UNIVERSITY OF SÃO PAULO
POLYTECHNIC SCHOOL

BRUNO THEOZZO

A robust optimization generic model for forest biorefineries design considering uncertainties on biomass growth and product selling prices

São Paulo
2022

BRUNO THEOZZO

A robust optimization generic model for forest biorefineries design considering uncertainties on biomass growth and product selling prices

Revised version

Text presented to the Graduate Program in Chemical Engineering at the Polytechnic School from the University of São Paulo for the Doctor of Science degree

Concentration area: Chemical Engineering
Advisor: Prof. Dr. Moises Teles dos Santos

São Paulo
2022

Este exemplar foi revisado e corrigido em relação à versão original, sob responsabilidade única do autor e com a anuência de seu orientador.

São Paulo, ______ de ____________________ de __________

Assinatura do autor: ________________________

Assinatura do orientador: ________________________

Catalogação-na-publicação

Theozzo, Bruno
A robust optimization generic model for forest biorefineries design considering uncertainties on biomass growth and product selling prices. / B. Theozzo – versão corr. -- São Paulo, 2022.
185 p.

Tese (Doutorado) - Escola Politécnica da Universidade de São Paulo. Departamento de Engenharia Química.

1.Otimização matemática 2.Otimização sob incerteza 3.Otimização robusta 4.Biorrefinaria florestal 5.Papel e celulose I.Universidade de São Paulo. Escola Politécnica. Departamento de Engenharia Química II.t.

THEOZZO, B. - **A robust optimization generic model for forest biorefineries design considering uncertainties on biomass growth and product selling prices.** Thesis (Doctor of Sciences in Chemical Engineering) - Polytechnic School, University of São Paulo, São Paulo, 2022.

Approved on __________________________________

Examination board:

Prof. Dr. __________________________________
Institution __________________________________
Decision __________________________________

Prof. Dr. __________________________________
Institution __________________________________
Decision __________________________________

Prof. Dr. __________________________________
Institution __________________________________
Decision __________________________________

Prof. Dr. __________________________________
Institution __________________________________
Decision __________________________________

Prof. Dr. __________________________________
Institution __________________________________
Decision __________________________________

ABSTRACT

THEOZZO, B. - **A robust optimization generic model for forest biorefineries design considering uncertainties on biomass growth and product selling prices** Thesis (Doctor of Sciences in Chemical Engineering) - Polytechnic School, University of São Paulo, São Paulo, 2022.

Biorefining emerges as a potential alternative for fossil-based industries by proposing the use of renewable biomass to produce chemicals, fuels, and energy. Several opportunities arise from a large set of available biorefining products, conversion technologies, sources of biomass, and integration points with other industries. The design of biorefineries that optimally explore this vast opportunity space is not trivial. Several tools have been proposed for this task. Among these, mathematical programming is highlighted as one of the most promising strategies due to its systematic evaluation of a large space of structural alternatives. The state-of-the-art mathematical programming-based frameworks deal with process synthesis challenges along with supply chain challenges under explicit spatial and temporal consideration. However, these frameworks cannot capture some particularities of forest systems, one of the most promising platforms for integrating biorefining operations. Thus, this thesis proposes an optimization generic model for biorefineries design able to account for the specificities of forest systems, under an MILP (Mixed-Integer Linear Problem) formulation for maximizing the operating net present value (NPV) over four interconnected layers of decision: (I) Forest dynamics, (II) Conversion systems, (III) Supply Chain, and (IV) Markets. The model also incorporates uncertainties in biomass productivity and product selling prices under a robust optimization formulation to ensure the operation's profitability and feasibility even on the materialization of the worst-case values for the uncertain parameters. The degree of conservatism of the solution is controlled through the description of the uncertainties within the intersection of a box and polyhedral sets. The model is applied to a case study on the design of a eucalyptus biorefinery in Brazil to produce bleached pulp (used for papermaking), lignin (used as a cement additive), and electricity. The case study showed that biomass dynamics played a vital role in the core strategic decisions, with biomass availability and forest distances driving decisions on all other layers. The adequate consideration of the supply networks was also relevant, as some highly productive forest lands become financially attractive in scenarios with reduced logistic costs. The model was demonstrated useful for minimum selling price estimation for products that might not be considered financially attractive under the nominal values for the input parameters. The choice of conservatism degree was demonstrated as an important feature of the model. Under a full conservative approach, the entire biorefinery operation was considered financially unattractive, contrasting with the nominal case scenario that indicates an opportunity of over 136 billion BRL (around 27 billion USD) in net present value. The over-conservatism on forest uncertainties is especially harmful as it proposes a 70% excessive usage of land to ensure a stable wood supply. This excessive land usage might compete with land for food crops. In between, some still conservative designs were proposed that could provide a robustness level consistent with the nature of the uncertain parameters and still benefit from the biorefining opportunities.

KEYWORDS: MILP, Optimization under Uncertainty, Robust Optimization, Forest Biorefinery, Pulp and Paper.

RESUMO

THEOZZO, B. – **Um modelo genérico de otimização robusta para o design de biorrefinarias florestais considerando incertezas na produtividade florestal e nos preços de venda dos produtos.** Tese (Doutor em Ciências em Engenharia Química) - Escola Politécnica, Universidade de São Paulo, São Paulo, 2022.

Biorrefinarias despontam como uma potencial alternativa para as indústrias baseadas em recursos fósseis ao propor a exploração de biomassa renovável para produção de químicos, combustíveis e energia. Diversas opções para bioprodutos, tecnologias de conversão, fontes de biomassa e pontos de integração com outras indústrias criam um amplo espaço de oportunidade a ser explorado. Contudo, propor uma configuração de biorrefinaria capaz de aproveitar esse espaço de forma ótima não é trivial. Diversas ferramentas foram propostas para esse fim. Entre essas, as baseadas em programação matemática são especialmente promissoras dada sua capacidade de avaliação sistêmica de um amplo espaço de alternativas estruturais. As ferramentas em estado da arte baseadas em programação matemática lidam com aspectos de síntese de processos integrados a toda a cadeia de fornecimento, com considerações temporais e espaciais. Contudo, essas ferramentas ainda não capturam algumas particularidades de sistemas florestais, sendo esses, uma das plataformas mais promissoras para a integração de operações de biorrefinaria. Com isso, esta tese propõe um modelo genérico de otimização para o design de biorrefinarias capaz de lidar com as particularidades de sistemas florestais, formulado como um Problema Inteiro-Misto Linear (MILP) para maximização do valor presente operacional líquido (NPV) sobre quatro camadas interconectadas de decisão: (I) Dinâmica Florestal, (II) Sistemas de Conversão, (III) Malha Logística e (IV) Mercado. O modelo também incorpora incertezas na produtividade da biomassa e nos preços de venda dos produtos via otimização robusta, garantindo viabilidade financeira-operacional mesmo na materialização dos piores casos para os parâmetros incertos. O grau de conservadorismo da solução é controlado pela descrição das incertezas como a união entre conjuntos intervalares e poliédricos. O modelo é aplicado em um estudo de caso para o design de uma biorrefinaria de eucalipto no Brasil produzindo polpa branqueada (matéria-prima para papel), lignina (uso como aditivo em cimentos) e energia elétrica. O estudo de caso mostrou que a dinâmica florestal tem um papel crítico nas decisões estratégicas. Por exemplo, disponibilidade de biomassa e distâncias florestais afetaram as decisões em todas as outras camadas do modelo. A consideração adequada das redes logísticas também se mostrou relevante, sendo capaz de tornar financeiramente atrativas plantações distantes de elevada produtividade florestal em cenários de redução de custos logísticos. O modelo também se mostrou útil para estimar o preço mínimo de venda de produtos que não são financeiramente atrativos nos cenários nominais. A possibilidade de controlar o grau de conservadorismo da solução se mostrou especialmente importante, sendo que, em uma abordagem completamente conservadora, a construção da biorrefinaria é considerada financeiramente inviável. Isso contrasta com a oportunidade de 136 bilhões de reais para o NPV no cenário nominal. O conservadorismo em excesso se mostrou especialmente prejudicial quando aplicado à produtividade florestal, resultando em um uso 70% superior de terras para garantir fornecimento estável de biomassa. Entre os extremos, cenários com conservadorismo controlado foram capazes de aproveitar a oportunidade financeira e ainda assim oferecer robustez consistente com a natureza dos parâmetros.

PALAVRAS-CHAVE: MILP, Otimização sob Incerteza, Otimização Robusta, Biorrefinaria Florestal, Papel e Celulose

LIST OF FIGURES

LIST OF TABLES

LIST OF ACRONYMS

ABTCP	Brazilian Pulp and Paper Producers Association
ANP	National Agency of Petroleum, Natural Gas and Biofuels
ANTAQ	Sea Transportation National Agency
BEKP	Bleached Eucalyptus Kraft Pulp
BFD	Block Flow Diagram
CBGTL	Coal, Biomass, and Natural Gas to Liquid
CHP	Combined Heat and Power
COFINS	Contribution to the financing of Social Security
CSCO	Chemical Species/Conversion Operator
CSLL	Social Contribution on Net Profit
FAMATO	Agriculture and Livestock Federation from Mato Grosso
FOB	Free on Board
FT	Fischer-Tropsch
GHG	Greenhouse Gases emission
IBÁ	Brazilian Tree Institute
IBGE	Brazilian Institute of Geography and Statistics
ICMS	Tax on Goods and Services Circulation
IPCA	Brazilian Price-Index to the Consumer
IRPJ	Income Tax for Legal Person
LGHG	Lifecycle Greenhouse Gases emission
LP	Linear Problem
MADM	Multi-Attribute Decision-Making
MILP	Mixed-Integer Linear Problem
MOO	Multi-Objective Optimization
NCM	Mercosur Common Nomenclature
NPV	Net Present Value
P&P	Pulp and Paper
P&W	Printing and Writing paper
PIS	Social Integration Program
PSE	Process System Engineering
SAA	Sample-Average Algorithm

SG&A	Selling, General, and Administrative expenses
UF	Federative Units
USA	United States of America
WECD	World Commission on Environment and Development

LIST OF SYMBOLS

admt	Air-dried metric ton, unit of measurement
BRL	Brazilian currency (Real)
EUR	European Union’s currency (Euro)
ft	feet, unit of measurement
kg	Kilogram, unit of measurement
km	Kilometer, unit of measurement
kWh	Kilowatts-hour, unit of measurement
GJ	Gigajoules, unit of measurement
ha	Hectare, unit of measurement
m^3	Cubic meter, unit of measurement
MJ	Mega-Joules, unit of measurement
MW	Megawatt, unit of measurement
MWh	Megawatt-hour, unit of measurement
Nm^3	Normal cubic meter, unit of measurement
s	Second, unit of measurement
ton	Metric ton, unit of measurement
ton RM	Mass unit of measurement referenced to a process’ raw material
USD	United States of America’s currency (Dollar)

TABLE OF CONTENTS

1 INTRODUCTION

The term “Sustainable Development” was coined in 1987 by the World Commission on Environment and Development (WECD, 1987) as the “development that meets the needs of the present generation without compromising the ability of future generations to meet their needs”. This vision implies that industrial models that depend on finite resources - such as fossil oil - are intrinsically unsustainable. Still, they account for nearly 80% of the global energy supply (IEA, 2021) and source of 90% of all chemicals produced (MAITY, 2015).

Biorefining emerges as a potential alternative for these industries by proposing the use of renewable biomass for producing chemicals, fuels, and energy. Several types of biomass feedstock can be used for biorefining: lignocellulosic (DE BHOWMICK; SARMAH; SEN, 2018), oleochemical (SCHNEIDER; IACONI; LAROCCA, 2016), algal (CHANDRA et al., 2019), and others (KUMAR; VERMA, 2021), where lignocellulosic biomass is the most abundant of them (WU et al., 2020).

The lignocellulosic biomass consists of cellulose (35–50%), hemicellulose (20–35%), and lignin (5–30%) as its three major components (MANKAR et al., 2021). Each component is interwoven in a polymerics recalcitrant structure (BHATIA et al., 2020) that, once isolated, has the potential to be functionalized into more valuable products. Over 200 value-added compounds can be produced from lignocellulosic biomass (ISIKGOR; BECER, 2015) by a variety of conversion routes, such as thermochemical (KIRTANIA, 2018), enzymatic (BHARDWAJ; VERMA, 2021), and biological (BECKHAM et al., 2016) ones.

The lignocellulosic biomass has also been appointed as a promising biorefinery feedstock motivated by their non-seasonal availability, reduced acquisition costs, and/or diminished competition to food crops and arable lands (BHATIA et al., 2020; DE BHOWMICK; SARMAH; SEN, 2018; MENON; RAO, 2012; OKOLIE et al., 2021). However, even the lignocellulosic biorefinery setup having a clear value proposition, its commercial success at the industrial scale is still inadequate (SINGH et al., 2022).

One strategy for increasing the economic attractiveness of biorefinery projects is to consider the integration of the biorefining operations. The Integrated Biorefinery run as a multifunctional production unit, simultaneously producing biofuels, electricity, and a considerable number of chemicals from biomass (BRIDGWATER, 2003), which allows for energy and materials to be recovered within the operation, lowering raw-materials and energy consumptions (TAY et al., 2011). The integration of biorefining operations, can also be done into established production facilities, sharing raw materials, by-products, utilities, and infrastructure, which may result in economic advantages such as capital investment, and reduced operating and utility costs (RAFIONE et al., 2014).

Christopher (2013) highlights the Pulp and Paper (P&P) mills as a promising option for this integration strategy as they present the world largest non-food biomass collection system, are located near forest and agricultural residues, and have existing infrastructure to transport the raw materials and finished products. Also, the Kraft pulping process – the most common process for producing cellulose pulp from wood in P&P mills (SIXTA, 2006) - is particularly well suited as a receptor of the biorefining technologies, since part of lignin and hemicelluloses - which is normally burnt for energy recovery - can be extracted from biomass and used as a raw material to produce high value-added bioproducts (RAFIONE et al., 2014).

The possibilities for biorefining operations to be integrated to P&P facilities are numerous, such as the black liquor (MORYA et al., 2022), lignin (ABDELAZIZ et al., 2020), and hemicellulose (AJAO et al., 2018) valorization.

Brazil plays a leading role in the world's wood pulp production. It was the world's largest exporter of chemical wood pulp in 2018, with trade totaling 8.2 billion USD and representing 20.5% of the total export of chemical wood pulp (SUSAETA; ROSSATO, 2021). Nearly 87% of the total pulp production in Brazil comes from hardwoods (BRAZILIAN TREE INDUSTRY, 2021) which can be explained by the preeminence of eucalyptus plantations covering about 7.5 million hectares, which represents 77% of all Brazilian planted tree area (IBGE, 2020) and 32% of the estimated planted eucalyptus area in the world (ZHANG; WANG, 2021).

The Brazilian relevance in eucalyptus production is not only related to planted area but also to productivity metrics. The average eucalyptus productivity in Brazil is estimated at 35.7 m^3 ha^{-1} $year^{-1}$ comparing to around 30 for China and 25 for Indonesia (PENA-VERGARA et al., 2022) , two other relevant countries in eucalyptus productivity.

Besides increasing the economic attractiveness of the biorefining operation, higher biomass productivity also reduces the demand for arable lands - a major concern regarding the sustainable consolidation of the biorefinery model - that might lead to increased deforestation pressure (BORDONAL et al., 2018), and food and livestock feed competition (MUSCAT et al., 2020). On this regard, Lossau et al. (2015) have mapped over 37 million hectares of available residual lands[1] in Brazil that could be used for sustainable fuel crops expansion.

The availability for planted area expansion and the high biomass productivity enhances potential value of the P&P integrated biorefinery in Brazil. However, it also brings another dimension for the already complex opportunity space, increasing the difficulty for choosing among all the possible products to be produced, technological pathways, and biomass supply networks. This decision challenge is extremely complex as - even if the decisions are taken wisely - the biorefinery implementation leads to substantial investments that might start paying-off only after several years of operation.

The Process System Engineering (PSE) is one strategy for addressing such a challenge. According to Grosmann (2021), PSE is a discipline concerned with the systematic analysis and optimization of decision-making processes for the discovery, design, manufacture and distribution of chemical products.

[1] The classification of residual lands from Lossau et al. (2015) excludes lands that: (I) are already used by agriculture, livestock, and/or fibers production; (II) results in direct or indirect deforestation; (III) are under any form of legal protection; (IV) is associated with biodiversity loss; (V) compete for scarce freshwater, and/or (VI) cause land degradation or an increase in GHG emission due to fertilizers usage or land-use change.

Several PSE approaches were used for the design of integrated biorefineries. Ng, Ng, and Ng (2017) categorize them into hierarchical-based, insights-based, or mathematical optimization-based approaches.

The hierarchical approaches rely on rules derived from expert knowledge and are thus dependent upon the knowledge and experience of the designer (NG; NG; NG, 2017). This limitation is even more prominent for Biorefineries as most technologies are still under lower maturity levels. Examples of the use of hierarchical approaches for biorefineries design are the works of Ng et al. (2009) and Pham and El-Halwagi (2012).

The insights-based approaches include strategies such as the ternary diagram and pinch analysis that aim at finding superior design points by the graphical representation of process physical targets. The main limitation is that graphical methods are potentially tedious and inaccurate and may be limited to a maximum of three dimensions (NG; NG; NG, 2017). Examples on the use of pinch analysis for the design of biorefineries are the works of Martinez-Hernandez et al. (MARTINEZ-HERNANDEZ; SADHUKHAN; CAMPBELL, 2013; MARTINEZ-HERNANDEZ; TIBESSART; CAMPBELL, 2018).

Mathematical programming-based approaches consist of three steps: (I) the development of a representation of alternatives from which the optimum solution is selected; (II) the formulation of a mathematical program which generally involves discrete and continuous variables for the selection of the configuration and operating levels, respectively; (III) the solution of the optimization model from which the optimal solution is determined (GROSSMANN; GUILLÉN-GOSÁLBEZ, 2010). The mathematical programming approaches are preferred for the conceptual process design due to its systematic evaluation of a large space of structural alternatives (MENCARELLI et al., 2020), with main limitations given by the designer ability to define an appropriate search space, select a suitable degree of approximation, and solve the resulting optimization problems (CHEN; GROSSMANN, 2017).

Mathematical programming-based approaches are reviewed in chapter 2, in which is shown that the state-of-the-art applications tackle process design challenges (technological pathways and product portfolio selection) along with supply chain challenges (production capacities and logistic design and planning) under explicit spatial and temporal consideration.

These applications, however, cannot capture some particularities of forest-based systems, especially because forests demand several years of cultivation for reaching commercial maturity (DIAZ-BALTEIRO; RODRIGUEZ, 2006) and present a non-linear growth behavior during this period (RYAN et al., 2004).

To overcome this literature gap, this thesis proposes an optimization generic model for biorefineries design able to account for specificities of forest-based biorefineries. The system is modeled as an MILP (Mixed-Integer Linear Problem) over four interconnected layers of decision: (I) Forest dynamics, (II) Conversion technologies and production facilities implementation, (III) Storage facilities and logistic network, and (IV) Product portfolio and market demand fulfillment. The framework maximizes the net present value (NPV) of the cash flow generated throughout the model time horizon.

The feasibility of a real-world application of solutions derived from the model, however, depends on the accurate description of the input parameters, such as biomass productivity and product selling prices. This is a challenging task as prices are associated with high volatility (PÄTÄRI et al., 2016) and biomass productivity is highly affected by uncontrolled factors such as precipitation, plagues, and diseases. For instance, Binkley et al. (2017) reported that the same eucalyptus clone in Brazil presented a 50% difference in productivity on plantations separated by hundred kilometers.

To address this challenge, the model developed in Chapter 3 also proposes the incorporation of uncertainties in biomass productivity and product selling prices under a robust optimization formulation to ensure the operational and financial feasibility of the solution even on the worst-case materialization of the model parameters. As robust formulations tend to be over-conservative (BERTSIMAS; BROWN; CARAMANIS, 2011) the degree of conservatism of the solution is controlled through the description of the uncertainties within the intersection of a box and polyhedral sets, as proposed by Bertsimas and Sim (2004).

The model is applied to a case study on the design of a eucalyptus biorefinery in Brazil to produce bleached pulp (used for papermaking), lignin (used as cement additive), and electricity. Conclusions and recommendations for further works are then presented in Chapters 5 and 6, respectively.

2 LITERATURE REVIEW

According to Grossmann (2021), Process System Engineering (PSE) is a discipline concerned with the systematic analysis and optimization of decision-making processes for the discovery, design, manufacture and distribution of chemical products. PSE tools are known for handling complex process systems through a holistic view and a system thinking framework (KISS; GRIEVINK, 2020). This makes PSE very well positioned to navigate the vast opportunity space associated with the integrated biorefineries implementation.

As discussed in Chapter 1, several PSE tools have been applied to the design of biorefineries and those based on mathematical programming (or optimization) are the preferred for process design. These approaches are then the focus of this review.

Section 2.1 starts discussing how these optimization approaches have been deployed for the design of biorefineries. Some works on this regard have considered a more rigorous process representation resulting in non-linear optimization models. These formulations require specific solving procedures, such as the two-stage heuristic in the works of Gebrelassie, Waymire and You (2013), or the tailored branch-and-bound with successive piecewise linear approximation in the work of Gong and You (2014). This increased computational complexity for solving the optimization problem may prohibit solving large instances of the model. As the objective of this thesis is to provide a model integrating several decisions layers (forest, production process, supply chain and markets) on a more strategic level, the control of computational traceability is preferred over the rigorous representation of conversion process. Thus, the review will not cover non-linear optimization models.

Section 2.1 contemplates the works that proposed the optimal biorefineries design under a deterministic approach, i.e., supposing the input data are correct. However, some input parameters, such as biomass productivity and product selling prices, are influenced by several uncontrolled factors and are uncertain. Section 2.2 discusses how these uncertainties are managed by the optimization frameworks.

Sections 2.1 and 2.2 deal with the design of biorefineries for maximization of a single performance indicator, generally, an economic-related objective, such as the net present value (NPV) or operating profit. These indicators, however, do not evaluate the sustainability performance of the operation, which is a major claim for the biorefinery model adoption. The incorporation of sustainability assessment in the mathematical-programming frameworks is reviewed in Section 2.3. Then, Section 2.4 discusses how both sustainability and uncertainties considerations are integrated into the same optimization model. Finally, section 2.5 consolidates a general overview of the previous discussion and how it connects to the scope of this thesis.

It is worth noticing that sustainability assessments are not incorporated in the generic model developed in this thesis. However, they are reviewed in sections 2.3 and 2.4 as they represent important avenues for the suggested further works (discussed in Chapter 6).

2.1 OPTIMIZATION-BASED STRATEGIC DESIGN

Bao et al. (2011) proposed a linear programming (LP) framework for the screening of technological pathways for biomass conversion into products. The framework is based on a layered representation named Chemical species/conversion operator (CSCO) that alternates possible conversion technologies (Conversion Operators) and potential intermediate products (Chemical Species) using simple conversion factors. The framework was applied to the technological selection for gasoline production from cellulosic biomass. Pham and El-Halwagi (2012) proposed an LP framework for the screening of biorefineries technological pathways based on the optimization of a network of feedstocks, conversion steps, intermediates, and desired products. The framework was applied to the screening of technological pathways to produce fuel-grade alcohols from lignocellulosic biomass. González-Delgado, Kafarov, and El-Halwagi (2015) expanded the framework including post-optimization comparisons step and applied it to the technological pathway selection of algae conversion into fuels and chemicals. Gupta, Shastri, and Bhartyra (2016) proposed an MILP for the optimal technological pathway selection to produce biodiesel from microalgae cultivation.

Such methodologies are useful for deciding on technological aspects of biorefinery design. However, they do not incorporate location-specific information into the decision-making process. As biomass physical-chemical properties and availability are highly dependent on geography (SCHRÖDER; LAUVEN; GELDERMANN, 2018), this location-specific information should also be considered in the proposed decision-making process.

Dunnet, Adjiman, and Shah (2007) proposed a framework for designing biomass-based energy systems that explicitly decides on cultivation, harvesting, and the centralization or decentralization of processing facilities. However, the framework is applicable only to a local level as it does not consider the possibility of integrating supply and demand from different regions. The latter was proposed by Dunnet, Adjiman, and Shah (2008) on the synthesis of a bio-ethanol supply chain connecting rural and urban areas. The model was formulated as an MILP that considered hypothetical scenarios of geographical supply and demand distribution and showed that decentralized processing might be relevant for an efficient design of biomass-based energy systems. Zamboni, Shah, and Bezzo (2009a) proposed an MILP for the optimal design of biofuels supply chain, deciding over biomass supplier allocation, production site locations and capacity assignment, logistic distribution, and transport system. The framework was applied to the design of a corn-based ethanol system in Italy by optimizing economic criteria. Leduc et al. (2009) proposed an MILP for deciding on locations and capacities of biodiesel production plants from jatropha oil in India. An MILP for the design of a biofuel supply chain in Mississippi (USA) was proposed by Ekşioğlu et al. (2009), deciding on the number, size, and location of processing units to produce biofuel using the available biomass. Bowling, Ponce-Ortega, and El-Halwagi (2011) proposed an MILP for deciding on the centralization or decentralization of pretreatment facilities for biofuels supply chain.

Huang, Chen, and Fan (2010) incorporated the temporal dimension into the supply chain design of biofuels. They proposed a multistage MILP that accounts for temporal demand variability and the need for infrastructure expansion of processing capacities over time. Van Dyken, Bakken, and Skjelbred (2010) proposed a multi-period MILP for biofuels supply chain design that accounts for biomass properties variation during long-term processes such as passive drying during storage. Seasonality of biomass availability was incorporated by An, Wilhelm, and Searcy (2011) into an MILP framework for biofuels supply chain design in Central Texas (USA) and by Giuliano, Poletto, and Barletta (2016) into the process synthesis for the conversion of eucalyptus residues, wheat straw and olive tree pruning into levunilic acid, succinic acid and ethanol. Competition for biomass was incorporated into the design by Zimmer et al. (2017), who proposed an MILP framework for designing a synthetic fuel supply chain that considers biomass competition from combined heat and power (CHP) and householder consumers. Kostin et al. (2018) have proposed an MILP framework for designing a sugar and bioethanol supply chain in Brazil. The model decides on the locations of the production and storage facilities, their expansion policy, technology for conversion, and material flows.

Some works have also proposed the integration between process synthesis (conversion technologies pathway selection) to the supply chain design problem. Lim et al. (2013) proposed a multi-period MILP for technology selection and resource planning in an oil-extraction and cogeneration facility integrated into a rice mill. Cucek et al. (2014) proposed a multi-period spatially explicit MILP that considers seasonality and availability of resources, recycling of products, and total-site heat integration. The framework is applied to a biofuels supply chain from several feedstocks (corn grain, wheat, corn stover, wheat straw, switchgrass, forest thinning, waste cooking oil, and algae are) through several integrated conversion technologies (dry-grind process, biochemical conversion, gasification, catalytic mixed-alcohol synthesis, Fischer-Tropsch [FT] synthesis, hydrocracking, oil extraction, and transesterification). The framework represents an important advance in terms of an optimization tool for a holistic design.

A general feature of these works is that, when explicitly considering the spatial and temporal availability of biomass, they assume it presents a fixed cultivation timespan and/or that biomass productivity within this period is constant. These assumptions, however, do not hold for forest systems. For instance, eucalyptus usually present clear-cut ages of around 5 to 9 years in Brazil and 13 to 18 years in Spain

(DIAZ-BALTEIRO; RODRIGUEZ, 2006). Treating this long timespan as a fixed parameter may impose severe difficulties for an adequate design and planning of forest-based biorefineries. Also, Ryan et al. (2004) highlight that the growth behavior observed in forest plantations is not linear and shows an increase in aboveground wood production early in stand development, followed by a peak near the canopy closure and then a decline by 20–80% over years to centuries. This non-linear growth behavior along the cultivation time imposes severe difficulties to the practical application of former methodologies for forest-based biorefinery design. This dynamic behavior suggests that plantation and harvesting planning must be treated as decisions variables to be optimized with the other design variables. This is one of the literature gaps that this thesis aims to cover.

2.2 DESIGN UNDER UNCERTAINTY

Generally, the methodologies described in section 2.1 assume the correctness of input data. This data, however, may be associated with several uncertainties that might hinder the performance of design on real-world implementation. A review on the several sources of uncertainties in biorefineries supply chain is provided by Awudu and Zhang (2012). Some authors incorporate the evaluation of some of these uncertainties in their works.

Marvin et al. (2012) evaluated wherever the optimal deterministic biomass-to-ethanol supply chain would fail on ethanol prices variation. Gebrelassie, Waymere, and You (2013) evaluated the effects of diesel prices variation on the technological routes optimal selection for an algae-based biorefinery. Kelloway and Daoutidis (2014) evaluated the effect of product prices and feedstocks costs on the optimal configurations of a biorefinery to produce fuel and chemicals from different biomass. They also conducted a Monte Carlo sampling for identifying the most promising technologies and products.

Sampling methods were also employed by Santibãnez-Aguilar et al. (2016) for the generation of several scenarios solved individually by a deterministic MILP framework for a biorefinery system in Mexico. Statistical data from the collection of individual solutions was used for selecting the most robust structures for the supply chain.

These approaches try to provide information about the robustness of a solution facing uncertainty after the optimization stage has been concluded, which do not guarantee that the final solution is chosen optimally regarding the uncertainties. Some works handled uncertainties *a priori* the optimization stage through stochastic programming[2]. Dal-Mas et al. (2011) proposed a scenario-based MILP for the design of corn-to-ethanol supply chain in Italy under uncertainties on feedstock cost and product selling price. Kim, Realff, and Lee (2011) proposed a two-stage stochastic MILP for the supply chain design of biofuels in the southern USA under uncertainty on biomass supply, operating costs, and technological yields. In that work, the biomass is converted into bio-oil through fast-pyrolysis and then is further upgraded to biofuels via FT synthesis. The framework can decide on the decentralization of fast-pyrolysis units and the subsequent transference of the intermediate bio-oil to central larger upgrades facilities.

Walther, Schatka, and Spengler (2012) proposed a scenario-based approach for the design of a second-generation biodiesel supply chain in Germany. These authors present different strategies for incorporating the scenarios into the MILP model (Maxmin, Expected-value, Hodges-Lehmann, and Expected-value-expected-failure) accordingly to the risk-aversion of the decision-maker. Kostin et al. (2012) proposed a two-stage stochastic MILP for the design of bioethanol supply chains in Argentina under demand uncertainty. Gebreslassie, Yao, and You (2012) proposed a two-stage stochastic MILP framework for the hydrocarbon biorefinery supply chains design and planning under supply and demand uncertainties. Osmani and Zhang (2013) proposed a two-stage stochastic optimization model for the design of a lignocellulosic-based bioethanol supply chain under uncertainties on supply, demand, and prices. Azadeh, Vafa Arani, and Dashti (2014) proposed a stochastic linear programming framework for the design of biofuels supply chain considering demand and prices uncertainties. Product demands were assumed to be dependent upon their prices, which were

[2] An overview about stochastic programming frameworks and methods is presented in Birge and Louveaux (2011).

assumed to follow a Geometric Brownian Motion. Li and Hu (2014) proposed a two-stage stochastic MILP for the selection of location and capacity of decentralized fast-pyrolysis plants connected to a central upgrading facility for converting corn stover into transportation fuels in Iowa under feedstock availability, fuel price, capital costs, logistic costs, and technology advancement uncertainties. Tong et al. (2014b) expanded their deterministic MILP framework (TONG et al., 2014a) to a two-stage stochastic MILP formulation that integrates biorefineries decisions into existing petroleum supply chain infrastructure under price and demand uncertainties, including considerations on co-processing routes and product blending.

A key point is that stochastic optimization assumes that uncertainties have a known probability distribution (i.e., uncertainties are random). This imposes a severe challenge for situations lacking data for probability estimation or when the estimated probability is not representative of the future outcomes (i.e., when uncertainties are epistemic). For the latter case, Bertsimas, Brown, and Caramanis (2011) pointed out that robust optimization[3] may be the only reasonable alternative. Under a robust optimization approach, it is acceptable to obtain a suboptimal solution in respect to the nominal values of the data as long as this solution remains feasible and near-optimal when data changes (BERTSIMAS; SIM, 2004).

In the robust optimization method, a deterministic data set is defined within the uncertain space, and the best solution which is feasible for any realization of the data uncertainty in the given set is computed through the solution of the robust counterpart optimization problem (LI; FLOUDAS, 2012). For instance, the uncertainty can be represented by an interval-set that defines the range within an uncertain parameter can fluctuate.

However, a robust optimization hedging for this type of uncertainty representation yields very conservative solutions because it would require the solution to be robust to a scenario in which all uncertainty parameters assume their worst value at the same time. This may be a rare event in several real applications. A less

[3] An overview of robust optimization frameworks and methods is presented in Ben-Tal, El Gahoui, and Nemirovski (BEN-TAL; EL GAHOUI; NEMIROSVSKI, 2009).

conservative approach was proposed by Bertsimas and Sim (2004) considering that the random variable describing the uncertain parameter fluctuation is comprised not only within an interval-set but also within a polyhedral that relates several random variables with each other. Thus, the simultaneous occurrence of the worst value for all random variables within the same set is limited by the size of the polyhedral.

The robust optimization approach from Bertsimas and Sim (2004) has been applied by Mohseni, Pishvaee, and Sahebi (2016) to the strategic design of biodiesel from microalgae supply chain design under biomass productivity, resources availabilities, capital and operating costs, and biodiesel demand epistemic uncertainties.

The management of both random and epistemic uncertainties in supply chain optimization was proposed by Shabani and Sowlati. First, they developed a multi-stage stochastic framework for bioenergy supply chain planning under biomass demand random uncertainty (SHABANI et al., 2014) and then expanded the framework for a hybrid robust multi-stage optimization formulation that also considers epistemic uncertainty on the quality of supplied biomass (SHABANI; SOWLATI, 2016). Bairamzadeh, Saidi-Mehrabad, and Pishvaee (2018) proposed a hybrid robust optimization model for handling multiple types of uncertainties designing a bioethanol supply chain in Iran. Chemical conversion factors were taken as random uncertainty with a known probability distribution. Biomass yields were treated as fuzzy numbers with possibilities drawn from experts' knowledge. Fuel demands were treated as an interval of possible values. The final model integrates a robust scenario-based approach (MULVEY; VANDERBEI; ZENIOS, 1995) for handling the conversion uncertainties, a robust possibilist approach (PISHVAEE; RAZMI; TORABI, 2012) for handling the biomass yield uncertainties, and a robust convex formulation (BERTSIMAS; SIM, 2004) for handling demand uncertainties.

Besides the assurance of feasibility on the entire uncertainty set, another important source of conservatism of traditional robust formulations is the disregard of recourse (i.e., reactive actions after the realization of the uncertainty), which is a very unrealistic assumption in many cases, such as in problems involving investment and long-term contract decisions (GROSSMANN et al., 2016). Adjustable robust optimization formulations (BEN-TAL et al., 2004) propose the incorporation of recourse actions into the robust framework and thus provide an opportunity for less conservative designs.

The use of adjustable robust programming in biofuels supply chains design was proposed by Zhao and You (2019). They proposed a two-stage adaptive robust fractional programming model with a decision-dependent uncertainty set. The remaining production capacity at each manufacturing facility after the occurrence of unknown disruptions is modeled by an uncertainty set, which depends on facility-location decisions and production-capacity decisions. A data-driven procedure was also proposed for the definition of the uncertainty set.

In general, Stochastic and Robust Optimization are the two major approaches for the incorporation of uncertainties in the mathematical programming-based frameworks for biorefineries design. The first has the major drawback of relying on the probabilistic description of the uncertain parameters. This, even if accomplished, might not be representative of future outcomes. The latter has the major drawback of being overconservative. To circumvent this issue, recourse actions have been proposed as well as the description of the uncertainties on more assertive sets both through tighter mathematical description of the uncertain parameters' behavior and data-driven approaches.

2.3 SUSTAINABILITY METRICS IN OPTIMIZATION-BASED DESIGN

One of the major motivations for the adoption of biorefineries is their use of renewable resources in alternative to fossil ones. However, the renewability of raw materials does not necessarily imply a sustainable industrial model. A proper sustainability assessment should be conducted for ensuring a sustainable design of biorefineries.

In this direction, some works have incorporated sustainability-related metrics into optimization-based frameworks. Sharma, Sarker, and Romagnoli (2011) proposed an MILP framework for biorefinery design that maximizes the 'stakeholder value', an indicator that consolidates the operating cash flow with the monetization of environmental implications such as emission mitigation costs and credits. Monetization of emissions was also used by Osmani and Zhang (2014) for incorporation of the environmental impacts in the economic criteria subject to optimization. Zore, Cucek, and Kravanja (2017) proposed the concept of *Sustainability Profit* further expanded by Zore et al. (2018) to a *Sustainability Net Present Value*, a metric that combines a monetary expression for the economic, environmental, and social net present values into a composite measure of sustainability. This indicator was then maximized through an MILP for the renewable energy supply network considering biomass, waste, solar, wind, and geothermal energies on a European continental scale.

Elia et al. (2011) incorporated lifecycle greenhouse gases (LGHG) emissions into the design of hybrid coal, biomass, and natural gas to liquid (CBGTL) energy networks. The emissions were subject to a maximum allowed level, which stimulated the use of renewable resources. The adoption of carbon policies on design constraints was also proposed by Marufuzzaman, Eksioglu, and Huang (2014) for the design of biodiesel production supply chain from wastewater. Policies that impose a maximum allowed greenhouse gases (GHG) emission, tax on GHG emissions, and trade of emission credits were incorporated into a two-stage stochastic model and allowed the incorporation of environmental impact considerations into an uncertainty handling framework without the burdens of using multi-objective optimization strategies. Gonela, Zhang, and Osmani (2015) proposed a stochastic MILP for the design of a 2^{nd} generation bioethanol production that integrates with existing 1^{st} generation infrastructure in North Dakota (USA). Environmental impacts were incorporated into the methodology as restriction policies on the maximum allowed GHG emission and irrigated land usage.

The integration of environmental impact within the economic metric or its incorporation as operations constraints represents an advance towards more sustainable designs while keeping the computational benefits of having a single optimization objective. However, having explicit indicators for environmental performance allows designers to optimize for the environmental criteria and to manage its trade-offs with economic criteria.

Multi-objective optimization (MOO) methodologies[4] were proposed for the optimization of explicit indicators for environmental performance along with economic metrics. In MOO, the concept of optimality is replaced with Pareto-optimality. The Pareto-optimal solutions are those that cannot be improved in respect to one objective function without deteriorating their performance in at least one of the rest (MAVROTAS, 2009).

Zamboni, Shah, and Bezzo (2009b) expanded their former MILP framework (ZAMBONI; SHAH; BEZZO, 2009a) into an MOO between economic and environmental impact (LGHG) criteria applied to the design of a corn-based bioethanol supply chain in Italy. You and Wang (2011) proposed a bi-objective MILP framework that integrates technology and supply chain decisions optimizing LGHG emissions and economic criteria for a case study of biofuels production in the state of Iowa (USA).

Other environmental impact indicators other than GHG emissions were also considered in MOO frameworks. Bojarski et al. (2009) proposed an MILP for a biorefinery supply chain design in Europe considering both an economic metric and a sustainability metric given by the IMPACT2002+ (JOLLIET et al., 2003) that combines several damage categories into a single indicator. Santibañez-Aguilar et al. (2011) proposed an MILP for the Pareto-optimal selection of feedstock, processing technology, and product portfolio considering both economic and sustainability metrics given by the eco-indicator 99 (PRE-CONSULTANTS, 2000). Eason and Cremaschi (2014) proposed an MILP for the design of biofuel from biomass and the selection of technological pathways for different feedstocks that optimizes for cost, GHG emission, and energy recovery from biomass (i.e., how much energy originally presented in the feedstock is available as product).

[4] An overview on multi-objective optimization is presented in Collette and Siarry (2004).

These methodologies tried to approximate the Pareto-optimal curve via methods such as ε-constraint and weighted-sum. This curve approximation might be computationally expensive and requires a post-optimization analysis for reaching a final solution. To cope with that, fuzzy programming has been proposed as an alternative that does not try to approximate the entire Pareto-optimal curve. Tan et al. (2009) proposed an LP for product mix and conversion process selection in biorefineries that considers both environmental and economic objectives as fuzzy goals to be optimized simultaneously. Tay et al. (2011) proposed an MILP for the process synthesis of integrated biorefineries also considering environmental impact and economic performance as flexible fuzzy goals. Ng, Hassim, and Ng (2013) used fuzzy optimization for handling the biorefinery synthesis under economic, environmental, safety, and health optimization criteria. Yilmaz, Balaman, and Selim (2014) proposed an MILP with fuzzy goals for the design of a biogas supply chain for both maximizing the total operating profit (economic criteria) and minimizing the weighted unused waste biomass amount in the supply regions (sustainability criteria).

The social dimension, along with the economic and environmental ones, is one of the basic pillars of sustainability. However, its incorporation in mathematical programming-based frameworks is still in its infancy. You et al. (2012) incorporated the number of accrued jobs as social optimization criteria along with environmental impact (LGHG) and economic criteria (total annualized cost) into a multi-objective MILP for the design of a cellulosic ethanol supply chain in Illinois (USA). Pérez-Fortes et al. (2012) proposed an MILP that optimizes economic (NPV), environmental (Impact 2002+), and social criteria (creation of jobs). The social indicator was taken as the number of sites to receive a production facility with the assumption that these facilities may generate a positive social impact in the communities that receive them. The framework was applied to a case study of electricity generation from biomass in Ghana. El-Halwagi et al. (2013) proposed a framework for hydrogen from biomass design that optimizes for both economic and safety criteria, namely total annual cost and a cumulative risk index. Gonela et al. (2015) proposed a stochastic MILP for the design of 2nd generation bioethanol supply chains that accounts for the existing 1st generation infrastructure. The amount of 1st generation biofuel produced was taken as a metric for social impact with the understanding that 1st generation biofuel production increases the pressure on food prices due to land competition. Environmental impact was taken in terms of GHG emissions and was integrated into the framework as a constraint that imposes a maximum allowed emission level.

When the social dimension is incorporated into the decision framework along with environmental and economic aspects, the proper assessment of the Pareto curve is more challenging and might become impractical for real-life applications. To overcome this issue, a solution raking methodology has been employed by Medina-González et al. (MEDINA-GONZÁLEZ et al., 2017; MEDINA-GONZÁLEZ; ESPUÑA; PUIGJANER, 2018) to retrieve the solution that best matches decision-maker preferences from the Pareto-optimal set.

To avoid several evaluations of the optimization model for approximating the Pareto-optimal curve, a multi-attribute decision-making (MADM) method was incorporated into an MILP framework in the work of Wheeler et al. (2018) for retrieving a single Pareto-optimal point that reflects the preferences of decision-makers towards each objective. The framework was applied to the bioethanol supply chain design in Argentina.

In general, sustainability assessment of biorefineries is done by means of GHG emissions or other methodologies to aggregate several environmental impact dimensions into a single indicator. The evaluation of the social component is still incipient with some efforts on the evaluation of job creation, operational risks, and food-price pressure. The sustainability indicators are integrated into the optimization as constraints (such as limiting GHG emissions) or aggregated together with the economic criteria into a single objective. MOO frameworks are also developed trying to approximate the Pareto-optimal curve for economic and a second sustainability indicator. This approach, however, might be impractical on real-life applications for more than two objectives. On this regard, fuzzy optimization seems an interesting strategy for handling more than two objectives optimally without trying to approximate the Pareto-curve.

2.4 MULTI-OBJECTIVE OPTIMIZATION UNDER UNCERTAINTY

Section 2.3 presented several works that integrated economic and sustainability performance into multi-objective optimization models. However, these works are deterministic in nature, and, as discussed in section 2.2, the adequate evaluation of the uncertainties in input parameters is of great value in biorefineries design. Some works proposed the integration of the multi-objective optimizations models with the incorporation of uncertainties in the optimization.

Giarola, Bezzo, and Shah (2013) proposed a two-stage stochastic MILP for the design of 1st and 2nd generation bioethanol supply chains under market uncertainties that integrates an economic objective (expected NPV) and GHG emissions into a single objective through the definition of a weighting factor that composes the two objectives into one. The weighting factor can be varied to explore different trade-off configurations between economic and environmental performances. Cheali et al. (2015) also proposed the integration of several sustainability indicators into a single objective of a stochastic optimization for the synthesis of a bioethanol-upgrading biorefinery under product prices uncertainties. The authors propose a single sustainability score weighting up to five indicators describing economic, environmental, health/safety, and operational aspects. A sustainability ratio describing the score of the new proposed process flowsheet to a benchmark is taken as the optimization objective.

Yilmaz Balaman and Selim (2015) treated uncertainties in land availability policies as fuzzy parameters and incorporated them in a multi-objective fuzzy goal programming for designing a biomass-to-biogas supply chain.

Bairamzadeh, Pishvaee, and Saidi-Mehrabad (2016) proposed a multi-objective robust possibilistic programming for the design of biofuels supply chain that maximizes the economic performance and social impact (job creation) while minimizing environmental impact (eco-indicator 99). Uncertain market prices, biofuel demands, and environmental impact coefficients are treated as fuzzy numbers. The different objectives are aggregated using a weighted-sum fuzzy aggregation function. The framework was applied to a case study of a lignocellulosic biomass-to-biofuel supply chain in Iran.

Gao and You (2017) proposed a bi-objective two-stage stochastic mixed-integer fractional linear program for the design of a hydrocarbon biorefinery in Illinois (USA) optimizing for both cost and environmental impact under supply and demand uncertainties. The cost and environmental impact are normalized to a product functional unit (gasoline-equivalent gallon). This normalization makes the model non-linear (fractional) with higher complexity. A specific methodology for solving the resulting optimization problem was presented by the authors.

Medina-González et al. (2017) extended the work of Pérez-Fortes et al. (2012) for consideration of supply uncertainties on the bioenergy supply chain planning that optimizes for economic, environmental, and social criteria. They proposed a two-stage stochastic program for handling uncertainties with a Sample-Average Algorithm (SAA) (AHMED; SHAPIRO, 2002) for its solution. Although the framework accounts for multiple objectives, the solution stage for the stochastic problem considers only the maximization of the economic criteria due to the computational complexity of the multi-objective stochastic optimization. The incorporation of social and environmental impact evaluations is conducted in a post-optimization step using the so-called ELETRE solution ranking methodologies from the solutions obtained during the SAA stage. Medina-González, Espuña, and Puigjaner (2018) further extended the framework to include a scenario reduction stage aiming at the mitigation of the computational complexities of the framework.

2.5 GENERAL CONCLUSIONS ABOUT LITERATURE REVIEW

Section 2.1 discussed the importance of integrating the biomass supply chain into biorefinery design and showed that state-of-the-art mathematical programming-based approaches can tackle process design challenges (technological pathways and product portfolio selection) along with supply chain challenges (production capacities and logistic design and planning) under explicit spatial and temporal consideration. However, these works adopt some premises for the biomass dynamics that do not hold for forest systems due to their non-linear growth behavior. Chapter 3 proposes a generic optimization model to cover this literature gap.

Beyond those complex growth dynamics, the biomass productivity is dependent on several uncontrolled factors and its estimation is highly uncertain. Section 2.2 shows that several works deal with the integration of uncertainties in in the mathematical programming-based frameworks for biorefineries design. Generally, they rely on two major strategies: Stochastic and Robust Optimization.

Stochastic Optimization has the major drawback of relying on the probabilistic description of the uncertain parameters. This, even if accomplished, might not be representative of future outcomes. On the other hand, Robust Optimization has the major drawback of yielding over-conservative solutions. To overcome this excessive conservatism, some works proposed the incorporation of recourse actions into the decision space and/or the description of the uncertainties on more assertive mathematical sets.

Chapter 3 also proposes a methodology for incorporating uncertainties associated to biomass growth and product selling prices to the generic optimization model.

The incorporation of the uncertainties in the optimization model is important for ensuring economic and operational feasibility of the solutions even on stressful scenarios. However, given one the major motivators for biorefineries adoption relies on sustainability claims, the incorporation of sustainability metrics is also important to the decision framework.

Section 2.3 shows that the sustainability assessment of biorefineries is commonly done by means of computing the life cycle GHG emissions of the operation. Other environmental impact dimensions may also be evaluated and aggregated into a single impact indicator. The evaluation of the social component is still incipient with some efforts towards the evaluation of job creation, operational risks, and food-price pressure.

The sustainability indicators are often integrated into the optimization model as constraints (such as limiting the GHG emissions level) or aggregated together with the economic criteria into a single optimization objective. The aggregation is often done via weighted average, reflecting the decision-making priorities towards each objective or by means of monetizing the environmental performance and integrating them into the operating cash flow, such as in the cases of incurring cost for mitigating environmental impacts or credits.

The sustainability performance has also been taken as an objective along with the economic criteria in MOO frameworks that try to obtain the approximated Pareto-optimal curve for the multiple objectives. This approach, however, might be impractical on real-life applications for more than two objectives. On this regard, fuzzy optimization seems an interesting strategy for handling more than two objectives optimally without trying to approximate the Pareto-curve.

The explicit incorporation of sustainability metrics as a single or multi-objective optimization strategy is not contemplated in the scope of this thesis but is recommended as further works in the discussion of Chapter 6.

3 METHODOLOGY

The proposed methodology is based on a mathematical model that explicitly relates an economic objective to the strategic, tactical, and operating decisions for a biorefinery design. The decisions cover the entire biorefinery supply chain, ranging from which biomass species to plant at each location to which products to sell at each consumer location. The model is built for a broad applicability and allows the consideration of multiple biomass species, long-term non-linear biomass growth behavior, complex production processes topologies, and several tax collection schemes. On top of that, uncertainties on biomass productivity and product selling prices are handled optimally accordingly to the desired degree of conservatism for heading against the uncertainties' materialization. The applicability of the proposed model is illustrated in a case study presented in Chapter 4 on the design of a eucalyptus biorefinery in Brazil to produce bleached pulp (used for papermaking), lignin (used as cement additive), and electricity.

The mathematical model consists of an MILP formulation that interconnects four layers of decision (Figure 1). Each layer l is represented by a set of n_l possible instances: Set F (all the n_f possible forest locations); Set P (all the n_p possible production facilities locations); Set E (all the n_e possible storage facilities locations); and Set M (all the n_m possible consumers' markets to be attended). The interconnections' flows are referenced with a subscript q (or b) indicating a chemical species q from the Set Q (or a biomass b from Set B) and a subscript t indicating a period from the Set T.

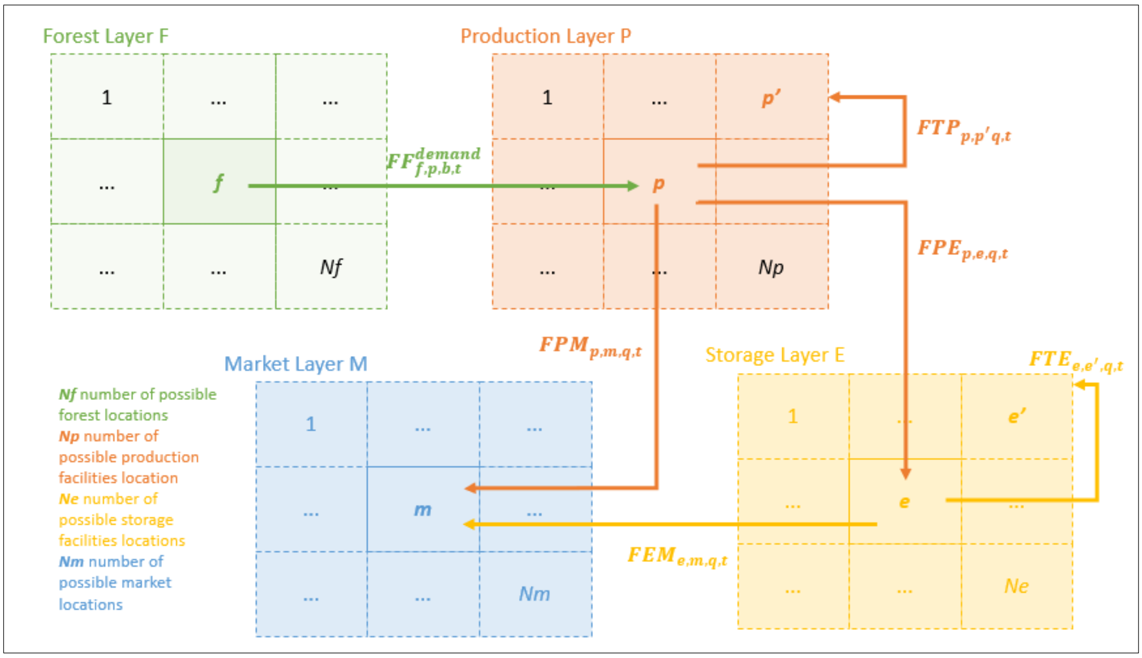

Figure 1 - The four layers of decision (Forest, Production, Storage, and Market) and its interconnections.
FFdemandf,p,b,t represents the amount of biomass b planted at a forest location f demanded by the production facility p at a period t; FTPp,p',q,t represents the amount of chemical species q transferred from a production facility p to a production facility p' at a period t. FPEp,e,q,t represents the amount of a chemical species q transferred from the production facility p to a storage location e at a period t. FPMp,m,q,t represents the amount of chemical species q sold directly to the market location m from the production facility p at a period t. FTEe,e',q,t represents the amount of chemical species q transfer from a storage facility e to a storage facility e' at a period t. FEMe,m,q,t represents the amount of chemical species q sold to the market location m from the storage facility e at a period t.

The formulation of the model's equations is presented in sections 3.1 to 3.3. Sections 3.1 discuss the forest dynamics modeling connecting decisions on land management and on biomass plantation, harvesting and transportation. Section 3.2 is devoted to the technological and supply chain modeling in which decisions on production facilities location and capacities, technological pathway, material transference, and product supply chain are discussed. Finally, section 3.3 connects all decisions from the previous sections into an economic modeling forming the objective function of the optimization problem. In all modeling sections, variables are formatted as **bold** meanwhile parameters are displayed in regular formatting.

3.1 FOREST DYNAMICS

Forest dynamics modeling is comprised of a set of multi-period land balances (section 3.1.1) that relates the dynamics of land acquisition, harvesting and planting, the modeling of biomass growth and production (section 3.1.2), the consideration of uncertainties on biomass productivity (section 3.1.3), and the constraints on post-operating periods that allows the perpetuity of the operation beyond the accounting period (section 3.1.4).

3.1.1 Multi-Period Land Balances

The main element for modeling forest dynamics is the land balance. Lands are classified as “planted” (land with a biomass *b* planted on) or “free” (no planted biomass), and as “owned” (lands self-possessed) or “thirds” (lands on third parties’ possession). The initial values for the available area for thirds and owned planted lands are represented, respectively, by the parameters $A_{f,b,i,initial}^{thirds}$ and $A_{f,b,i,initial}^{owned}$ for each forest unit *f* and each biomass *b* with age *i*. Thirds’ lands are available for buying at each period, but owned lands cannot be sold in any period.

The current quantity of available planted lands is updated at each period by forest operating decisions (land buying, harvesting, planting, and maintenance) and biomass growth dynamics. These updated quantities are represented by the variables $\boldsymbol{A_{f,b,i,t}^{thirds}}$ and $\boldsymbol{A_{f,b,i,t}^{owned}}$ for thirds and owned planted lands, respectively.

At each period *t* the decision of buying lands on a forest unit *f* planted with biomass *b* of age *i* ($\boldsymbol{A_{f,b,i,t}^{planted,bought}}$) is limited by the available thirds planted land at the previous period with age subtracted to one (eq. 1). The subtraction represents the aging of the biomass from the previous period to the next. For the first period, however, the equation is adapted using the initial land parameter with no age correction (eq. 2).

$$\boldsymbol{A_{f,b,i,t}^{planted,bought}} \leq \boldsymbol{A_{f,b,i-1,t-1}^{thirds}} \qquad \forall(f \in F, b \in B, i \neq \{0, imax\} \in I, t \neq 1 \in T) \quad \text{(eq. 1)}$$

$$\boldsymbol{A_{f,b,i,t=1}^{planted,bought}} \leq A_{f,b,i,initial}^{thirds} \qquad \forall(f \in F, b \in B, i \in I) \quad \text{(eq. 2)}$$

When biomass ages beyond the maximum age of *imax*, it will be considered the same as the *imax*-old biomass, as growth beyond the maximum allowed age is considered neglectable. Thus equation 1 is adapted into equation 3 for the maximum age.

$$\boldsymbol{A^{planted,bought}_{f,b,i=imax,t}} \leq \boldsymbol{A^{thirds}_{f,b,imax-1,t-1}} + \boldsymbol{A^{thirds}_{f,b,imax,t-1}} \qquad \forall(f \in F, b \in B, t \neq 1 \in T) \quad \text{(eq. 3)}$$

The 0-year-old biomass is the one that has been planted within the same period of consideration. Here it is assumed that third parties do not plant new biomass, i. e., any new plantation decision is done exclusively on the lands that are owned. Thus, for the age 0 equation 1 is adapted into equation 4.

$$\boldsymbol{A^{planted,bought}_{f,b,i=0,t}} = 0 \qquad \forall(f \in F, b \in B, t \in T) \qquad \text{(eq. 4)}$$

The assumption that third parties do not plant new biomass implies that the updated amount of land on third parties´ possession to be updated by the amount of land bought from them (eq. 5). This balance is adapted for the first period (eq. 6) and for the maximum allowed age *imax* (eq. 7).

$$\boldsymbol{A^{thirds}_{f,b,i,t}} = \boldsymbol{A^{thirds}_{f,b,i-1,t-1}} - \boldsymbol{A^{planted,bought}_{f,b,i,t}} \qquad \text{(eq. 5)}$$
$$\forall(f \in F, b \in B, i \neq \{0, imax\} \in I, t \neq 1 \in T)$$

$$\boldsymbol{A^{thirds}_{f,b,i,t=1}} = A^{thirds}_{f,b,i,initial} - \boldsymbol{A^{planted,bought}_{f,b,i,t=1}} \qquad \forall(f \in F, b \in B, i \in I) \qquad \text{(eq. 6)}$$

$$\boldsymbol{A^{thirds}_{f,b,i=imax,t}} = \boldsymbol{A^{thirds}_{f,b,imax,t-1}} + \boldsymbol{A^{thirds}_{f,b,imax-1,t-1}} - \boldsymbol{A^{planted,bought}_{f,b,imax,t}} \qquad \text{(eq. 7)}$$
$$\forall(f \in F, b \in B, t \neq 1 \in T)$$

Owned lands ($\boldsymbol{A^{owned}_{f,b,i,t}}$) are also updated at each period considering not only the bought and initially owned lands ($\boldsymbol{A^{planted,bought}_{f,b,i,t}}$ and $A^{owned}_{f,b,i,initial}$) but also the harvested lands ($\boldsymbol{A^{harvested}_{f,b,i,t}}$) in equations 8 and 9. The amount of owned land for a biomass b of age 0 is equal to the amount of land that was planted with the same biomass b at this period ($\boldsymbol{A^{newly\_planted}_{f,b,t}}$) as given by equation 10. For the maximum age, equation 11 is arranged analogously to equation 7.

$$\boldsymbol{A^{owned}_{f,b,i,t}} = \boldsymbol{A^{owned}_{f,b,i-1,t-1}} - \boldsymbol{A^{harvested}_{f,b,i,t}} + \boldsymbol{A^{planted,bought}_{f,b,i,t}} \quad \forall(f \in F, b \in B, i \neq \{0, imax\} \in I, t \neq 1 \in T) \qquad \text{(eq. 8)}$$

$$\boldsymbol{A^{owned}_{f,b,i,t=1}} = A^{owned}_{f,b,i,initial} - \boldsymbol{A^{harvested}_{f,b,i,t=1}} + \boldsymbol{A^{planted,bought}_{f,b,i,t=1}} \quad \forall(f \in F, b \in B, i \neq 0 \in I) \qquad \text{(eq. 9)}$$

$$\boldsymbol{A^{owned}_{f,b,i=0,t}} = \boldsymbol{A^{newly\_planted}_{f,b,t}} \qquad \forall(f \in F, b \in B, t \in T) \qquad \text{(eq. 10)}$$

$$\boldsymbol{A^{owned}_{f,b,i=imax,t}} = \boldsymbol{A^{owned}_{f,b,imax,t-1}} + \boldsymbol{A^{owned}_{f,b,imax-1,t-1}} - \boldsymbol{A^{harvested}_{f,b,imax,t}} + \boldsymbol{A^{planted,bought}_{f,b,imax,t}} \qquad \forall(f \in F, b \in B, t \neq 1 \in T) \qquad \text{(eq. 11)}$$

Free lands ($\boldsymbol{A^{free,owned}_{f,t}}$) are subject to similar balances considering harvesting and plantation as well as the initially owned free lands ($A^{free,owned}_{f,initial}$). For these balances, it should be considered that all planted land, once harvested, is converted to free land in the same period (equations 12 and 13). The bought free land ($\boldsymbol{A^{free,bought}_{f,t=1}}$) is limited to the area of free lands available on third parties' possession ($\boldsymbol{A^{free,thirds}_{f,t-1}}$ and $A^{free,thirds}_{f,initial}$) in equations 14 and 15. These lands are subject to update at each period accordingly to equations 16 and 17.

$$\boldsymbol{A^{free,owned}_{f,t}} = \boldsymbol{A^{free,owned}_{f,t-1}} + \boldsymbol{A^{free,bought}_{f,t}} + \sum_{b \in B} \sum_{i \in I} \boldsymbol{A^{harvested}_{f,b,i,t}} - \sum_{b \in B} \boldsymbol{A^{newly\_planted}_{f,b,t}} \qquad \forall(f \in F, t \neq 1 \in T) \qquad \text{(eq. 12)}$$

$$\boldsymbol{A^{free,owned}_{f,t=1}} = A^{free,owned}_{f,initial} + \boldsymbol{A^{free,bought}_{f,t=1}} + \sum_{b \in B} \sum_{i \in I} \boldsymbol{A^{harvested}_{f,b,i,t=1}} - \sum_{b \in B} \boldsymbol{A^{newly\_planted}_{f,b,t=1}} \qquad \forall(f \in F) \qquad \text{(eq. 13)}$$

$$\boldsymbol{A^{free,bought}_{f,t}} \leq \boldsymbol{A^{free,thirds}_{f,t-1}} \qquad \forall(f \in F, t \neq 1 \in T) \qquad \text{(eq. 14)}$$

$$\boldsymbol{A_{f,t=0}^{free,bought}} \leq A_{f,initial}^{free,thirds} \qquad \forall (f \in F) \qquad \text{(eq. 15)}$$

$$\boldsymbol{A_{f,t}^{free,thirds}} = \boldsymbol{A_{f,t-1}^{free,thirds}} - \boldsymbol{A_{f,t}^{free,bought}} \qquad \forall (f \in F, t \neq 1 \in T) \qquad \text{(eq. 16)}$$

$$\boldsymbol{A_{f,t=1}^{free,thirds}} = A_{f,initial}^{free,thirds} - \boldsymbol{A_{f,t=1}^{free,bought}} \qquad \forall (f \in F) \qquad \text{(eq. 17)}$$

3.1.2 Biomass Production

The harvested area is then translated into produced biomass accordingly to the amount of biomass that has grown in this area. This growth is given by the accumulated growth parameter ($Growth_{f,b,i,t}^{accumulated}$) which is used in equation 18 together with the harvesting efficiency of each biomass *b* ($\eta_b^{harvest}$). This converts the amount of harvested area into the amount of produced biomass ($\boldsymbol{FF_{f,b,t}^{harvested}}$) at each forest location *f* planted with biomass *b* with age *i* at the period of harvest *t*.

$$\boldsymbol{FF_{f,b,t}^{harvested}} = \eta_b^{harvest} \sum_{\boldsymbol{i} \in \boldsymbol{I}} Growth_{f,b,i,t}^{accumulated} \boldsymbol{A_{f,b,i,t}^{harvested}} \qquad \text{(eq. 18)}$$
$$\forall (f \in F, b \in B, t \in T)$$

The accumulated growth parameter for a given biomass *b* with age *i* on a forest location *f* at a period *t* may be written as the accumulated growth of the same biomass on the same forest on the last period (*t-1* and with age *i-1*) plus a mass increment on the current period ($Growth_{f,b,i,t}^{incremented}$) as stated by equation 19.

$$Growth_{f,b,i,t}^{accumulated} = Growth_{f,b,i-1,t-1}^{accumulated} + Growth_{f,b,i,t}^{increment} \qquad \text{(eq. 19)}$$

Equation 19 may be recursively summed on previous periods yielding equation 20, which states the accumulated growth at a given period as a sum of all previous growth increments. Negative indexes for the time dimension are allowed in equation 20. This condition represents the growth increment observed in past (pre-operation) periods.

$$Growth_{f,b,i,t}^{accumulated} = \sum_{n=0}^{i-1} Growth_{f,b,i-n,t-n}^{increment} \ \forall(f \in F, b \in B, i \in I, t \in T) \qquad \text{(eq. 20)}$$

Applying equation 20 into equation 18 yields equation 21, which relates the harvested area and produced biomass through the series of growth increments along the period of the plantation.

$$\boldsymbol{FF_{f,b,t}^{harvested}} = \eta_b^{harvest} \sum_{\boldsymbol{i \in I}} \sum_{n=0}^{i-1} Growth_{f,b,i-n,t-n}^{increment} \, \boldsymbol{A_{f,b,i,t}^{harvested}} \qquad \text{(eq. 21)}$$

3.1.3 Uncertainties On Biomass Production

The growth increments used for describing biomass production in section 3.1.2 depend upon precipitation, sun incidence, plagues attacks, and many other uncontrolled environmental factors. For handling the uncertain nature of these parameters, the procedure from Bertsimas an Sim (2004) is employed in this section.

The uncertainties on growth increment are represented by a random variable $\xi_{f,b,t}^{growth}$. Equation 22 defines the actual growth increment as a composition of a nominal (expected) growth ($\overline{Growth_{f,b,\iota}^{increment}}$) and a random fluctuation term, given by the product of the random variable $\xi_{f,b,t}^{growth}$ and a parameter representing the possible deviations from the nominal growth value ($\widetilde{Growth_{f,b,\iota}^{increment}}$).

$$Growth_{f,b,i,t}^{increment} = \overline{Growth_{f,b,\iota}^{increment}} + \xi_{f,b,t}^{growth} \widetilde{Growth_{f,b,\iota}^{increment}} \qquad \text{(eq. 22)}$$
$$\forall(f \in F, b \in B, i \in I, t \in T)$$

The random variable represents uncertainties arising from a series of phenomena whose probabilities are hard to estimate and that might not hold for future outcomes, such as precipitation, plagues, and other environmental factors. As discussed in section 2.2, a robust optimization framework is preferred for such a situation. In this type of method, a deterministic data set is defined within the uncertain space, and the best solution which is feasible for any realization of the data uncertainty in the given set is computed through the solution of the robust counterpart optimization problem (LI; FLOUDAS, 2012).

Thus, it is important to define the space of all possible realization of these uncertainties, i.e., to define the sets containing all possible realizations for the random variable $\xi_{f,b,t}^{growth}$. The first definition is that the random variable is constrained within an interval set given by a constant $\psi_{f,b,t}^{growth}$ as in equation 23.

$$\left|\xi_{f,b,t}^{growth}\right| \leq \psi_{f,b,t}^{growth}\ \forall(f \in F, b \in B, t \in T) \qquad \text{(eq. 23)}$$

However, the interval-set representation for the random variable is a very conservative approach. It supposes that all uncertainty parameters assume their worst value at the same time which may be a rare event in several real applications. A less conservative approach was proposed by Bertsimas and Sim (2004) considering that the random variable is comprised not only within an interval-set but also within a polyhedron that relates several random variables with each other (Figure 2). Thus, the simultaneous occurrence of the worst value for all random variables within the same set is limited by the size of the polyhedron. The polyhedral set for incremental growth random variable is given by equation 24 as a function of a constant $\Gamma_{f,b}^{growth}$.

$$\sum_{\boldsymbol{i} \in \boldsymbol{I}} \left|\xi_{f,b,t-i}^{growth}\right| \leq \Gamma_{f,b}^{growth}\ \forall(f \in b, b \in B) \qquad \text{(eq. 24)}$$

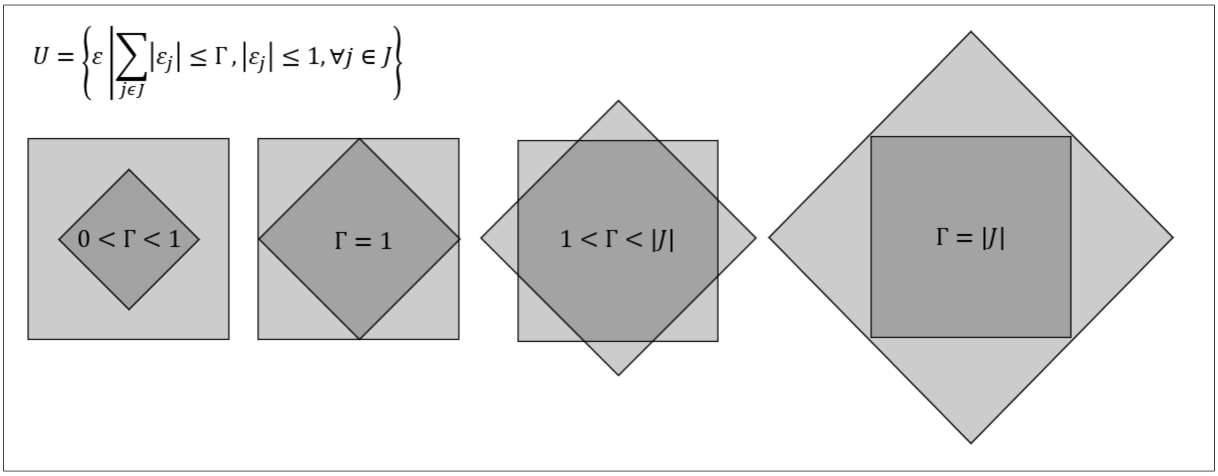

Figure 2 – Geometrical representation of the uncertainty set U for different values of the polyhedral constant Γ.
The resulting set is given by the intersection between the polyhedral and the box and is visually represented by the darker grey color. The lower the constant Γ the lower the possibility space for the random variable which yield a less conservative uncertainty representation. Source: adapted from Li and Floudas (2012)

For deriving the robust counterpart for this uncertainty set, equation 21 is reformulated as an inequality (eq. 25). This reformulation does not alter the optimal solution of the problem as harvesting lands beyond the minimum for satisfying the demands imposed to $\boldsymbol{FF_{f,b,t}^{harvested}}$ would imply in unnecessary extra-costs, reducing the objective function.

$$\boldsymbol{FF_{f,b,t}^{harvested}} - \eta_b^{harvest} \sum_{\boldsymbol{i} \in \boldsymbol{I}} \sum_{n=0}^{i-1} Growth_{f,b,i-n,t-n}^{increment} \boldsymbol{A_{f,b,i,t}^{harvested}} \leq 0 \qquad \text{(eq. 25)}$$
$$\forall (f \in F, b \in B, t \in T)$$

The robust counterpart for equation 25 is then given by equations 26 to 29 with the introduction of three auxiliary variables[5] ($\boldsymbol{U_{f,b,i,n,t}^{harvest}}$, $\boldsymbol{W_{f,b,i,n,t}^{harvest}}$, and $\boldsymbol{Z_{f,b,i,t}^{harvest}}$) accordingly to the procedure described by Li and Floudas (2012).

[5] These variables are used as mathematical artifacts for ensuring the main variables behave accordingly to the uncertainty sets formulation. No physical interpretation of them is necessary.

$$\boldsymbol{FF_{f,b,t}^{harvested}} - \eta_b^{harvest} \sum_{\boldsymbol{i} \in \boldsymbol{I}} \left(\sum_{n=0}^{i-1} \overline{Growth_{f,b,\iota-n}^{increment}}\, \boldsymbol{A_{f,b,i,t}^{harvested}} - \psi_{f,b,t}^{growth} \sum_{\boldsymbol{n=0}}^{\boldsymbol{i-1}} \boldsymbol{W_{f,b,i,n,t}^{harvest}} - \Gamma_{f,b}^{growth} \boldsymbol{Z_{f,b,i,t}^{harvest}} \right) \leq 0 \quad \text{(eq. 26)}$$

$$\forall (f \in F, b \in B, t \in T)$$

$$\boldsymbol{W_{f,b,i,n,t}^{harvest}} + \boldsymbol{Z_{f,b,i,t}^{harvest}} \geq \boldsymbol{U_{f,b,\mathrm{i},\mathrm{n},t}^{harvest}} \widetilde{Growth_{f,b,n}^{increment}} \quad \text{(eq. 27)}$$

$$\forall (f \in F, b \in B, i \in I, n \in \{I\ , n < i\}, t \in T)$$

$$\boldsymbol{A_{f,b,i,t}^{harvested}} \leq \boldsymbol{U_{f,b,\mathrm{i},\mathrm{n},t}^{harvest}} \quad \forall (f \in F, b \in B, \in I, n \in \{I\ , n < i\}, t \in T) \quad \text{(eq. 28)}$$

$$-\boldsymbol{U_{f,b,\mathrm{i},\mathrm{n},t}^{harvest}} \leq \boldsymbol{A_{f,b,i,t}^{harvested}} \quad \forall (f \in F, b \in B, \in I, n \in \{I\ , n < i\}, t \in T) \quad \text{(eq. 29)}$$

The uncertainties on biomass growth will affect the amount of harvested biomass that should still satisfy demand biomass ($\boldsymbol{FF_{f,p,b,t}^{demand}}$) by all the production facilities (eq. 30).

$$\boldsymbol{FF_{f,b,t}^{harvested}} = \sum_{\boldsymbol{p} \in \boldsymbol{P}} \boldsymbol{FF_{f,p,b,t}^{demand}} \quad \forall (f \in F, b \in B, t \in T) \quad \text{(eq. 30)}$$

The first periods on the time horizon (from 1 to $t_{construction}$) are dedicated to infrastructure building and thus are not operational. During this period, the biomass demand is imposed to be null (eq. 31).

$$\boldsymbol{FF_{f,p,b,t}^{demand}} = 0 \qquad \forall (f \in F, p \in P, b \in B, t \in \{1, t_{construction}\}) \quad \text{(eq. 31)}$$

3.1.4 Land Balance On Perpetuity

The model optimizes the decisions within the operational periods of set T. However, the biorefinery operation is supposed to be run indefinitely. Since only the revenues within the set T are accounted in the NPV calculation (section 3.3.4), the optimal solution will probably include only enough planted lands for supplying biomass to the operational periods. This implies that the optimal solution will not allow a stable operation for the periods subsequently to the operational period T, i.e., the biorefinery is not built to be run indefinitely.

For avoiding this situation, a land balance on perpetuity (post operation periods) is proposed. The perpetuity set ($T^{perpetuity}$) is an artificial set of periods defined from t_{last} + 1 (the next to the last operational period) to $2\ t_{last}$ + 1. The decisions variables taken for this period are not used for estimating the cash flows on perpetuity[6], they are only introduced for imposing that operating decision on accounting periods (set T) are taken in a way that enables the operation' sustain through perpetuity.

On perpetuity, land balances equations are adapted considering that no more land can be bought, i.e., all the harvested biomass must come from land that were acquired during the accounting period (equations 32 to 35).

$$\boldsymbol{A}_{\boldsymbol{f},\boldsymbol{t}'}^{\boldsymbol{free,owned}} = \boldsymbol{A}_{\boldsymbol{f},\boldsymbol{t}'-\boldsymbol{1}}^{\boldsymbol{free,owned}} + \sum_{b \in B} \sum_{i \in I} \boldsymbol{A}_{\boldsymbol{f},\boldsymbol{b},\boldsymbol{i},\boldsymbol{t}'}^{\boldsymbol{harvested}} - \sum_{b \in B} \boldsymbol{A}_{\boldsymbol{f},\boldsymbol{b},\boldsymbol{t}'}^{\boldsymbol{planted}} \quad \forall (f \in F, t' \in T^{perpetuity}) \qquad \text{(eq. 32)}$$

$$\boldsymbol{A}_{\boldsymbol{f},\boldsymbol{b},\boldsymbol{i},\boldsymbol{t}'}^{\boldsymbol{owned}} = \boldsymbol{A}_{\boldsymbol{f},\boldsymbol{b},\boldsymbol{i}-\boldsymbol{1},\boldsymbol{t}'-\boldsymbol{1}}^{\boldsymbol{owned}} - \boldsymbol{A}_{\boldsymbol{f},\boldsymbol{b},\boldsymbol{i},\boldsymbol{t}'}^{\boldsymbol{harvested}} \quad \forall (f \in F, b \in B, i \neq \{0, imax\} \in I, \quad t' \in T^{perpetuity}) \qquad \text{(eq. 33)}$$

$$\boldsymbol{A}_{\boldsymbol{f},\boldsymbol{b},\boldsymbol{i}=\boldsymbol{0},\boldsymbol{t}'}^{\boldsymbol{owned}} = \boldsymbol{A}_{\boldsymbol{f},\boldsymbol{b},\boldsymbol{t}'}^{\boldsymbol{newly\_planted}} \quad \forall (f \in F, b \in B, t' \in T^{perpetuity}) \qquad \text{(eq. 34)}$$

$$\boldsymbol{A}_{\boldsymbol{f},\boldsymbol{b},\boldsymbol{i}=\boldsymbol{imax},\boldsymbol{t}'}^{\boldsymbol{owned}} = \boldsymbol{A}_{\boldsymbol{f},\boldsymbol{b},\boldsymbol{imax},\boldsymbol{t}'-\boldsymbol{1}}^{\boldsymbol{owned}} + \boldsymbol{A}_{\boldsymbol{f},\boldsymbol{b},\boldsymbol{imax}-\boldsymbol{1},\boldsymbol{t}'-\boldsymbol{1}}^{\boldsymbol{owned}} - \boldsymbol{A}_{\boldsymbol{f},\boldsymbol{b},\boldsymbol{imax},\boldsymbol{t}'}^{\boldsymbol{harvested}} \quad \forall (f \in F, b \in B, t' \in T^{perpetuity}) \qquad \text{(eq. 35)}$$

While equations 32 to 35 impose that no more lands can be bought - i.e. that the land balances should be sustained only with the lands already bought on the

[6] The perpetuity cash flow generation estimation is discussed in Section 3.3.4 using only the decisions from the operation set T.

accounting period - equation 36 imposes that the amount of harvested land for each biomass and each age should be at least as large as the mean harvested land for each biomass and each age during the accounting period. This set of constraints allows land balances to be built in a way that all periods in the perpetuity present enough biomass for sustaining a consistent operational level.

$$\boldsymbol{A}_{\boldsymbol{f},\boldsymbol{b},\boldsymbol{i},\boldsymbol{t}'}^{\boldsymbol{harvested}} \geq \frac{\sum_{t \in T} \boldsymbol{A}_{\boldsymbol{f},\boldsymbol{b},\boldsymbol{i},\boldsymbol{t}'}^{\boldsymbol{harvested}}}{t_{last}+1} \quad \forall (f \in F, b \in B, i \in I, t' \in T^{perpetuity}) \qquad \text{(eq. 36)}$$

3.2 PRODUCTION DYNAMICS

The production dynamics modeling is comprised by the conversion process description and production mass balances (section 3.2.1), the consumption and production of utilities and wastes (section 3.2.2), and the logistics network connecting production, storages and market units (section 3.2.3).

3.2.1 Conversion Processes

The biomass demand from forest to production facility is transformed into pseudo-component flows ($\boldsymbol{FFP}_{\boldsymbol{p},\boldsymbol{q},\boldsymbol{t}}$) accordingly to a composition parameter ($x_{f,b,q}$) on equation 37.

$$\boldsymbol{FFP}_{\boldsymbol{p},\boldsymbol{q},\boldsymbol{t}} = \sum_{f \in F} \sum_{b \in B} x_{f,b,q} \boldsymbol{FF}_{\boldsymbol{f},\boldsymbol{p},\boldsymbol{b},\boldsymbol{t}}^{\boldsymbol{demand}} \quad \forall (p \in P, q \in Q, t \in T) \qquad \text{(eq. 37)}$$

In this formulation, a pseudo-component is the mathematical representation of process raw-materials or products, such as wood, chemical pulp, and precipitated lignin. Each pseudo-component is associated with an extensive measurement unit, such as kilogram or cubic meters. Caution should be taken for ensuring consistency across measurement units among the pseudo-components and their conversion factors (described further in this section).

Each pseudo-component *q* at each production facility *p* is subject to a mass balance (equations 38 and 39). The inputs of pseudo-component *q* in the production facility *p* are given by the amount of the pseudo-component *q* stored in the same facility *p* on the previous period *t-1* ($\boldsymbol{mp_{p,q,t-1}}$ or $mp_{p,q,initial}$), the amount of the pseudo-component *q* received in a material transference from other production facilities *p'* in the same period *t* ($\boldsymbol{FTP_{p',p,q,t}}$), and by the amount of the pseudo-component *q* produced by the same production facility *p* by each technology *z* in the same period *t* ($\boldsymbol{FPZ_{p,z,q,t}}$). The outputs are given by the amount of pseudo-component *q* transferred to other production facilities *p´* in the period *t* ($\boldsymbol{FTP_{p,p',q,t}}$), the amount of pseudo-component *q* transferred to the storage facilities *e* in the same period *t* ($\boldsymbol{FPE_{p,e,q,t}}$), the amount of pseudo-component *q* sold at a consumer market *m* at the same period *t* ($\boldsymbol{FPM_{p,m,q,t}}$), the amount of pseudo-component *q* fed to each conversion technology *z* within the same production facility *p* at the same period *t* ($\boldsymbol{FZ_{p,z,q,t}}$), and the amount of pseudo-component *q* stored in the same production facility *p* in the same period *t* for use in the next period ($\boldsymbol{mp_{p,q,t}}$).

$$\begin{aligned}\boldsymbol{FFP_{p,q,t}} + \boldsymbol{mp_{p,q,t-1}} + \sum_{\boldsymbol{p'\in P}} \boldsymbol{FTP_{p',p,q,t}} + \sum_{\boldsymbol{z\in Z}} \boldsymbol{FPZ_{p,z,q,t}} \\ = \sum_{\boldsymbol{z\in Z}} \boldsymbol{FZ_{p,z,q,t}} + \sum_{\boldsymbol{p'\in P}} \boldsymbol{FTP_{p,p',q,t}} + \sum_{\boldsymbol{e\in E}} \boldsymbol{FPE_{p,e,q,t}} \\ + \sum_{\boldsymbol{m\in M}} \boldsymbol{FPM_{p,m,q,t}} + \boldsymbol{mp_{p,q,t}} \qquad \forall(p \in P, q \in Q, t \neq 1 \in T)\end{aligned} \quad \text{(eq. 38)}$$

$$\begin{aligned}\boldsymbol{FFP_{p,q,t=1}} + mp_{p,q,initial} + \sum_{\boldsymbol{p'\in P}} \boldsymbol{FTP_{p',p,q,t=1}} + \sum_{\boldsymbol{z\in Z}} \boldsymbol{FPZ_{p,z,q,t=1}} \\ = \sum_{\boldsymbol{z\in Z}} \boldsymbol{FZ_{p,z,q,t=1}} + \sum_{\boldsymbol{m\in M}} \boldsymbol{FPM_{p,m,q,t=1}} + \sum_{\boldsymbol{e\in E}} \boldsymbol{FPE_{p,e,q,t=1}} \\ + \sum_{\boldsymbol{p'\in P}} \boldsymbol{FTP_{p,p',q,t=1}} + \boldsymbol{mp_{p,q,t=1}} \qquad \forall(p \in P, q \in Q)\end{aligned} \quad \text{(eq. 39)}$$

The transference between the same production unit ($p = p'$) is imposed to be null (eq. 40).

$$\boldsymbol{FTP_{p,p,q,t}} = 0 \qquad \forall(p \in P, q \in Q, t \in T) \qquad \text{(eq. 40)}$$

The chemical species storage and transfer should be null if the production facility *p* is not built (equations 41 and 42). The decision of building or not a production facility on location *p* is represented by the binary variable $\boldsymbol{yp_p}$ that takes 1 if it is decided to build the facility and 0 otherwise. A big-M[7] is defined for each of the equations ($M^{arm,p,q}$ and $M^{transf,p,q}$). It should be sufficiently large for not restricting the upper bounds of the continuous variable if the binary is *true*.

$$\boldsymbol{mp_{p,q,t}} \leq M^{arm,p,q}\boldsymbol{yp_p} \qquad \forall(p \in P, q \in Q, t \in T) \qquad \text{(eq. 41)}$$

$$\boldsymbol{FTP_{p,p',q,t}} \leq M^{transf,p,q}\boldsymbol{yp_{p'}} \qquad \forall(p, p' \in P, q \in Q, t \in T) \qquad \text{(eq. 42)}$$

The pseudo-component *q* can only be fed to a conversion technology *z* if this technology is built within production facility *p*. The decision of building the technology *z* within a production facility *p* is given by the binary variable $\boldsymbol{ypz_{p,z}}$. A big-M parameter ($M^{tec,z,q}$) is also used for this relation (eq. 43).

$$\boldsymbol{FZ_{p,z,q,t}} \leq M^{tec,z,q}\boldsymbol{ypz_{p,z}} \qquad \forall(p \in P, z \in Z, q \in Q, t \in T) \qquad \text{(eq. 43)}$$

Any pseudo-component can only be fed to technologies that can convert it. The representation of the ability of a technology *z* to convert a pseudo-component *q* is given by the sum of the conversion factors of *q* into other pseudo-components ($conv\_q_{z,q,qprod}$) or into a utility *uprod* ($conv\_u_{z,q,uprod}$). In this model, the possibility of converting a pseudo-component *q* into a utility *u* is considered. One example is the burn of black liquor that generates steam. If this sum is null, then the technology is not able to convert the given pseudo-component and its fed quantity must also be null. Equation 44 imposes this relation through a big-M-like parameter ($M^{conversion,z,q}$).

[7] The Big-M is a formulation strategy for representing if-then relations in mathematical programming. An overview on the topic is available in Raman and Grossmann (1994).

$$\boldsymbol{FZ_{p,z,q,t}} \leq M^{conversion,z,q} \left(\sum_{q_{prod}} conv_{q_{z,q,qprod}} + \sum_{u_{prod}} conv_{u_{z,q,uprod}} \right) \quad \forall (p \in P, z \in Z, q \in Q, t \in T) \qquad \text{(eq. 44)}$$

The amount of a pseudo-component *qprod* produced by a technology *z* is given by the sum of the products between the amount of other pseudo-components *q* fed to technology and the conversion factor from these pseudo-components *q* to *qprod* (eq. 45).

$$\boldsymbol{FPZ_{p,z,qprod,t}} = \sum_{\boldsymbol{q \in Q}} \boldsymbol{FZ_{p,z,q,t}}\, conv_{q_{z,q,qprod}} \quad \forall (p \in P, z \in Z, qprod \in Q, t \in T) \qquad \text{(eq. 45)}$$

The total amount of a pseudo-component *q* produced at a facility *p* is given by the sum of the productions by each technology within facility *p* (eq. 46).

$$\boldsymbol{FP_{p,qprod,t}} = \sum_{\boldsymbol{z \in Z}} \boldsymbol{FPZ_{p,z,qprod,t}} \qquad \forall (p \in P, qprod \in Q, t \in T) \qquad \text{(eq. 46)}$$

3.2.2 Utilities And Wastes Modeling

Technologies may also produce residues and effluents ($\boldsymbol{FRZ_{p,z,r,t}}$), given by a conversion factor ($conv\_r_{z,q,r}$) analogous to the conversion of pseudo-components (eq. 47).

$$\boldsymbol{FRZ_{p,z,r,t}} = \sum_{\boldsymbol{q \in Q}} \boldsymbol{FZ_{p,z,q,t}}\, conv\_r_{z,q,r} \qquad \forall (p \in P, z \in Z, r \in R, t \in T) \qquad \text{(eq. 47)}$$

A technology *z* when processing the pseudo-component *q* may also demand an amount of utility. This demand per unit of processed pseudo-component *q* is described by the consumption factor $utl_{z,q,u}$. The total utilities needed by a particular technology *z* ($\boldsymbol{FU^{needed}_{p,z,u,t}}$) is given by the sum of the utility needs for each pseudo-component conversion and the demand of utilities that are used on conversion to other utilities ($\boldsymbol{FU^{interconversion}_{p,z,u,t}}$), such as steam fed to the turbine for electricity generation (eq. 48).

$$\boldsymbol{FU^{needed}_{p,z,u,t}} = \sum_{\boldsymbol{q \in Q}} utl_{z,q,u} \boldsymbol{FZ_{p,z,q,t}} + \boldsymbol{FU^{interconversion}_{p,z,u,t}} \quad \forall (p \in P, z \in Z, u \in U, t \in T) \qquad \text{(eq. 48)}$$

Utilities may also be produced. This production may arise from the conversion of a pseudo-component into a utility - such as the burn of black liquor producing steam - or the interconversion of another utility - such as the conversion of steam into electricity through a steam turbine – as described by equation 49. The yields for these conversions are defined by the parameters $conv\_u_{z,q,u_{prod}}$ and $conv\_intu_{z,u,u_{prod}}$, respectively, and may only occur if the technology *z* is implemented within production facility *p* (eq. 50). If technology *z* has only null conversion terms for a given utility, the feed flow must be null (eq. 51).

$$\boldsymbol{FU^{produced}_{p,z,u_{prod},t}} = \sum_{\boldsymbol{q \in Q}} \boldsymbol{FZ_{p,z,q,t}}\, conv_{u_{z,q,u_{prod}}} + \sum_{\boldsymbol{u \in U}} \boldsymbol{FU^{interconversion}_{p,z,u,t}}\, conv_{intu_{z,u,u_{prod}}} \quad \forall \left(p \in P, z \in Z, u_{prod} \in U, t \in T\right) \qquad \text{(eq. 49)}$$

$$\boldsymbol{FU^{interconversion}_{p,z,u,t}} \leq M^{tec,z,u} \boldsymbol{ypz_{p,z}} \quad \forall (p \in P, z \in Z, u \in U, t \in T) \qquad \text{(eq. 50)}$$

$$\boldsymbol{FU^{interconversion}_{p,z,u,t}} \leq M^{tec,z,u} \sum_{u_{prod}} conv_{intu_{z,u,uprod}} \quad \forall (p \in P, z \in Z, u \in U, t \in T) \qquad \text{(eq. 51)}$$

A utility balance within each production facility *p* is given by equation 52 in which the difference of needed and produced utilities must be equal to the difference between bought ($\boldsymbol{FU_{p,u,t}^{bought}}$) and sold ($\boldsymbol{FU_{p,u,t}^{sold}}$) utilities. The buying and selling of utilities may only occur within the same production unit and must not surpass market supply and demands (equations 53 and 54).

$$\boldsymbol{FU_{p,u,t}^{bought}} - \boldsymbol{FU_{p,u,t}^{sold}} = \sum_{\boldsymbol{z \in Z}} \boldsymbol{FU_{p,z,u,t}^{needed}} - \sum_{\boldsymbol{z \in Z}} \boldsymbol{FU_{p,z,u,t}^{produced}} \quad \forall(p \in P, u \in U, t \in T) \qquad \text{(eq. 52)}$$

$$\boldsymbol{FU_{p,u,t}^{bought}} \leq M^{supply,p,u} \quad \forall(p \in P, u \in U, t \in T) \qquad \text{(eq. 53)}$$

$$\boldsymbol{FU_{p,u,t}^{sold}} \leq M^{demand,p,u} \quad \forall(p \in P, u \in U, t \in T) \qquad \text{(eq. 54)}$$

3.2.3 Logistics And Consumer Markets

Analogous to equation 38, a mass balance is imposed on each storage facility (eq. 55) considering at each period *t* the amount of pseudo-component *q* kept under storage ($\boldsymbol{me_{e,q,t}}$), the transference between storage facilities ($\sum_{\boldsymbol{e' \in E}} \boldsymbol{FTE_{e',e,q,t}} - \sum_{\boldsymbol{e' \in E}} \boldsymbol{FTE_{e,e',q,t}}$), the amount received by production facilities ($\sum_{\boldsymbol{p \in P}} \boldsymbol{FPE_{p,e,q,t}}$), the amount sold to markets ($\sum_{\boldsymbol{m \in M}} \boldsymbol{FEM_{e,m,q,t}}$), and the stored amount of the pseudo-component in the previous period ($\boldsymbol{me_{e,q,t-1}}$).

$$\boldsymbol{me_{e,q,t}} = \sum_{\boldsymbol{e' \in E}} \boldsymbol{FTE_{e',e,q,t}} - \sum_{\boldsymbol{e' \in E}} \boldsymbol{FTE_{e,e',q,t}} + \sum_{\boldsymbol{p \in P}} \boldsymbol{FPE_{p,e,q,t}} - \sum_{\boldsymbol{m \in M}} \boldsymbol{FEM_{e,m,q,t}} + \boldsymbol{me_{e,q,t-1}} \quad \forall(e \in E, q \in Q, t \neq 1 \in T) \qquad \text{(eq. 55)}$$

The transference flows are conditioned to the decision of building the receiving storage facility ($\boldsymbol{ye_e}$) in equations 56 and 57. Transference between the same storage unit *e* is imposed to be null (eq. 58).

$$\boldsymbol{FPE_{p,e,q,t}} \leq M^{transf,e,q} \boldsymbol{ye_e} \qquad \forall (p \in P, m \in M, q \in Q, t \in T) \qquad \text{(eq. 56)}$$

$$\boldsymbol{FTE_{e,e',q,t}} \leq M^{transf,e,q} \boldsymbol{ye_{e'}} \qquad \forall (e, e' \in E, q \in Qt \in T) \qquad \text{(eq. 57)}$$

$$\boldsymbol{FTE_{e,e,q,t}} = 0 \qquad \forall (e \in E, q \in Q, t \in T) \qquad \text{(eq. 58)}$$

For the first period, equation 55 is adjusted considering the initially available inventory ($me_{e,q,initial}$) in equation 59.

$$\boldsymbol{me_{e,q,t=1}} = \sum_{p \in P} \boldsymbol{FPE_{p,e,q,t=1}} - \sum_{m \in M} \boldsymbol{FEM_{e,m,q,t=1}} + \sum_{e' \in E} \boldsymbol{FTE_{e',e,q,t=1}} - \sum_{e' \in E} \boldsymbol{FTE_{e,e',q,t=1}} + me_{e,q,initial} \ \forall (e \in E, q \in Q) \qquad \text{(eq. 59)}$$

A minimum storage policy may also be implemented setting the parameter m_q^{min}. This parameter represents the fraction of the total attended demand ($\sum_{m \in M} \boldsymbol{FM_{m,q,t}}$) that must be kept under storage at each period (eq. 60).

$$\sum_{p \in P} \boldsymbol{mp_{p,q,t}} + \sum_{e \in E} \boldsymbol{me_{e,q,t}} \geq m_q^{min} \sum_{m \in M} \boldsymbol{FM_{m,q,t}} \ \forall (q \in Q, t \in T) \qquad \text{(eq. 60)}$$

The amount of pseudo-components sold to consumer markets is given by equation 61 and is limited by the demand for each market location at each period ($Fdem_{m,q,t}$) in equation 62.

$$\boldsymbol{FM_{m,q,t}} = \sum_{p \in P} \boldsymbol{FPM_{m,q,t}} + \sum_{e \in E} \boldsymbol{FEM_{m,q,t}} \ \forall (m \in M, q \in Q, t \in T) \qquad \text{(eq. 61)}$$

$$\boldsymbol{FM_{m,q,t}} \leq Fdem_{m,q,t} \ \forall (m \in M, q \in Q, t \in T) \qquad \text{(eq. 62)}$$

3.3 FINANCIAL MODELING

The financial modeling is comprised of forest, storage and production investments (section 3.3.1), operating costs (section 3.3.2), revenues (section 3.3.3), and the consolidation of all those elements into the net present value used as the objective function of the optimization problem (section 3.3.4).

3.3.1 Investments

Forest investments are given by equation 63 accordingly to the amounts and prices of planted and free land bought at each forest unit and period ($i_{f,b,i,t}^{planted}$ and $i_{f,t}^{free}$). The total forest investment at each period is the sum of investments on all forest units at this period (eq. 64).

$$\boldsymbol{I_{f,t}^{forest}} = \sum_{\boldsymbol{b \epsilon B}} \sum_{\boldsymbol{i \epsilon I}} i_{f,b,i,t}^{planted} \boldsymbol{A_{f,b,i,t}^{planted,bought}} + i_{f,t}^{free} \boldsymbol{A_{f,t}^{free,bought}} \quad \forall (f \in F, t \in T) \qquad \text{(eq. 63)}$$

$$\boldsymbol{I_{t}^{forest,total}} = \sum_{\boldsymbol{f \in F}} \boldsymbol{I_{f,t}^{forest}} \qquad \forall t \in T \qquad \text{(eq. 64)}$$

The productive investments are dependent upon the installed production capacities, which are taken as the maximum flow over all periods for each chemical or utility technology, and production facility. The maximum function (equations 65 to 66) is written linearly according to the procedure described in Smith and Taskin (2007).

$$\boldsymbol{FZ_{p,z,q}^{max}} \geq \boldsymbol{FZ_{p,z,q,t}} \; \forall (p \in P, z \in Z, q \in Q, t \in T) \qquad \text{(eq. 65)}$$

$$\boldsymbol{FU_{p,z,u}^{interconversion,max}} \geq \boldsymbol{FU_{p,z,u,t}^{interconversion}} \; \forall (p \in P, z \in Z, u \in U, t \in T) \qquad \text{(eq. 66)}$$

Production investments are estimated from a known reference investment ($i_{z,q}^{prod\_q}$ or $i_{z,u}^{prod\_u}$) used for implemented a given reference production capacity for the technology *z* for processing a pseudo-component *q* ($FZ_{z,q}^{ref}$) or utility *u* ($FU_{z,u}^{ref}$). The actual production investment is estimated through an power function (eq. 67) for scaling the reference capacity to the actual production capacity. Typically, the scale exponent is taken as 0.6 for describing the gains of scale associated with production investments, as described in McKetta Jr (1993).

$$\boldsymbol{I_{p,z}^{production}} = \sum_{q \in Q} i_{z,q}^{prod\_q} \left(\frac{\boldsymbol{FZ_{p,z,q}^{max}}}{FZ_{z,q}^{ref}} \right)^{n^{prod\_q,z,q}} + \sum_{u \in U} i_{z,u}^{prod\_u} \left(\frac{\boldsymbol{FU_{p,z,u}^{interconversion,max}}}{FU_{z,q}^{ref}} \right)^{n^{prod\_u,z,u}} \quad \forall (p \in P, z \in Z) \qquad \text{(eq. 67)}$$

Non linearities imposes several limitations in the optimization procedure. Therefore, Equation 67 is then linearized accordingly to the procedure described in Bergamini et al. (2008). A vector is defined with some points in the capacity level domain ($FZ_{z,q}^{ref,vetor} = [FZ_{z,q}^{ref,1}, FZ_{z,q}^{ref,2}, \ldots, FZ_{z,q}^{ref,n\_lin\_prod+1}]$). At each of these points, the approximated piecewise-linear function will match the original power function. In between those points, the function is linearly interpolated using auxiliary segmentation variables ($\boldsymbol{\delta_{z,q,p,n}^{lin\_prod\_q}}$ ∊ Non-Negative Reals and $\boldsymbol{w_{z,q,p,n}^{lin\_prod\_q}}$ ∊ {0, 1}). A visual representation of the proposed approach is displayed in Figure 3.

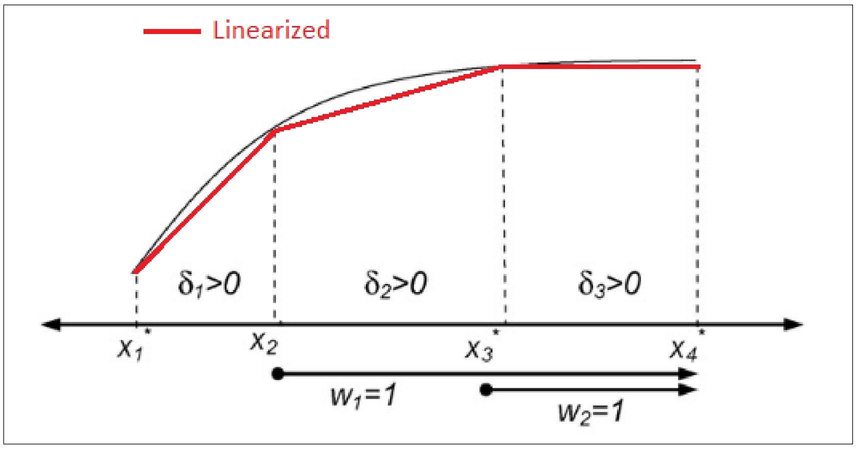

Figure 3 – Visual representation of the linearization procedure.
At each reference point xi the linearized and real curve have the same values. In between two reference points, the curve is approximated by a line. Source: Adapted from Bergamini et al. (2008).

The installed capacity ($\boldsymbol{FZ_{p,z,q}^{max}}$) is then given by equation 68 as function of the continuous delta variables.

$$\boldsymbol{FZ_{p,z,q}^{max}} = FZ_{z,q}^{ref,1} + \sum_{\boldsymbol{n=1}}^{\boldsymbol{n\_lin\_prod}} \boldsymbol{\delta_{p,z,q,n}^{lin\_prod\_q}} \qquad \forall(p \in P, z \in Z, q \in Q) \qquad \text{(eq. 68)}$$

The linearized production investment ($\boldsymbol{\tilde{I}_{p,z,q}^{prod,q}}$) is then given by equation 69.

$$\begin{aligned}&\boldsymbol{\tilde{I}_{p,z,q}^{prod,q}} \\ &= i_{z,q}^{prod\_q,q}\left(\frac{FZ_{z,q}^{ref,1}}{FZ_{z,q}^{ref}}\right)^{n^{prod\_q,,z,q}} \\ &+ \sum_{1}^{n\_lin\_prod} \frac{i_{z,q}^{prod_q,q}\left(\frac{FZ_{z,q}^{ref,n+1}}{FZ_{z,q}^{ref}}\right)^{n^{prod_q,z,q}} - i_{z,q}^{prod_q,q}\left(\frac{FZ_{z,q}^{ref,n}}{FZ_{z,q}^{ref}}\right)^{n^{prod_q,z,q}}}{FZ_{z,q}^{ref,n+1} - FZ_{z,q}^{ref,n}} \boldsymbol{\delta_{p,z,q,n}^{lin_{prod}}} \\ &\forall(p \in P, z \in Z, q \in \mathrm{Q})\end{aligned} \qquad \text{(eq. 69)}$$

The interpolation behavior of the auxiliary variables ($\boldsymbol{\delta_{z,q,p,n}^{lin\_prod\_q}}$ and $\boldsymbol{w_{z,q,p,n}^{lin\_prod\_q}}$) is ensured by the set of inequalities displayed in equation 70.

$$\begin{cases} \left(FZ_{z,q}^{ref,2} - FZ_{z,q}^{ref,1}\right)\boldsymbol{w_{p,z,q,1}^{lin_{prod_q}}} \le \boldsymbol{\delta_{p,z,q,1}^{lin_{prod_q}}} \le \left(FZ_{z,q}^{ref,2} - FZ_{z,q}^{ref,1}\right) \\ \vdots \\ \left(FZ_{z,q}^{ref,n+1} - FZ_{z,q}^{ref,n}\right)\boldsymbol{w_{p,z,q,n}^{lin_{prod_q}}} \le \boldsymbol{\delta_{p,z,q,n}^{lin_{prod_q}}} \le \left(FZ_{z,q}^{ref,n+1} - FZ_{z,q}^{ref,n}\right)\boldsymbol{w_{p,z,q,n-1}^{lin_{prod_q}}} \\ \vdots \\ \boldsymbol{\delta_{p,z,q,n_{lin_{prod}}}^{lin_{prod}}} \le \left(FZ_{z,q}^{ref,n_{lin_{prod}}+1} - FZ_{z,q}^{ref,n_{lin_{prod}}}\right)\boldsymbol{w_{p,z,q,n_{lin_{prod}}-1}^{lin_{prod_q}}} \\ \boldsymbol{w_{p,z,q,n}^{lin_{prod_q}}} \in \{0,1\}, n = 1,2 \dots \dots, n_{lin_{prod}} - 1 \end{cases} \qquad \text{(eq. 70)}$$

$$\forall(p \in P, z \in Z, q \in Q)$$

The utility interconversion modeling follows analogously. The installed capacity in a production unit *p* for converting a utility *u* by a technology *z* ($\boldsymbol{FU_{p,z,u}^{interconversion,max}}$) is given by equation 71 as a function of the continuous auxiliary variable $\boldsymbol{\delta_{p,z,u,n}^{lin\_prod\_u}}$. The interpolation behavior is imposed by equation 72 through the binary auxiliary variables $\boldsymbol{w_{p,z,u,n}^{lin_{prod\_u}}}$. The linearized investment ($\boldsymbol{\tilde{I}_{p,z,u}^{prod,u}}$) associated with the installed capacity is given by equation 73. Equation 74 imposes a null capacity if the technology is not able to convert the reference utility through a big-M-like parameter ($M^{conv,z,u}$) and equation 75 conditions the technology capacity installment to the production unit *p* construction.

$$\boldsymbol{FU_{p,z,u}^{interconversion,max}} = FU_{z,u}^{ref,1} + \sum_{\boldsymbol{n=1}}^{\boldsymbol{n_{lin_{prod}}}} \boldsymbol{\delta_{p,z,u,n}^{lin_{prod_u}}} \qquad \text{(eq. 71)}$$

$$\forall (p \in P, z \in Z, u \in U)$$

$$\begin{cases} \left(FU_{z,u}^{ref,2} - FU_{z,u}^{ref,1}\right)\boldsymbol{w_{p,z,u,2}^{lin_{prod_u}}} \leq \boldsymbol{\delta_{p,z,u,1}^{lin_{prod_u}}} \leq \left(FU_{z,u}^{ref,2} - FU_{z,u}^{ref,1}\right)\boldsymbol{w_{p,z,u,1}^{lin_{prod_u}}} \\ \vdots \\ \left(FU_{z,u}^{ref,n+1} - FU_{z,u}^{ref,n}\right)\boldsymbol{w_{p,z,u,n+1}^{lin_{prod_u}}} \leq \boldsymbol{\delta_{p,z,u,n}^{lin_{prod_u}}} \leq \left(FU_{z,u}^{ref,n+1} - FU_{z,u}^{ref,n}\right)\boldsymbol{w_{p,z,u,n}^{lin_{prod}}} \\ \vdots \\ \boldsymbol{\delta_{p,z,u,n_{lin_{prod}}}^{lin_{prod_u}}} \leq \left(FU_{z,u}^{ref,n_{lin_{prod}}+1} - FZ_{z,u}^{ref,n_{lin_{prod}}}\right)\boldsymbol{w_{p,z,u,n_{lin_{prod}}-1}^{lin_{prod_u}}} \\ \boldsymbol{w_{p,z,u,n}^{lin_{prod_u}}} \in \{0,1\}, n = 1,2 \ldots\ldots, n_{lin_{prod}} \end{cases} \qquad \text{(eq. 72)}$$

$$\forall (p \in P, z \in Z, u \in U)$$

$$\boldsymbol{\tilde{I}_{p,z,u}^{prod,u}} = i_{z,u}^{prod_u,u}\left(\frac{FU_{z,u}^{ref,1}}{FU_{z,u}^{ref}}\right)^{n^{prod_u,z,u}} + \sum_{1}^{n_{lin_{prod}}} \frac{i_{z,u}^{prod,u}\left(\frac{FU_{z,u}^{ref,n+1}}{FU_{z,u}^{ref}}\right)^{n^{prod_u,z,u}} - i_{z,u}^{prod_u,u}\left(\frac{FU_{z,u}^{ref,n}}{FU_{z,u}^{ref}}\right)^{n^{prod_u,z,u}}}{FU_{z,u}^{ref,n+1} - FU_{z,u}^{ref,n}} \boldsymbol{\delta_{p,z,u,n}^{lin_{prod_u}}} \qquad \text{(eq. 73)}$$

$$\forall (p \in P, z \in Z, u \in \mathrm{U}$$

$$\boldsymbol{w_{p,z,u,n}^{lin_{prod_u}}} \leq M^{conv,z,u} \sum_{u_{prod}} conv_{intu_{z,u,uprod}} \qquad \text{(eq. 74)}$$

$$\forall (p \in P, z \in Z, u \in \mathrm{U}, n \in N_{lin_{Prod}})$$

$$\boldsymbol{w_{p,z,u,n}^{lin\_prod\_u}} \leq \boldsymbol{ypz_{p,z}} \quad \forall (p \in P, z \in Z, u \in \mathrm{U}, n \in N_{lin_{Prod}}) \qquad \text{(eq. 75)}$$

The total investment on a technology *z* within production facility *p* ($\tilde{\boldsymbol{I}}_{\boldsymbol{p,z}}^{\boldsymbol{production}}$) is then given by the sum of the linearized investment for each chemical and utility (eq. 76) and the total productive investment ($\boldsymbol{I}^{\boldsymbol{production,total}}$) by the sum over all technologies and production facilities (eq. 77).

$$\tilde{\boldsymbol{I}}_{\boldsymbol{p,z}}^{\boldsymbol{production}} = \sum_{\boldsymbol{q}\in\boldsymbol{Q}} \tilde{\boldsymbol{I}}_{\boldsymbol{p,z,q}}^{\boldsymbol{prod\_q}} + \sum_{\boldsymbol{u}\in\boldsymbol{U}} \tilde{\boldsymbol{I}}_{\boldsymbol{p,z,u}}^{\boldsymbol{prod\_u}} \; \forall(p \in P, z \in Z) \qquad \text{(eq. 76)}$$

$$\boldsymbol{I}^{\boldsymbol{production,total}} = \sum_{\boldsymbol{p}\in\boldsymbol{P}} \sum_{\boldsymbol{z}\in\boldsymbol{Z}} \tilde{\boldsymbol{I}}_{\boldsymbol{p,z}}^{\boldsymbol{production}} \qquad \text{(eq. 77)}$$

Storage investments are modeled analogously to the production investments. The storage investment ($\boldsymbol{I}_{\boldsymbol{e}}^{\boldsymbol{storage,E}}$ for layer E or $\boldsymbol{I}_{\boldsymbol{p}}^{\boldsymbol{storage,P}}$ for layer P) is also considered as an exponential function of the installed storage capacity ($\boldsymbol{me}_{\boldsymbol{e,q}}^{\boldsymbol{max}}$ or $\boldsymbol{mp}_{\boldsymbol{p,q}}^{\boldsymbol{max}}$), a reference storage capacity (me_q^{ref} or mp_q^{ref}), and its respective reference investment ($i_q^{storage\_e}$ and $i_q^{storage\_p}$) as described by equations 78 and 83. The installed capacity is given as the linearized maximum of all stored volumes in all operational periods (equations 79 and 84) and is described as a function of the auxiliary continuous variables ($\boldsymbol{\delta}_{\boldsymbol{e,q,n}}^{\boldsymbol{lin\_arm\_e}}$ and $\boldsymbol{\delta}_{\boldsymbol{q,p,n}}^{\boldsymbol{lin\_arm\_p}}$) in equations 80 and 85. The interpolation behavior is imposed by equations 81 and 86 using the auxiliary binary variables ($\boldsymbol{w}_{\boldsymbol{e,q,n}}^{\boldsymbol{lin\_arm\_e}}$ and $\boldsymbol{w}_{\boldsymbol{p,q,n}}^{\boldsymbol{lin\_arm\_p}}$) and the segmentation capacities vector ($me_q^{ref,x}$ and $mp_q^{ref,x}$). The linearized investment ($\tilde{\boldsymbol{I}}_{\boldsymbol{e,q}}^{\boldsymbol{storage.E}}$ or $\tilde{\boldsymbol{I}}_{\boldsymbol{p,q}}^{\boldsymbol{storage.P}}$) is given by equations 82 and 87.

$$\boldsymbol{I}_{\boldsymbol{e}}^{\boldsymbol{storage,E}} = \sum_{\boldsymbol{q}\in\boldsymbol{Q}} i_q^{storage\_e} \left(\frac{\boldsymbol{me}_{\boldsymbol{e,q}}^{\boldsymbol{max}}}{me_q^{ref}}\right)^{n^{storage,q}} \qquad \forall(e \in E, q \in Q) \qquad \text{(eq. 78)}$$

$$\boldsymbol{me}_{\boldsymbol{e,q}}^{\boldsymbol{max}} \geq \boldsymbol{me}_{\boldsymbol{e,q,t}} \; \forall(e \in E, q \in Q, t \in T) \qquad \text{(eq. 79)}$$

$$\boldsymbol{me}_{\boldsymbol{e,q}}^{\boldsymbol{max}} = me_q^{ref,1} + \sum_{\boldsymbol{n=1}}^{n\_\boldsymbol{lin\_arm\_e}} \boldsymbol{\delta}_{\boldsymbol{e,q,n}}^{\boldsymbol{lin\_arm\_e}} \qquad \forall(e \in E, q \in Q) \qquad \text{(eq. 80)}$$

$$\begin{cases} \left(me_q^{ref,2} - me_q^{ref,1}\right)\boldsymbol{w_{e,q,2}^{lin_{arm_e}}} \le \boldsymbol{\delta_{e,q,1}^{lin_{arm_e}}} \le \left(me_q^{ref,2} - me_q^{ref,1}\right)\boldsymbol{w_{e,q,1}^{lin_{arm_e}}} \\ \dots \\ \left(me_q^{ref,n+1} - me_q^{ref,n}\right)\boldsymbol{w_{e,q,n+1}^{lin_{arm_e}}} \le \boldsymbol{\delta_{e,q,n}^{lin_{arm_e}}} \le \left(me_q^{ref,n+1} - me_q^{ref,n}\right)\boldsymbol{w_{e,q,n}^{lin_{arm_e}}} \\ \dots \\ \boldsymbol{\delta_{e,q,N_{lin_{arm_e}}}^{lin_{arm_e}}} \le \left(me_q^{ref,N+1} - me_q^{ref,N}\right)\boldsymbol{w_{e,q,N_{lin_{arm_e}}}^{lin_{arm_e}}} \\ \boldsymbol{w_{e,q,n}^{lin_{arm_e}}} \in \{0,1\}, n = 1,2 \dots \dots, n_{lin_{arm_e}} \end{cases}$$

$$\forall (e \in E, q \in Q) \qquad \text{(eq. 81)}$$

$$\boldsymbol{\tilde{I}_{e,q}^{storage.E}} = i_q^{storage\_e}\left(\frac{me_q^{ref,1}}{me_q^{ref}}\right)^{n^{storage,q}} + \sum_{1}^{N} \frac{i_q^{storage_e}\left(\frac{me_q^{ref,n+1}}{me_q^{ref}}\right)^{n^{storage,q}} - i_q^{storage_e}\left(\frac{me_q^{ref,n}}{me_q^{ref}}\right)^{n^{storage,q}}}{me_q^{ref,n+1} - me_q^{ref,n}}\ \boldsymbol{\delta_{e,q,n}^{lin_{arm_e}}}$$

$$\forall (\mathrm{e} \in E, q \in \mathrm{Q}) \qquad \text{(eq. 82)}$$

$$\boldsymbol{I_p^{storage,P}} = \sum_{\boldsymbol{q \in Q}} i_q^{storage\_p}\left(\frac{\boldsymbol{mp_{p,q}^{max}}}{mp_q^{ref}}\right)^{n^{storage,q}} \qquad \forall (p \in P, q \in Q) \qquad \text{(eq. 83)}$$

$$\boldsymbol{mp_{p,q}^{max}} \ge \boldsymbol{mp_{p,q,t}} \ \ \forall (p \in P, q \in Q, t \in T) \qquad \text{(eq. 84)}$$

$$\boldsymbol{mp_{p,q}^{max}} = mp_q^{ref,1} + \sum_{\boldsymbol{n=1}}^{\boldsymbol{n\_lin\_arm\_p}} \boldsymbol{\delta_{q,p,n}^{lin\_arm\_p}} \qquad \forall (p \in P, q \in Q) \qquad \text{(eq. 85)}$$

$$\begin{cases} \left(mp_q^{ref,2} - mp_q^{ref,1}\right)\boldsymbol{w_{p,q,2}^{lin_{arm_p}}} \le \boldsymbol{\delta_{p,q,1}^{lin_{arm_p}}} \le \left(mp_q^{ref,2} - mp_q^{ref,1}\right)\boldsymbol{w_{p,q,1}^{lin_{arm_p}}} \\ \dots \\ \left(mp_q^{ref,n+1} - mp_q^{ref,n}\right)\boldsymbol{w_{p,q,n+1}^{lin_{arm_p}}} \le \boldsymbol{\delta_{p,q,n}^{lin_{arm_p}}} \le \left(mp_q^{ref,n+1} - mp_q^{ref,n}\right)\boldsymbol{w_{p,q,n}^{lin_{arm_p}}} \\ \dots \\ \boldsymbol{\delta_{p,q,N_{lin_{arm_p}}}^{lin_{arm_p}}} \le \left(mp_q^{ref,N+1} - mp_q^{ref,N}\right)\boldsymbol{w_{p,q,N_{lin_{arm_p}}}^{lin_{arm_p}}} \\ \boldsymbol{w_{p,q,n}^{lin_{arm_p}}} \in \{0,1\}, n = 1,2 \dots, n_{lin_{arm_p}} \end{cases}$$

$$\forall (p \in P, q \in Q) \qquad \text{(eq. 86)}$$

$$\tilde{\boldsymbol{I}}_{\boldsymbol{p,q}}^{\boldsymbol{storage.P}} = i_q^{storage\_p}\left(\frac{mp_q^{ref,1}}{mp_q^{ref}}\right)^{n^{storage,q}} + \sum_{1}^{N}\frac{i_q^{storage_p}\left(\frac{mp_q^{ref,n+1}}{mp_q^{ref}}\right)^{n^{storage,q}} - i_q^{storage_p}\left(\frac{mp_q^{ref,n}}{mp_q^{ref}}\right)^{n^{storage,q}}}{mp_q^{ref,n+1} - mp_q^{ref,n}}\,\boldsymbol{\delta}_{\boldsymbol{p,q,n}}^{\boldsymbol{lin_{arm_p}}} \quad \forall(\mathrm{p} \in P, q \in \mathrm{Q}) \qquad \text{(eq. 87)}$$

The total investment in storage ($\boldsymbol{I}^{\boldsymbol{storage}}$) is given by the sum of linearized investments on layers E and P (eq. 88).

$$\boldsymbol{I}^{\boldsymbol{storage}} = \sum_{\boldsymbol{e}\in\boldsymbol{E}}\sum_{\boldsymbol{q}\in\boldsymbol{Q}}\tilde{\boldsymbol{I}}_{\boldsymbol{e,q}}^{\boldsymbol{storage,E}} + \sum_{\boldsymbol{p}\in\boldsymbol{P}}\sum_{\boldsymbol{q}\in\boldsymbol{Q}}\tilde{\boldsymbol{I}}_{\boldsymbol{p,q}}^{\boldsymbol{storage,P}} \qquad \text{(eq. 88)}$$

3.3.2 Operating Costs

Operating costs are comprised of costs on forest maintenance (section 3.3.2.1), harvesting (section 3.3.2.2), biomass transportation (3.3.2.3), production (3.3.2.4), pseudo-components transportation (3.3.2.5 and 3.3.2.7), and storage (3.3.2.6). Those costs are consolidated in a single variable in section 3.3.2.8.

3.3.2.1 Maintenance Of Forest Lands Costs

Planted and free lands that were bought must be maintained from the period they were bought until the end of the operational time horizon. The costs of land maintenance for planted and free land ($\boldsymbol{C}_{\boldsymbol{f,b,t}}^{\boldsymbol{maintenance,F}}$ and $\boldsymbol{C}_{\boldsymbol{f,t}}^{\boldsymbol{maintenance,F,free}}$) are given by equations 89 and 90 as a function of the unitary costs ($c_{f,b,i,t}^{maintenance,F}$ and $c_{f,t}^{maintenance,F,free}$) and the area of owned land. The total forest maintenance cost ($\boldsymbol{C}_{\boldsymbol{t}}^{\boldsymbol{maintenance,F,total}}$) is given by equation 91.

$$\boldsymbol{C}_{\boldsymbol{f},\boldsymbol{b},\boldsymbol{t}}^{\boldsymbol{maintenance},\boldsymbol{F}} = \sum_{i \in I} c_{f,b,i,t}^{maintenance,F} \boldsymbol{A}_{\boldsymbol{f},\boldsymbol{b},\boldsymbol{i},\boldsymbol{t}}^{\boldsymbol{owned}} \quad \forall (f \in F, b \in B, t \in T) \qquad \text{(eq. 89)}$$

$$\boldsymbol{C}_{\boldsymbol{f},\boldsymbol{t}}^{\boldsymbol{maintenance},\boldsymbol{F},\boldsymbol{free}} = c_{f,t}^{maintenance,F,free} \boldsymbol{A}_{\boldsymbol{f},\boldsymbol{t}}^{\boldsymbol{free},\boldsymbol{owned}} \quad \forall (f \in F, t \in T) \qquad \text{(eq. 90)}$$

$$\boldsymbol{C}_{\boldsymbol{t}}^{\boldsymbol{maintenance},\boldsymbol{F},\boldsymbol{total}} = \sum_{\boldsymbol{f} \in \boldsymbol{F}} \left(\sum_{\boldsymbol{b} \in \boldsymbol{B}} \boldsymbol{C}_{\boldsymbol{f},\boldsymbol{b},\boldsymbol{t}}^{\boldsymbol{maintenance},\boldsymbol{F}} + \boldsymbol{C}_{\boldsymbol{f},\boldsymbol{t}}^{\boldsymbol{maintenance},\boldsymbol{F},\boldsymbol{free}} \right) \ \forall t \in T \qquad \text{(eq. 91)}$$

3.3.2.2 Harvesting Costs

The harvesting cost of a biomass *b* at a forest location *f* in a period *t* ($\boldsymbol{C}_{\boldsymbol{f},\boldsymbol{b},\boldsymbol{t}}^{\boldsymbol{harvest}}$) is also defined accordingly to a unitary harvesting cost ($c_{f,b,i,t}^{harvest}$) and the harvested area (eq. 92). The total harvesting cost ($\boldsymbol{C}_{\boldsymbol{t}}^{\boldsymbol{harvest},\boldsymbol{total}}$) at each period *t* is given by equation 93.

$$\boldsymbol{C}_{\boldsymbol{f},\boldsymbol{b},\boldsymbol{t}}^{\boldsymbol{harvest}} = \sum_{i \in I} c_{f,b,i,t}^{harvest} \boldsymbol{A}_{\boldsymbol{f},\boldsymbol{b},\boldsymbol{i},\boldsymbol{t}}^{\boldsymbol{harvested}} \ \forall (f \in F, b \in B, t \in T) \qquad \text{(eq. 92)}$$

$$\boldsymbol{C}_{\boldsymbol{t}}^{\boldsymbol{harvest},\boldsymbol{total}} = \sum_{\boldsymbol{f} \in \boldsymbol{F}} \sum_{\boldsymbol{b} \in \boldsymbol{B}} \boldsymbol{C}_{\boldsymbol{f},\boldsymbol{b},\boldsymbol{t}}^{\boldsymbol{harvest}} \quad \forall t \in T \qquad \text{(eq. 93)}$$

3.3.2.3 Biomass Transportation Costs

Harvested biomass is transferred to the production layer. The cost of transportation ($\boldsymbol{C}_{\boldsymbol{f},\boldsymbol{p},\boldsymbol{t}}^{\boldsymbol{transp},\boldsymbol{biomass}.\boldsymbol{FP}}$) is given by a unitary transportation cost ($c_{f,p,b,t}^{transp,biomass}$) and the amount of the transported biomass ($\boldsymbol{FF}_{\boldsymbol{f},\boldsymbol{p},\boldsymbol{b},\boldsymbol{t}}^{\boldsymbol{demand}}$) in equation 94. The total transportation cost in each period ($\boldsymbol{C}_{\boldsymbol{t}}^{\boldsymbol{transp},\boldsymbol{biomass}}$) is given by the sum of the transportation costs of all pairs of origins *f* and destinations *p* in that period (eq. 95).

$$\boldsymbol{C}_{\boldsymbol{f},\boldsymbol{p},\boldsymbol{t}}^{\boldsymbol{transp},\boldsymbol{biomass},\boldsymbol{FP}} = \sum_{b \in B} c_{f,p,b,t}^{transp,biomass} \boldsymbol{FF}_{\boldsymbol{f},\boldsymbol{p},\boldsymbol{b},\boldsymbol{t}}^{\boldsymbol{demand}} \ \forall (f \in F, p \in P, t \in T) \qquad \text{(eq. 94)}$$

$$C_{t}^{transp,biomass} = \sum_{f \in F} \sum_{p \in P} C_{f,p,t}^{transp,biomass,FP} \quad \forall t \in T \qquad \text{(eq. 95)}$$

3.3.2.4 Production Costs

The production cost of a production facility *p* at a period *t* ($\boldsymbol{C_{p,t}^{production,P}}$) is given by the sum of the individual costs of each technology *z* installed in the production facility *p* (equation 96). These costs are composed by a fixed term ($c_{p,z,t}^{prod,fix}\boldsymbol{ypz_{p,z}}$) conditioned to the binary decision of building (or not) the technology *z* within the production facility *p*, a variable cost term associated with the amount of pseudo-component and utilities processed ($\sum_{q \in Q} c_{p,z,q,t}^{prod,var_q}\boldsymbol{FZ_{p,z,q,t}}$ and $\sum_{u \in U} c_{p,z,u,t}^{prod,var_u}\boldsymbol{FU_{p,z,ut}^{interconversion}}$), effluents generated ($\sum_{r \in R} c_{p,r,t}^{residue}\boldsymbol{FRZ_{p,z,r,t}}$), and utilities bought ($\sum_{u \in U} c_{p,u,t}^{utility}\boldsymbol{FU_{p,u,t}^{bought}}$).

$$\begin{aligned} \boldsymbol{C_{p,t}^{production,P}} = \sum_{z \in Z} \Bigg(& c_{p,z,t}^{prod,fix}\boldsymbol{ypz_{p,z}} + \sum_{q \in Q} c_{p,z,q,t}^{prod,var,q}\boldsymbol{FZ_{p,z,q,t}} \\ & + \sum_{u \in U} c_{p,z,u,t}^{prod,var,u}\boldsymbol{FU_{p,z,ut}^{interconversion}} \\ & + \sum_{r \in R} c_{p,r,t}^{residue}\boldsymbol{FRZ_{p,z,r,t}} \Bigg) \\ & + \sum_{u \in U} c_{p,u,t}^{utility}\boldsymbol{FU_{p,u,t}^{bought}} \; \forall (p \in P, t \in T) \end{aligned} \qquad \text{(eq. 96)}$$

Total production cost at each period *t* ($\boldsymbol{C_{t}^{production}}$) is given by the sum of production costs of each facility *p* (eq. 97).

$$\boldsymbol{C_{t}^{production}} = \sum_{p \in P} \boldsymbol{C_{p,t}^{production}} \quad \forall\, t \in T \qquad \text{(eq. 97)}$$

3.3.2.5 Pseudo-Components Transportation Costs From Production

From production facilities, some chemicals are transferred to other facilities, storage units, and consumer markets. These transferences are associated with transportation costs ($\boldsymbol{C_{p,p',q,t}^{transp,PP}}$, $\boldsymbol{C_{p,e,q,t}^{transp,PE}}$ and $\boldsymbol{C_{p,m,q,t}^{transp,PM}}$) given by a unitary cost dependent on the origin, destination, pseudo-component, and period ($c_{p,p',q,t}^{transp,PP}$, $c_{p,e,q,t}^{transp,PE}$and $c_{p,m,q,t}^{transp,PM}$) and the amount of transported material ($\boldsymbol{FTP_{p,p',q,t}}$, $\boldsymbol{FPE_{p,e,q,t}}$ and $\boldsymbol{FPM_{p,m,q,t}}$) as described by equations 98 to 100.

$$\boldsymbol{C_{p,p',q,t}^{transp,PP}} = c_{p,p',q,t}^{transp,PP} \boldsymbol{FTP_{p,p',q,t}} \; \forall (p, p' \in P, q \in Q, t \in T) \qquad \text{(eq. 98)}$$

$$\boldsymbol{C_{p,e,q,t}^{transp,PE}} = c_{p,e,q,t}^{transp,PE} \boldsymbol{FPE_{p,e,q,t}} \; \forall (p \in P, e \in E, q \in Q, t \in T) \qquad \text{(eq. 99)}$$

$$\boldsymbol{C_{p,m,q,t}^{transp,PM}} = c_{p,m,q,t}^{transp,PM} \boldsymbol{FPM_{p,m,q,t}} \; \forall (p \in P, m \in M, q \in Q, t \in T) \qquad \text{(eq. 100)}$$

Total transportation costs from layer P at a period *t* ($\boldsymbol{C_{t}^{transp,P}}$) is given by the sum of the individual costs for all pseudo-components, coming from all origins on layer P, and going to all destinations in layers P, E, and M (eq. 101).

$$\boldsymbol{C_{t}^{transp,P}} = \sum_{q \in Q} \sum_{p \in P} \left(\sum_{p' \in P} \boldsymbol{C_{p,p',q,t}^{transp,PP}} + \sum_{e \in E} \boldsymbol{C_{p,e,q,t}^{transp,PE}} + \sum_{m \in M} \boldsymbol{C_{p,m,q,t}^{transp,PM}} \right) \qquad \text{(eq. 101)}$$
$$\forall t \in T$$

3.3.2.6 Storage Costs

The storage costs in a storage facility *e* ($\boldsymbol{C_{e,t}^{storage,E}}$) is also composed of a fixed cost term associated with the decision of building the facility ($c_{e,t}^{stor,E,fix} \boldsymbol{ye_e}$ or $c_{p,t}^{stor,P,fix} \boldsymbol{yp_p}$) and variable costs accordingly to the amount under storage ($\sum_{\boldsymbol{q \in Q}} c_{e,q,t}^{stor,E,var} \boldsymbol{me_{e,q,t}}$) as described by equation 102. The storage cost in a production facility *p* ($\boldsymbol{C_{p,t}^{storage,P}}$), however, is composed of only a variable cost term ($\sum_{\boldsymbol{q \in Q}} c_{p,q,t}^{stor,P,var} \boldsymbol{mp_{p,q,t}}$) as described by equation 104, once the fixed costs of the production facility installation are supposed to be already incorporated into the production cost definition. The total storage costs at a period t in layer E ($\boldsymbol{C_t^{storage,E}}$) and layer P ($\boldsymbol{C_{p,t}^{storage,P}}$) are given by the sum of the individual facilities costs in that period as described by equations 103 and 105.

$$\boldsymbol{C_{e,t}^{storage,E}} = c_{e,t}^{stor,E,fix}\boldsymbol{ye_e} + \sum_{\boldsymbol{q \in Q}} c_{e,q,t}^{stor,E,var}\boldsymbol{me_{e,q,t}} \ \forall(e \in E, t \in T) \qquad \text{(eq. 102)}$$

$$\boldsymbol{C_t^{storage,E}} = \sum_{\boldsymbol{e \in E}} \boldsymbol{C_{e,t}^{storage,E}} \ \forall t \in T \qquad \text{(eq. 103)}$$

$$\boldsymbol{C_{p,t}^{storage,P}} = \sum_{\boldsymbol{q \in Q}} c_{p,q,t}^{stor,P,var}\boldsymbol{mp_{p,q,t}} \ \forall(p \in P, t \in T) \qquad \text{(eq. 104)}$$

$$\boldsymbol{C_t^{storage,P}} = \sum_{\boldsymbol{p \in P}} \boldsymbol{C_{p,t}^{storage,P}} \ \forall t \in T \qquad \text{(eq. 105)}$$

3.3.2.7 Pseudo-Components Transportation Costs From Storage Facilities

Transference costs from a storage facility *e* in layer E to another storage facility *e'* ($\boldsymbol{C_{e,e',q,t}^{transp,EE}}$) or to a consumer market *m* ($\boldsymbol{C_{e,m,q,t}^{transp,EM}}$) are modeled analogously to costs in layer P as a function of a unitary cost dependent on the origin, destination, pseudo-component, and period ($c_{e,e',q,t}^{transp,EE}$ and $c_{e,m,q,t}^{transp,EM}$) and the amount of transported material ($\boldsymbol{FTE}_{e,e',\boldsymbol{q,t}}$ and $\boldsymbol{FEM_{e,m,q,t}}$) as described by equations 106 and 107. The total transportation cost on transferences from layer E at a period t ($\boldsymbol{C_t^{transp,E}}$) is given by the sum of individual transference costs for all pseudo-components, from all origins in layer E, to all destinations in both layers E and M, as described by equation 108.

$$\boldsymbol{C_{e,e',q,t}^{transp,EE}} = c_{e,e',q,t}^{transp,EE}\boldsymbol{FTE}_{e,e',\boldsymbol{q,t}} \ \forall(e, e' \in E, q \in Q, t \in T) \qquad \text{(eq. 106)}$$

$$\boldsymbol{C_{e,m,q,t}^{transp,EM}} = c_{e,m,q,t}^{transp,EM}\boldsymbol{FEM_{e,m,q,t}} \ \forall(e \in E, m \in M, q \in Q, t \in T) \qquad \text{(eq. 107)}$$

$$\boldsymbol{C_t^{transp,E}} = \sum_{q \in Q} \sum_{e \in E} \left(\sum_{e' \in P} \boldsymbol{C_{q,e,e',t}^{transp,EE}} + \sum_{m \in M} \boldsymbol{C_{q,e,m,t}^{transp,EM}} \right) \ \forall t \in T \qquad \text{(eq. 108)}$$

3.3.2.8 Total Operating Costs

The total operating cost at a period t ($\boldsymbol{C_t^{total}}$) is then given by the sum of forest maintenance costs, harvesting, biomass transportation, production, storage, and chemicals transportation (eq. 109).

$$\boldsymbol{C_t^{total}} = \boldsymbol{C_t^{maintenance,F,total}} + \boldsymbol{C_t^{harvest,F}} + \boldsymbol{C_t^{transp,biomassa}} + \boldsymbol{C_t^{production}} + \boldsymbol{C_t^{storage,E}} + \boldsymbol{C_t^{storage,P}} + \boldsymbol{C_t^{transp,P}} + \boldsymbol{C_t^{transp,E}} \ \forall t \in T \qquad \text{(eq. 109)}$$

3.3.3 Revenues

Operating revenues comes from the sales of pseudo-components (section 3.3.3.1) and utilities (section 3.3.3.3). The uncertainties in selling prices directly affect the revenue calculation and are discussed in section 3.3.3.2 and 3.3.3.4 for pseudo-components and utilities, respectively.

Revenues are used to calculate profit taxes, as discussed in section 3.3.3.5. However, the uncertainty on revenue generation must be considered under a robust optimization lens for the profit tax calculation. This robust consideration is discussed in section 3.3.3.6.

3.3.3.1 Revenues From Pseudo-Components

Operating revenues come from the selling of chemicals on market (layer M) and utilities on production sites (layer P). The deterministic revenues from chemical sales ($\boldsymbol{RP_{p,m,q,t}}$ for sales coming from layer P or $\boldsymbol{RE_{e,m,q,t}}$ for sales coming from layer E) are given by equations 110 and 111 considering the product selling price on location M

($pq_{m,q,t}$), an origin-destination dependent tax term ($tax^{sales,P}_{p,m,q}$ or $tax^{sales,E}_{e,m,q}$) and the amount of product sold ($\boldsymbol{FPM_{p,m,q,t}}$ or $\boldsymbol{FEM_{e,m,q,t}}$).

$$\boldsymbol{RP_{p,m,q,t}} = pq_{m,q,t}\left(1 - tax^{sales,P}_{p,m,q}\right)\boldsymbol{FPM_{p,m,q,t}} \quad \forall\ (p \in P, m \in M, q \in Q, t \in T) \qquad \text{(eq. 110)}$$

$$\boldsymbol{RE_{e,m,q,t}} = pq_{m,q,t}\left(1 - tax^{sales,E}_{e,m,q}\right)\boldsymbol{FEM_{e,m,q,t}} \quad \forall\ (e \in E, m \in M, q \in Q, t \in T) \qquad \text{(eq. 111)}$$

3.3.3.2 Uncertainty In Chemicals' Selling Prices

Product selling prices are considered uncertain parameters in this work. Analogously to biomass growth modeling in section 3.1.3, the price is decomposed into an expected or nominal value for the parameter ($\overline{pq}_{m,q,t}$) and a possible fluctuation term ($\widetilde{pq}_{m,q,t}$) as described in equation 112. The uncertainty is represented by a random variable $\xi^{price}_{m,q,t}$ constrained within an interval set given by the constant $\psi^{price}_{m,q,t}$ (eq. 113) and a polyhedral given by the constant $\Gamma^{price}_{m,q}$ (eq. 114).

$$pq_{m,q,t} = \overline{pq}_{m,q,t} + \xi^{price}_{m,q,t}\widetilde{pq}_{m,q,t} \forall (m \in M, q \in Q, t \in T) \qquad \text{(eq. 112)}$$

$$\left|\xi^{price}_{m,q,t}\right| \leq \psi^{price}_{m,q,t}\ \forall (m \in M, q \in Q, t \in T) \qquad \text{(eq. 113)}$$

$$\sum_{t}\left|\xi^{price}_{m,q,t}\right| \leq \Gamma^{price}_{m,q}\ \forall (m \in M, q \in Q) \qquad \text{(eq. 114)}$$

The formulation of the robust counterparts of equations 110 and 111, however, would not benefit from the polyhedral set approach because only a single uncertain parameter is included in the same constraint. Thus, instead of explicitly evaluating revenues at each period, all revenues are brought to present value and summed together into the variables $\boldsymbol{RP^{present\ value}_{p,m,q}}$ (eq. 115) or $\boldsymbol{RE^{present\ value}_{e,m,q}}$ (eq. 116) representing the present value of revenues from the sale of a pseudo-component *q* on a market *m* from a production facility *p* or a storage facility *e*.

For the present value calculation, revenues are supposed to occur in the middle of each period *t* (*t + 0.5*, given *t* is 0-indexed) discounted by the interest rate int_rate. The last term in the equation represents the operation's perpetuity and considers the mean profit along the operational period with no yearly growth to occur subsequently to the last time horizon period, i.e., $t_{last} + 1$.

$$\boldsymbol{RP}_{\boldsymbol{p,m,q}}^{\boldsymbol{present\ value}} = \left(1 - tax_{p,m,q}^{sales,P}\right)\left(\sum_{t \in T} \frac{pq_{m,q,t}\boldsymbol{FPM}_{\boldsymbol{p,m,q,t}}}{(1 + int_{rate})^{t\ +\ 0.5}} + \frac{\frac{\left(\frac{\sum_{t \in T} pq_{m,q,t}\boldsymbol{FPM}_{\boldsymbol{p,m,q,t}}}{t_{last} + 1}\right)}{int_{rate}}}{(1 + int_{rate})^{t\_last\ +\ 1}}\right) \forall (\mathrm{p} \in P, m \in M, q \in Q) \quad \text{(eq. 115)}$$

$$\boldsymbol{RE}_{\boldsymbol{e,m,q}}^{\boldsymbol{present\ value}} = \left(1 - tax_{e,m,q}^{sales,E}\right)\left(\sum_{t \in T} \frac{pq_{m,q,t}\boldsymbol{FEM}_{\mathbf{em},\boldsymbol{q,t}}}{(1 + int_{rate})^{t\ +\ 0.5}} + \frac{\frac{\left(\frac{\sum_{t \in T} pq_{m,q,t}\boldsymbol{FEM}_{\boldsymbol{e,m,q,t}}}{t_{last} + 1}\right)}{int_{rate}}}{(1 + int_{rate})^{t\_last\ +\ 1}}\right) \forall (\mathrm{e} \in E, m \in M, q \in Q) \quad \text{(eq. 116)}$$

For simplification, equations 115 and 116 are rearranged as equations 117 and 118. Also, they are converted to inequalities to match the pattern reported in Li and Floudas (2012) for deriving the robust counterpart. This conversion to inequality does not alter the optimal solution to the problem as revenues are always maximized accordingly to the objective function formulated in section 3.3.4.

$$\boldsymbol{RP}_{\boldsymbol{p,m,q}}^{\boldsymbol{present\ value}} - \left(1 - tax_{p,m,q}^{sales,P}\right)\sum_{t\in T}\left(\frac{1}{(1+int_{rate})^{t\,+\,0.5}} + \frac{1}{(t_{last}+1).\,int_{rate}.\,(1+int_{rate})^{t\_last\,+\,1}}\right)pq_{m,q,t}\boldsymbol{FPM}_{\boldsymbol{p,m,q,t}} \leq 0 \ \ \forall(p \in P, m \in M, q \in Q) \quad \text{(eq. 117)}$$

$$\boldsymbol{RE}_{\boldsymbol{e,m,q}}^{\boldsymbol{present\ value}} - \left(1 - tax_{e,m,q}^{sales,E}\right)\sum_{t\in T}\left(\frac{1}{(1+int_{rate})^{t\,+\,0.5}} + \frac{1}{(t_{last}+1).\,int_{rate}.\,(1+int_{rate})^{t\_last\,+\,1}}\right)pq_{m,q,t}\boldsymbol{FEM}_{\boldsymbol{e,m,q,t}} \leq 0 \ \ \forall(e \in E, m \in M, q \in Q) \quad \text{(eq. 118)}$$

The robust counterpart according to the procedure by Li and Floudas (2012) for equation 115 is then given by equations 119 to 122 and for equation 116 by equations 122 to 126, with the introduction of the auxiliary variables ($\boldsymbol{W}_{\boldsymbol{p,m,q,t}}^{\boldsymbol{revenue,P}}$, $\boldsymbol{Z}_{\boldsymbol{m,q}}^{\boldsymbol{revenue,P}}$, $\boldsymbol{U}_{\boldsymbol{p,m,q,t}}^{\boldsymbol{revenue,P}}$, $\boldsymbol{W}_{\boldsymbol{e,m,q,t}}^{\boldsymbol{revenue,E}}$, $\boldsymbol{Z}_{\boldsymbol{m,q}}^{\boldsymbol{revenue,E}}$ and $\boldsymbol{U}_{\boldsymbol{e,m,q,t}}^{\boldsymbol{revenue,E}}$).

$$\boldsymbol{RP}_{\boldsymbol{p,m,q}}^{\boldsymbol{present\ value}} - \left(1 - tax_{p,m,q}^{sales,P}\right)\sum_{t\in T}\left(\frac{1}{(1+int_{rate})^{t\,+\,0.5}} + \frac{1}{(t_{last}+1).\,int_{rate}.\,(1+int_{rate})^{t_{last}+\,1}}\right)\overline{pq}_{m,q,t}\boldsymbol{FPM}_{\boldsymbol{p,m,q,t}} + \sum_{t\in T}\Psi_{m,q,t}^{price}\boldsymbol{W}_{\boldsymbol{p,m,q,t}}^{\boldsymbol{revenue,P}} - \Gamma_{m,q}^{price}\boldsymbol{Z}_{\boldsymbol{m,q}}^{\boldsymbol{revenue,P}} \leq 0 \quad \text{(eq. 119)}$$

$$\forall (\mathrm{p} \in P, m \in M, q \in Q)$$

$$\boldsymbol{W}_{\boldsymbol{p,m,q,t}}^{\boldsymbol{revenue,P}} + \boldsymbol{Z}_{\boldsymbol{p,m,q}}^{\boldsymbol{revenue,P}} \geq \left(1 - tax_{p,m,q}^{sales,P}\right)\left(\frac{1}{(1+int_{rate})^{t\,+\,0.5}} + \frac{1}{(t_{last}+1).\,int_{rate}.\,(1+int_{rate})^{t_{last}+\,1}}\right)\widetilde{pq}_{m,q,t}\boldsymbol{U}_{\boldsymbol{p,m,q,t}}^{\boldsymbol{revenue,P}} \quad \forall (\mathrm{p} \in P, m \in M, q \in Q, t \in T) \qquad \text{(eq. 120)}$$

$$\boldsymbol{FPM}_{\boldsymbol{p,m,q,t}} \leq \boldsymbol{U}_{\boldsymbol{p,m,q,t}}^{\boldsymbol{revenue,P}} \quad \forall (\mathrm{p} \in P, m \in M, q \in Q, t \in T) \qquad \text{(eq. 121)}$$

$$-\boldsymbol{U}_{\boldsymbol{p,m,q,t}}^{\boldsymbol{revenue,P}} \leq \boldsymbol{FPM}_{\boldsymbol{p,m,q,t}} \quad \forall (\mathrm{p} \in P, m \in M, q \in Q, t \in T) \qquad \text{(eq. 122)}$$

$$\boldsymbol{RE}_{\boldsymbol{e,m,q}}^{\boldsymbol{present\ value}} - \left(1 - tax_{e,m,q}^{sales,E}\right)\sum_{t\in T}\left(\frac{1}{(1+int_{rate})^{t\,+\,0.5}} + \frac{1}{(t_{last}+1).\,int_{rate}.\,(1+int_{rate})^{t_{last}+\,1}}\right)\overline{pq}_{m,q,t}\boldsymbol{FEM}_{\boldsymbol{e,m,q,t}} + \sum_{t\in T}\Psi_{m,q,t}^{price}\boldsymbol{W}_{\boldsymbol{e,m,q,t}}^{\boldsymbol{revenue,E}} - \Gamma_{m,q}^{price}\boldsymbol{Z}_{\boldsymbol{m,q}}^{\boldsymbol{revenue,E}} \leq 0 \quad \forall (\mathrm{e} \in E, m \in M, q \in Q) \qquad \text{(eq. 123)}$$

$$\boldsymbol{W}_{\boldsymbol{e,m,q,t}}^{\boldsymbol{revenue,E}} + \boldsymbol{Z}_{\boldsymbol{e,m,q}}^{\boldsymbol{revenue,E}} \geq \left(1 - tax_{e,m,q}^{sales,E}\right)\left(\frac{1}{(1+int_{rate})^{t\,+\,0.5}} + \frac{1}{(t_{last}+1).\,int_{rate}.\,(1+int_{rate})^{t_{last}+\,1}}\right)\widetilde{pq}_{m,q,t}\boldsymbol{U}_{\boldsymbol{e,m,q,t}}^{\boldsymbol{revenue,E}} \quad \forall (e \in E, m \in M, q \in Q, t \in T) \qquad \text{(eq. 124)}$$

$$\boldsymbol{FEM}_{\boldsymbol{e,m,q,t}} \leq \boldsymbol{U}_{\boldsymbol{e,m,q,t}}^{\boldsymbol{revenue,E}} \quad \forall (e \in E, m \in M, q \in Q, t \in T) \qquad \text{(eq. 125)}$$

$$-\boldsymbol{U}_{\boldsymbol{e,m,q,t}}^{\boldsymbol{revenue,E}} \leq \boldsymbol{FEM}_{\boldsymbol{e,m,q,t}} \quad \forall(e \in E, m \in M, q \in Q, t \in T) \qquad \text{(eq. 126)}$$

The present value for the chemical sales revenue during the entire operating period ($\boldsymbol{RQ}^{\boldsymbol{present\_value}}$) is then given by equation 127.

$$\boldsymbol{RQ}^{\boldsymbol{present\_value}} = \sum_{m\in M}\sum_{q\in Q}\left(\sum_{p\in P}\boldsymbol{RP}_{\boldsymbol{p,m,q}}^{\boldsymbol{present\ value}} + \sum_{e\in E}\boldsymbol{RE}_{\boldsymbol{e,m,q}}^{\boldsymbol{present\ value}}\right) \qquad \text{(eq. 127)}$$

3.3.3.3 Revenues From Utilities Sales

Besides chemicals, utilities can also be sold, but only within the location it was produced (layer P). Thus, revenues from utilities do not account for origin-destination dependent tax terms. The present value for revenues coming from selling a utility *u* sold in a production facility *p* ($\boldsymbol{RU}_{\boldsymbol{p,u}}^{\boldsymbol{present\ value}}$) is then given by equation 128 as a function of the uncertain utility selling prices ($pu_{p,u,t}$), analogously to equations 117 and 118. The total present value revenue from utility sales is given by equation 129.

$$\boldsymbol{RU}_{\boldsymbol{p,u}}^{\boldsymbol{present\ value}} - \left(1 - tax_{p,u}^{sales,U}\right)\sum_{t\in T}\left(\frac{1}{(1+int_{rate})^{t\,+\,0.5}} + \frac{1}{(t_{last}+1).\,int_{rate}.\,(1+int_{rate})^{t_{last}+\,1}}\right) pu_{p,u,t}\boldsymbol{FU}_{\boldsymbol{p,u,t}}^{\boldsymbol{sold}} \leq 0 \qquad \text{(eq. 128)}$$

$$\boldsymbol{RU}^{\boldsymbol{present\_value}} = \sum_{p\in P}\sum_{u\in U}\boldsymbol{RU}_{\boldsymbol{p,u}}^{\boldsymbol{present\ value}} \qquad \text{(eq. 129)}$$

3.3.3.4 Uncertainty In Utilities' Selling Price

The uncertainty representation of the utilities selling prices is given by equations 130 to 132, analogously to the chemical selling prices on equations 112 to 114, considering an expected or nominal value for the utility selling price ($\overline{pu}_{p,\mathrm{u},t}$), a possible fluctuation term ($\widetilde{pu}_{p,u,t}$) and a random variable for the uncertainty representation ($\xi_{p,u,t}^{price,u}$) that is constrained in a polyhedral and interval-sets given by the constants $\psi_{p,u,t}^{price,u}$ and $\Gamma_{p,u}^{price,u}$, respectively.

$$pu_{p,\mathrm{u},t} = \overline{pu}_{p,\mathrm{u},t} + \xi_{p,u,t}^{price,u}\widetilde{pu}_{p,u,t} \forall(p \in P, u \in U, t \in T) \qquad \text{(eq. 130)}$$

$$\left|\xi_{p,u,t}^{price,u}\right| \leq \psi_{p,u,t}^{price,u} \; \forall(p \in P, u \in U, t \in T) \qquad \text{(eq. 131)}$$

$$\sum_{t}\left|\xi_{p,u,t}^{price,u}\right| \leq \Gamma_{p,u}^{price,u} \; \forall(p \in P, u \in U) \qquad \text{(eq. 132)}$$

The robust counterpart for the present value of the utility sales revenue ($\boldsymbol{RU_{p,u}^{present\ value}}$) is then given by equations 133 to 136 considering the auxiliary variables $\boldsymbol{W_{p,u,t}^{revenue,u}}$, $\boldsymbol{Z_{p,u}^{revenue,u}}$ and $\boldsymbol{U_{p,u,t}^{revenue,util}}$.

$$\begin{aligned} &\boldsymbol{RU_{p,u}^{present\ value}} \\ &\quad - \sum_{t \in T}\left(\frac{1}{(1+int_{rate})^{t\,+\,0.5}} \right. \\ &\quad \left. + \frac{1}{(t_{last}+1).\, int_{rate}.\,(1+int_{rate})^{t_{last}+\,1}}\right)\overline{pu}_{p,u,t}\boldsymbol{FU_{p,u,t}^{sold}} \\ &\quad + \sum_{t \in T}\psi_{p,u,t}^{price,u}\boldsymbol{W_{p,u,t}^{revenue,util}} - \Gamma_{p,u}^{price,u}\boldsymbol{Z_{p,u}^{revenue,u}} \leq 0 \\ &\qquad \forall(p \in P, u \in U) \end{aligned} \qquad \text{(eq. 133)}$$

$$\begin{aligned} &\boldsymbol{W_{p,u,t}^{revenue,u}} + \boldsymbol{Z_{p,u}^{revenue,u}} \\ &\geq \left(\frac{1}{(1+int_{rate})^{t\,+\,0.5}} \right. \\ &\left. + \frac{1}{(t_{last}+1).\, int_{rate}.\,(1+int_{rate})^{t_{last}+\,1}}\right)\widetilde{pu}_{p,u,t}\boldsymbol{U_{p,u,t}^{revenue,u}} \\ &\qquad \forall(p \in P, u \in U, t \in T\ ) \end{aligned} \qquad \text{(eq. 134)}$$

$$\boldsymbol{FU_{p,u,t}^{sold}} \leq \boldsymbol{U_{p,u,t}^{revenue,u}} \quad \forall(p \in P, u \in U, t \in T\ ) \qquad \text{(eq. 135)}$$

$$-\boldsymbol{U}_{\boldsymbol{p,u,t}}^{\boldsymbol{revenue,u}} \leq \ \boldsymbol{FU}_{\boldsymbol{p,u,t}}^{\boldsymbol{sold}} \quad \forall (p \in P, u \in U, t \in T\ ) \qquad \text{(eq. 136)}$$

3.3.3.5 Profit Taxes

For the robust counterpart formulation, revenues from all periods were grouped into a single variable at present value. However, profit taxes calculation requires an explicit evaluation of revenues at each period because these taxes are only applied to periods with positive profits. Thus, defining $\boldsymbol{R}_{\boldsymbol{t}}^{\boldsymbol{total}}$ as the total revenue for the operation (both from chemical and utility sales) and $\boldsymbol{tax}_{\boldsymbol{t}}^{\boldsymbol{profit}}$ the profit taxes at a period *t*, the profit at this period ($\boldsymbol{L_t}$) can be expressed by equation 137.

$$\boldsymbol{L_t} = \boldsymbol{R}_{\boldsymbol{t}}^{\boldsymbol{total}} - \boldsymbol{C}_{\boldsymbol{t}}^{\boldsymbol{total}} - \boldsymbol{I}_{\boldsymbol{t}}^{\boldsymbol{forest}} - \boldsymbol{tax}_{\boldsymbol{t}}^{\boldsymbol{profit}} \quad \forall\ t \in T \qquad \text{(eq. 137)}$$

The tax on profit is defined accordingly to a rate (tax_{rate}^{profit}) applied to the accounting profit. The accounting profit consists of the difference between total revenues and total operating expenditures at each period ($\boldsymbol{R}_{\boldsymbol{t}}^{\boldsymbol{total}} - \boldsymbol{C}_{\boldsymbol{t}}^{\boldsymbol{total}} - \boldsymbol{I}_{\boldsymbol{t}}^{\boldsymbol{forest}}$). Depreciation of investments may be discounted from the accounting profit. The total productive and storage investments ($\boldsymbol{I}^{\boldsymbol{production}} + \boldsymbol{I}^{\boldsymbol{storage}}$) are depreciated during a certain time ($t_{depreciation}$). This tax profit formulation for periods of depreciation is given by equation 138 and for non-depreciation periods by equation 139. As profit taxes are only incident on positive profits, they will be defined through inequalities, which does not alter the optimal solution as profit taxes directly reduces the objective function defined in section 3.3.4 and will not assume on optimality any value beyond the strict minimum imposed by equations 138 and 139.

$$\boldsymbol{tax}_{\boldsymbol{t}}^{\boldsymbol{Profit}} \geq tax_{rate}^{profit} \left(\boldsymbol{R}_{\boldsymbol{t}}^{\boldsymbol{total}} - \boldsymbol{C}_{\boldsymbol{t}}^{\boldsymbol{total}} - \boldsymbol{I}_{\boldsymbol{t}}^{\boldsymbol{forest}} - \frac{\left(\boldsymbol{I}^{\boldsymbol{production}} + \boldsymbol{I}^{\boldsymbol{storage}} \right)}{t_{depreciation}} \right) \quad \forall \mathrm{t} \leq \mathrm{t}_{\mathrm{depreciation}} \in T \qquad \text{(eq. 138)}$$

$$\boldsymbol{tax_t^{Profit}} \geq tax_{rate}^{profit}\left(\boldsymbol{R_t^{total}} - \boldsymbol{C_t^{total}} - \boldsymbol{I_t^{forest}}\right) \quad \forall \mathrm{t} > \mathrm{t_{depreciation}} \in T \qquad \text{(eq. 139)}$$

3.3.3.6 Estimation Of Revenues At Each Period For Taxes Calculation

As profit tax formulation needs explicit isolation of revenues at each period and the revenues at each period are dependent upon the uncertain prices, the worst-case scenario will be considered, i.e., the maximum price for each chemical will be taken for calculating $\boldsymbol{R_t^{total}}$ (eq. 140). This representation leads to an underestimation of the real operating NPV as it expects all prices to be at their highest for taxes calculation.

$$\boldsymbol{R_t^{total}} = \sum_{\boldsymbol{m} \in \mathrm{M}} \sum_{\boldsymbol{q} \in \boldsymbol{Q}} \Big(\overline{pq}_{m,q,t} + \min(\psi_{m,q,t}^{price,q}, \Gamma_{m,q}^{price,q})\ \widetilde{pq}_{m,q,t}\Big)\left(\sum_{\boldsymbol{p} \in \mathrm{P}} \big(1 - tax_{p,m,q}^{sales,P}\big)\boldsymbol{FPM_{p,m,q,t}} + \sum_{\boldsymbol{e} \in \mathrm{E}} \big(1 - tax_{e,m,q}^{sales,E}\big)\boldsymbol{FEM_{e,m,q,t}}\right) + \sum_{\boldsymbol{p} \in \mathrm{P}} \sum_{\boldsymbol{u} \in \boldsymbol{U}} \Big(\overline{pu}_{p,u,t} + \min(\psi_{p,u,t}^{price,u}, \Gamma_{p,u}^{price,u})\ \widetilde{pu}_{p,u,t}\Big)\big(1 - tax_{p,u}^{sales,U}\big)\boldsymbol{FU_{p,u,t}^{sold}} \qquad \text{(eq. 140)}$$

The term $\left(\overline{pq}_{m,q,t} + \min(\psi_{m,q,t}^{price,q}, \Gamma_{m,q}^{price,q})\ \widetilde{pq}_{m,q,t}\right)$ in equation 140 represents the maximum possible selling price for a pseudo-component *q* on a market *m* at a period *t*. It is given by the nominal value of price summed the positive incidence of the uncertain price. The term $\min(\psi_{m,q,t}^{price,q}, \Gamma_{m,q}^{price,q})$ represents the maximum positive value allowed for the variable $\xi_{m,q,t}^{price}$ in equation 112 when constrained within an interval set given by the constant $\psi_{m,q,t}^{price}$ (eq. 113) and a polyhedral given by the constant $\Gamma_{m,q}^{price}$ (eq. 114).

3.3.4 Objective Function

The objective function is defined as the Net Present Values ($\boldsymbol{NPV}$) of the cash flow generated on the operational time horizon. Production and Storage Investments are incidents in the first period of operation and profit is incident in the middle of each period *t* with no perpetuity growth analogously to equations 115 and 116. Equations 141 to 143 give the present value for cost, forest investments, and profit taxes, and equation144 the NPV.

$$\boldsymbol{C}^{\boldsymbol{present\ value}} = \sum_{\boldsymbol{t}\in\mathrm{T}} \left(\frac{\boldsymbol{C}_{\boldsymbol{t}}^{\boldsymbol{total}}}{(1 + int_{rate})^{t+0.5}} \right) + \frac{\frac{\left(\frac{\sum_{\boldsymbol{t}\in\mathrm{T}} \boldsymbol{C}_{\boldsymbol{t}}^{\boldsymbol{total}}}{t_{last} + 1} \right)}{int_{rate}}}{(1 + int_{rate})^{t_{last} + 1}} \quad \text{(eq. 141)}$$

$$\boldsymbol{I}^{\boldsymbol{forest,present\ value}} = \sum_{\boldsymbol{t}\in\mathrm{T}} \left(\frac{\boldsymbol{I}_{\boldsymbol{t}}^{\boldsymbol{forest}}}{(1 + int_{rate})^{t+0.5}} \right) + \frac{\frac{\left(\frac{\sum_{\boldsymbol{t}\in\mathrm{T}} \boldsymbol{I}_{\boldsymbol{t}}^{\boldsymbol{forest}}}{t_{last} + 1} \right)}{int_{rate}}}{(1 + int_{rate})^{t_{last} + 1}} \quad \text{(eq. 142)}$$

$$\boldsymbol{tax}^{\boldsymbol{profit,present\ value}} = \sum_{\boldsymbol{t}\in\mathrm{T}} \left(\frac{\boldsymbol{tax}_{\boldsymbol{t}}^{\boldsymbol{profit}}}{(1 + int_{rate})^{t+0.5}} \right) + \frac{\frac{\left(\frac{\sum_{\boldsymbol{t}\in\mathrm{T}} \boldsymbol{tax}_{\boldsymbol{t}}^{\boldsymbol{profit}}}{t_{last} + 1} \right)}{int_{rate}}}{(1 + int_{rate})^{t_{last} + 1}} \quad \text{(eq. 143)}$$

$$\begin{aligned} \boldsymbol{NPV} = \boldsymbol{RQ}^{\boldsymbol{present\ value}} + \boldsymbol{RU}^{\boldsymbol{present\ value}} - \boldsymbol{I}^{\boldsymbol{Production}} - \boldsymbol{I}^{\boldsymbol{Storage}} \\ - \boldsymbol{I}^{\boldsymbol{forest,present\ value}} - \boldsymbol{C}^{\boldsymbol{present\ value}} \\ - \boldsymbol{tax}^{\boldsymbol{profit,present\ value}} \end{aligned} \quad \text{(eq. 144)}$$

The choice of the NPV as the economic objective is motivated by its ability to integrate into the same indicator cash flows generated in different time periods and compare them regarding the cost of capital. This leads to a fair evaluation of investments trade-offs, such as the decision of centralizing or decentralizing production facilities. In the first option, initial investments are lower for a same total production capacity due to gains of scale, but the longer distances from biomass sourcing and consumer markets might impose larger logistic costs during the several years of biorefinery operation.

4 CASE STUDY

The case study consists of the design of a eucalyptus-based biorefinery producing paper-grade Bleached Eucalyptus Kraft Pulp (BEKP), electricity, and lignin in Brazil. This case will be used to illustrate how the generic model developed in the previous section can be instantiated and applied to the design of forest-based biorefineries.

4.1 DATA GATHERING

Section 4.1.1 presents the sets used by the mathematical model. These sets define the dimension for the input parameters discussed in Sections 4.1.2 (Forest), 4.1.3 (Technology), 4.1.4 (Logistics), and 4.1.5 (Market). A spreadsheet with the collected values for the input parameters will be made available upon request.

4.1.1 Sets Definition

The choice for the potential locations for forest, production, storage, and market layers is discussed in sections 4.1.1.1, 4.1.1.4, 4.1.1.5, and 4.1.1.3, respectively. The choice of which biomass species and ages to be considered is discussed in section 4.1.1.2. The available conversion technologies are presented in section 4.1.1.6 while the pseudo-component, utilities, and residues in section 4.1.1.7. The periods of operational, construction, and depreciation is presented in section 4.1.1.8.

4.1.1.1 Set F – Forest Units

The forest layer will be segmented following the Brazilian political division into 27 Federative Units (*Unidades Federativas,* UF). Climate and/or geological criteria could be another approach for forest segmentation. For instance, Binkley et al. (2017) reported a 3 times higher biomass growth for forests distant only 100 km, which indicates that a climate-geological segmentation of the Forest Layer should be preferred over a political one if data is available.

The top-10 UFs regarding eucalyptus planted area accordingly to the IBÁ (Brazilian Tree Institute) mapping are considered into the forest unit set (INSTITUTO BRASILEIRO DE ÁRVORES, 2015). Goiás and Tocantins UFs are not within this list but will also be considered into the forest unit's set as they are, respectively, the 3rd and 5th largest UFs regarding lands available for plantation (hereafter called free lands), accordingly to Lossau et al. (2015). These states together represent more than 95% of the total eucalyptus-planted land and more than 83% of all free lands in Brazil as discussed in Sections 4.1.2.1 and 4.1.2.2. The list of all UFs considered in the model is displayed in Table 1.

Table 1 - List of all federative units (UFs) considered in the forest unit's set F.

Forest unit ID	Federative Unit (UF)
1	Bahia
2	Espírito Santo
3	Goiás
4	Maranhão
5	Mato Grosso
6	Mato Grosso do Sul
7	Minas Gerais
8	Paraná
9	Rio Grande do Sul
10	Santa Catarina
11	São Paulo
12	Tocantins

4.1.1.2 Sets B And I – Biomass Species And Ages

The biomass species considered are *E. urophylla* and *E. grandis x E. camaldulensis*. These species are the top performers in the Tropical and Subtropical Zones[8], respectively, in the eucalyptus productivity map in Brazil by Binkley et al. (2017). A list of all considered biomass species in the model is presented in Table 2.

Table 2 - List of all eucalyptus species considered in biomass species' set B.

Biomass species ID	Eucalyptus species
1	*E. urophylla*
2	*E. grandis x E. camaldulensis*

[8] Top performer among species that were planted on both zones. Some species were planted only on one zone and were not considered for this case study as data would be missing for some forest units.

The growth of these biomass species is modeled over twelve years, i.e., the set I that comprises all biomass ages in the model is given by all integers from 0 to 12, inclusive. When biomass ages beyond the maximum age of 12, it will be considered the same as the 12-years-old biomass, as growth beyond the maximum allowed age is considered neglectable. The 0-year-old biomass is the one that has been planted within the same period of consideration.

4.1.1.3 Set M – Consumer Markets

The market layer is the only one that contains both domestic and external locations. According to the Brazilian Pulp and Paper Producers Association (ABTCP) sector report (FARINHA E SILVA; BUENO; NEVES, 2017) , Europe, China, and North America represent over 89% of the Brazilian pulp exports. These three locations will comprise the set of all potential overseas markets, a subset of the Set M with all potential market locations (Table 3).

Table 3 - List of all federative units (UFs) and overseas locations considered in the market unit's set M.

Market unit ID	Location
1	Bahia
2	Goiás
3	Mato Grosso do Sul
4	Paraná
5	Rio Grande do Sul
6	Santa Catarina
7	São Paulo
8	Alagoas
9	Rio de Janeiro
10	Pará
11	Ceará
12	Minas Gerais
13	Distrito Federal
14	Paraíba
15	Sergipe
16	Espírito Santo
17	Europe
18	China
19	North America

The domestic locations included in set M were chosen given by all Brazilian UFs that present installed capacity for print and write (P&W) and tissue papers, the major products driving BEKP demand as discussed further in section 4.1.5.3. UFs that do not present tissue or P&W production capacities but are relevant to the lignin market are also included in the set M. The UFs were included until 90% of all mapped cement production capacity (the major application for lignin considered in this case study[9]) was represented in the Set M.

4.1.1.4 Set P – Production Facilities

The Set P with all possible production facilities locations will be defined as the union of the forest and domestic consumer markets' locations sets. This enables production facilities to be close to the biomass supply or consumers' demands. The production facilities produce Bleached Eucalyptus Kraft Pulp (BEKP) with the possibility of having both Lignin and Electricity as co-products. The list of all UFs considered in the model is displayed in Table 4.

Table 4. List of all federative units (UFs) considered in the production unit's set P.

Production unit ID	Federative Unit (UF)
1	Alagoas
2	Bahia
3	Ceará
4	Distrito Federal
5	Espírito Santo
6	Goiás
7	Maranhão
8	Mato Grosso
9	Mato Grosso do Sul
10	Minas Gerais
11	Pará
12	Paraíba
13	Paraná
14	Pernambuco
15	Rio de Janeiro
16	Rio Grande do Sul
17	Santa Catarina
18	São Paulo
19	Sergipe
20	Tocantins

[9] The use of lignin in cement and other construction materials is discussed by Jędrzejczak et al. (2021).

4.1.1.5 Set E – Storage Facilities

The set with all storage facilities locations is defined as the union of all production facilities locations set and all the ports' locations. These ports' locations are introduced to enable overseas markets to be accessed through sea freight. A representative port is chosen for each of the Brazilian political regions with access to the sea (North, Northeast, Southeast, and South). The representative port of each region is taken as the port with the greatest cargo movement in that region according to the statistical annual report by ANTAQ (Sea Transportation National Agency) (AGÊNCIA NACIONAL DE TRANSPORTE AQUAVIÁRIO, 2021): Vila do Conde (Pará, North), Suape (Pernambuco, Northeast), Santos (São Paulo, Southeast) e Paranaguá (Paraná, South). These port locations correspond to an important subset of the Set E in modeling overseas freight. The list of all locations (port and no-port locations) included in Set E is displayed in Table 5.

Table 5 - List of all federative units (UFs) and ports considered in the storage unit's set E.

Storage unit ID	Federative Unit (UF)
1	Alagoas
2	Bahia
3	Ceará
4	Distrito Federal
5	Espírito Santo
6	Goiás
7	Maranhão
8	Mato Grosso
9	Mato Grosso do Sul
10	Minas Gerais
11	Pará
12	Paraíba
13	Paraná
14	Paranaguá
15	Pernambuco
16	Rio de Janeiro
17	Rio Grande do Sul
18	Santa Catarina
19	Santos
20	São Paulo
21	Sergipe
22	Suape
23	Tocantins
24	Vila do Conde

4.1.1.6 Set Z – Technologies

The most common process to produce cellulose pulp is the Kraft process (SIXTA, 2006) and is considered the base technological process in the model. The Kraft process consists of several operations grouped here into four: (I) Wood Preparation, responsible for the processing of raw wood into wood chips for cooking; (II) Kraft Cooking, responsible for the heat and chemical treatment of the woodchips for removing lignin; (III) Bleaching, responsible for removing the residual lignin and other chromophores compounds from the pulp. This step will also comprise the drying and packaging operations; and (IV) Chemical Recovery, comprising a set of operations to recover the inorganic chemicals used in cooking through burning the lignin-rich liquor (black liquor) on a recovery boiler.

As the chemical recovery stage burns the black liquor, steam is generated. The steam can be used in other operations and/or for electricity generation on a steam turbine. A biomass boiler will also be considered to burn the residuals from wood preparation (wood fines) and generate additional steam.

The burn of black liquor, however, may not be the most strategic decision as lignin presents a high potential to be used as a chemical (HOLLADAY et al., 2007). Therefore, an acid precipitation stage is considered for lignin recovery from the black liquor via acidification with CO_2 and sulfuric acid. A Block Flow Diagram (BFD) comprising all technologies considered in the model is shown in Figure 4 and a complete list of all technologies is displayed in Table 6.

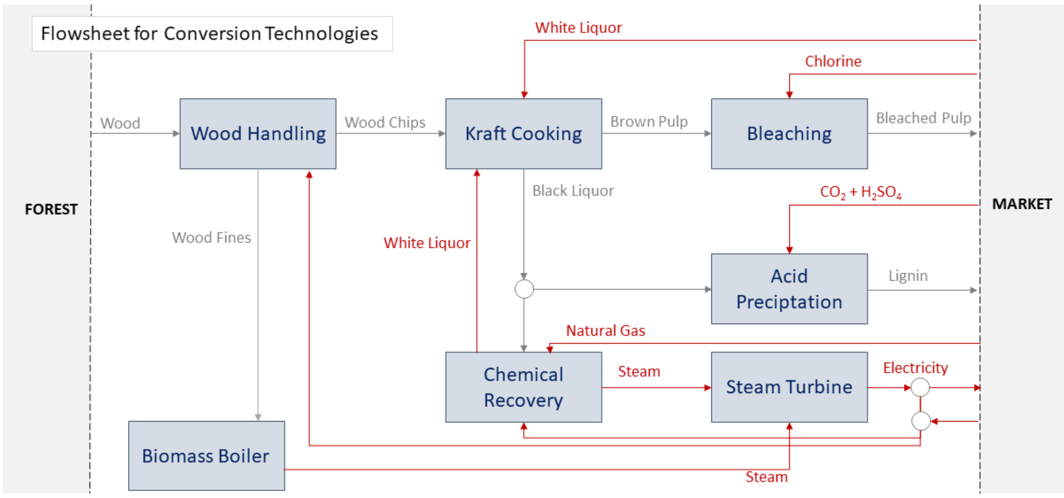

Figure 4 - A visual representation of conversion technologies considered in the model. Technologies are represented as blue rectangles. Chemical pseudo-components and utility flow are represented as grey and red arrows, respectively. Wood species come from the forest Layer. Bleached Pulp and Lignin can be sold to markets. White Liquor, Chlorine, Natural Gas, CO2, and H2SO4 can be bought from the market. Electricity can be either bought or sold to the market.

Table 6 - List of all technologies considered in set Z.

Technology ID	Technology
1	Wood Handling
2	Kraft Cooking
3	Acid Precipitation
4	Chemical Recovery
5	Bleaching
6	Steam Turbine
7	Biomass Boiler

4.1.1.7 Sets Q, U, And R – Pseudo-Components, Utilities, And Effluents

The BFD in Figure 4 highlights pseudo-components and utilities flows. The flowsheet starts with a generic component “wood” representing the eucalyptus biomass. It is known that different Eucalyptus species are associated with different chemical compositions (CARRILLO et al., 2018; OHRA-AHO et al., 2018). However, for the scope of this work, it is assumed that all eucalyptus species from all forest units yield biomass with the same chemical and physical characteristics.

Wood chips and fines are the results of wood handling operations. The latter is used as burning fuel in biomass boilers and the first is cooked for lignin removal from cellulose. During cooking, lignin and some other wood components are dissolved in the cooking liquor. The remainder solid product (Brown Pulp) is separated from the cooking liquor (Black Liquor) and subject to a bleaching and drying process that yields a final marketable product (Bleached Pulp). The lignin dissolved in the black liquor can be extracted in an acid-precipitation stage yielding powder lignin, another marketable product. This completes the list of chemical pseudo-components considered in the model displayed in Table 7.

Besides chemical pseudo-components, utilities should also be considered in the model. The difference between them is that chemical pseudo-components may be stored, transferred to other production facilities, and sold to consumer markets. Utilities may not be stored nor transferred and can only be bought or sold within the same production facility location in which they are produced.

Table 7 - List of all chemical pseudo-components included in the pseudo-components set Q.

Pseudo-component ID	Pseudo-component
1	Wood
2	Wood Chips
3	Brown Pulp
4	Black Liquor
5	Lignin
6	Bleached Pulp
7	Wood Fines

Electricity is employed in every production process mentioned in Section 4.1.1.6. Natural gas is also used as an auxiliary energy source in chemical recovery processes. White Liquor is taken as a representative utility pseudo-component for the kraft cooking chemicals and chlorine as a representative for the bleaching chemicals. Lignin precipitation requires Carbon Dioxide (CO_2) and Sulfuric Acid (H_2SO_4). These utilities compose the Set U displayed in Table 8.

Table 8. List of all utilities included in the utilities set U.

Utility ID	Utility
1	Electricity
2	White Liquor
3	Steam
4	Chlorine
5	CO_2
6	H_2SO4
7	Natural Gas

The production processes also generate some effluents and residues that must be managed. In this work, no distinction between types of effluent or residues will be made and the Set R is represented by a single pseudo-component named *effluent*. Effluent treatment units are not modelled explicitly, but all the effluent generated is associated with an effluent treatment cost representing the disposal or treatment of such effluent, as described in section 4.1.3.6.

4.1.1.8 Set T – Periods

The time horizon for the model will be of 20 years. The idle time between a production or storage investment is made until facilities are completely operational is taken as 2 years. Depreciation time for investments is considered as 10 years.

4.1.2 Forest Parameters

Forest parameters that must be inputted into the model are: (I) planted land profiles from third parties and self-owned at each forest unit for all biomass species of all ages (section 4.1.2.1); (II) free land profiles at each forest unit (section 4.1.2.2); (III) growth characteristics and chemical composition of each biomass species at each age and each forest location (section 4.1.2.3); (IV) harvesting efficiency for each biomass (section 4.1.1.4); (V) forest operating costs (Section 4.1.2.5); and (VI) acquisition prices for third parties' lands (section 4.1.2.6).

4.1.2.1 Planted Lands

According to IBÁ (INSTITUTO BRASILEIRO DE ÁRVORES, 2015), Brazil has a total of 7.74 million hectares of planted forest. 72% of those are planted with eucalyptus and 21% with pine. Also, only 7 UFs (Minas Gerais, São Paulo, Paraná, Mato Grosso do Sul, Bahia, Santa Catarina, and Rio Grande do Sul) are responsible for 82% of all planted forest lands in the country, 80% of all eucalyptus-planted lands and 96% of all pine-planted lands. The complete data for each UF is displayed in Table 9.

The top 10 UFs regarding planted land will be considered in the forest unit Set F as already mentioned in Section 4.1.1.1. These UFs are Minas Gerais, São Paulo, Paraná, Mato Grosso do Sul, Bahia, Santa Catarina, Rio Grande do Sul, Mato Grosso, Espírito Santo, and Maranhão.

According to the IBÁ mapping, only 34% of all planted forest lands belong to the Pulp and Paper segment. Thus, the available lands considered in the model will be 34% of those reported in Table 9 for each forest unit.

Table 9 - Map of planted forest lands in Brazil.

Federative Unit	Eucalyptus		Pine		Others		**Total**	
	[ha]	[%]	[ha]	[%]	[ha]	[%]	[ha]	[%]
Minas Gerais	1,400,232	*25.2%*	39,674	*2.4%*	5,313	*1.0%*	**1,445,219**	***19%***
São Paulo	976,186	*17.6%*	123,996	*7.5%*	90,147	*16.9%*	**1,190,329**	***15%***
Paraná	224,089	*4.0%*	673,769	*41.0%*	16,255	*3.1%*	**914,113**	***12%***
Mato Grosso do Sul	803,699	*14.5%*	7,135	*0.4%*	23,000	*4.3%*	**833,834**	***11%***
Bahia	630,808	*11.3%*	6,499	*0.4%*	34,000	*6.4%*	**671,307**	***9%***
Santa Catarina	112,944	*2.0%*	541,162	*32.9%*	6,645	*1.2%*	**660,751**	***9%***
Rio Grande do Sul	309,125	*5.6%*	184,585	*11.2%*	103,592	*19.5%*	**597,302**	***8%***
Mato Grosso	187,090	*3.4%*	0	*0.0%*	113,249	*21.3%*	**300,339**	***4%***
Espírito Santo	228,781	*4.1%*	2,660	*0.2%*	15,000	*2.8%*	**246,441**	***3%***
Maranhão	211,334	*3.8%*	0	*0.0%*	0	*0.0%*	**211,334**	***3%***
Pará	125,110	*2.3%*	0	*0.0%*	72,368	*13.6%*	**197,478**	***3%***
Tocantins	115,564	*2.1%*	430	*0.0%*	45,876	*8.6%*	**161,870**	***2%***
Goiás	124,297	*2.2%*	9,087	*0.6%*	5,000	*0.9%*	**138,384**	***2%***
Amapá	60,025	*1.1%*	0	*0.0%*	1,936	*0.4%*	**61,961**	***1%***
Piauí	31,212	*0.6%*	0	*0.0%*	0	*0.0%*	**31,212**	***0%***
Others	18,157	0.3%	56,140	3.4%	0	0.0%	**74,297**	**1%**
Total	**5,558,653**	***100%***	**1,645,137**	***100%***	**532,381**	***100%***	**7,736,171**	***100%***

Source: IBÁ (INSTITUTO BRASILEIRO DE ÁRVORES, 2015)

The mapping, however, does not differentiate lands according to eucalyptus species and neither include their respective age. Thus, it is assumed in the case study that Paraná, Santa Catarina, and Rio Grande do Sul have all their lands planted exclusively with biomass *E. grandis x E. camaldulensis* that has presented the higher productivity in the subtropical zones in the study conducted by Binkley et al. (2017). All other UFs are supposed to be planted with *E. urophylla*, the most productive biomass for the tropical zone in the same study. Regarding age, it is assumed that lands' age has a normal distribution with a mean of 5 years and a variance of 2 for all forest units.

Finally, for the complete characterization of planted lands profile, it is considered that all lands are owned by third parties and are available for buying at the prices discussed in section 4.1.2.6.

4.1.2.2 Free Lands

The adoption of biorefineries may imply a higher demand for arable lands. For this adoption to be sustainable, expansion must be conducted in a way that preserves highly biodiverse ecosystems, does not threaten the production and supply of food, and mitigates GHG emissions due to deforestation and land-use change.

In this direction, Lossau et al. (2015) mapped the Brazilian territory for lands that are available for sustainable biofuels production. This classification (named *residual III* lands) excludes lands that: (I) are already used by agriculture, livestock, and/or fibers production; (II) results in direct or indirect deforestation; (III) are under any form of legal protection; (IV) is associated with biodiversity loss; (V) compete for scarce freshwater, and/or (VI) cause land degradation or an increase in GHG emission due to fertilizers usage or land-use change. The area of free lands suited for sustainable plantation is displayed in Table 10.

Table 10 shows that Goiás and Piauí are relevant regarding available lands for plantation and are also included in the Set F of all forest units considered in the model along with the major UFs regarding planted forest areas. Figure 5 shows the total eucalyptus planted land and free land available for plantation for each Brazilian UF.

Table 10 **–** Mapping of available lands for sustainable plantation for biofuels production in Brazil.

Federative Unit	Total Area		Residual I		Residual II		Residual III	
	[kha]	[%]	[kha]	[%]	[kha]	[%]	[kha]	[%]
Minas Gerais	58,931	*6.9%*	19,629	*22.9%*	12,547	*30.0%*	12,547	*33%*
Bahia	56,683	*6.6%*	9,003	*10.5%*	4,271	*10.2%*	4,271	*11%*
Goiás	34,185	*4.0%*	6,637	*7.8%*	3,482	*8.3%*	3,482	*9%*
São Paulo	24,909	*2.9%*	4,426	*5.2%*	3,305	*7.9%*	3,305	*9%*
Tocantins	27,931	*3.3%*	7,359	*8.6%*	2,775	*6.6%*	2,550	*7%*
Maranhão	32,977	*3.9%*	4,823	*5.6%*	2,284	*5.5%*	1,879	*5%*
Mato Grosso	90,853	*10.7%*	5,064	*5.9%*	2,362	*5.6%*	1,835	*5%*
Mato Grosso do Sul	35,859	*4.2%*	2,347	*2.7%*	1,427	*3.4%*	1,427	*4%*
Paraná	19,932	*2.3%*	1,692	*2.0%*	1,306	*3.1%*	1,306	*3%*
Piauí	25,318	*3.0%*	3,380	*3.9%*	1,138	*2.7%*	1,138	*3%*
Rio Grande do Sul	26,896	*3.2%*	2,080	*2.4%*	1,112	*2.7%*	1,112	*3%*
Espírito Santo	4,623	*0.5%*	1,248	*1.5%*	794	*1.9%*	794	*2%*
Rio de Janeiro	4,374	*0.5%*	1,410	*1.6%*	779	*1.9%*	779	*2%*
Santa Catarina	9,523	*1.1%*	924	*1.1%*	576	*1.4%*	576	*2%*
Pernambuco	9,872	*1.2%*	472	*0.6%*	236	*0.6%*	236	*1%*
Ceará	14,984	*1.8%*	293	*0.3%*	176	*0.4%*	176	*0%*
Paraíba	5,682	*0.7%*	236	*0.3%*	173	*0.4%*	173	*0%*
Rio Grande do Norte	5,311	*0.6%*	230	*0.3%*	128	*0.3%*	128	*0%*
Sergipe	2,197	*0.3%*	101	*0.1%*	46	*0.1%*	46	*0%*
Alagoas	2,791	*0.3%*	49	*0.1%*	27	*0.1%*	27	*0%*
Distrito Federal	582	*0.1%*	221	*0.3%*	12	*0.0%*	12	*0%*
Rondônia	23,893	*2.8%*	681	*0.8%*	362	*0.9%*	0	*0%*
Acre	16,512	*1.9%*	43	*0.1%*	39	*0.1%*	0	*0%*
Amazonas	156,935	*18.4%*	2,315	*2.7%*	388	*0.9%*	0	*0%*
Roraima	22,574	*2.6%*	4,270	*5.0%*	167	*0.4%*	0	*0%*
Pará	124,289	*14.6%*	5,677	*6.6%*	1,880	*4.5%*	0	*0%*
Amapá	14,099	*1.7%*	997	*1.2%*	49	*0.1%*	0	*0%*
Total	**852,715**	***100%***	**85,607**	***100%***	**41,841**	***100%***	**37,799**	***100%***

Source: Lossau et al. (2015).

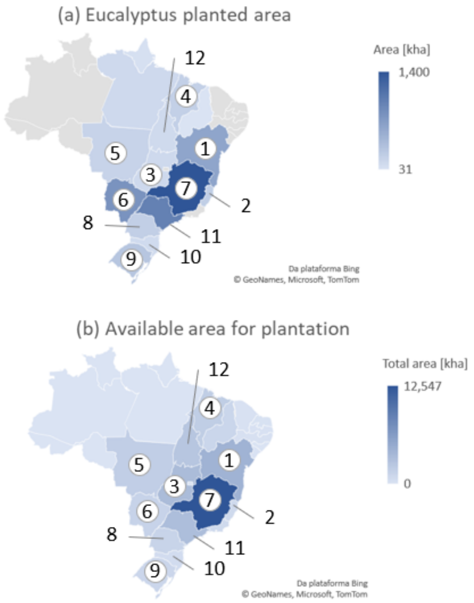

Forest units considered on model	
Bahia	1
Espírito Santo	2
Goiás	3
Maranhão	4
Mato Grosso	5
Mato Grosso do Sul	6
Minas Gerais	7
Paraná	8
Rio Grande do Sul	9
Santa Catarina	10
São Paulo	11
Tocantins	12

Figure 5 - Total eucalyptus planted area (a) and free land available for plantation (b) for each Brazilian federal unit.
Federal units chosen as potential forest units for the model were marked with an identification number that can be matched on the adjacent table. Source: Based on data from (a) IBÁ (INSTITUTO BRASILEIRO DE ÁRVORES, 2015) and (b) Lossau et al. (2015).

4.1.2.3 Productivity, Growth, And Chemical Composition

This work adopts the logistic curve as a description of forest biomass growth[10] (eq. 145), in which biomass volume (V) is considered as a logistic function of the stand year (t), the maximum asymptotic volume (V_{max}) and a coefficient α that represents the inflection point of biomass growth, in years.

$$V = \frac{V_{max}}{1 + e^{\alpha - t}} \quad \text{(eq. 145)}$$

The value of α is taken as 4 for all biomass species in all forest units. This parameter was chosen as an approximation to the middle year of typical eucalyptus rotations in Brazil of 5 to 9 years, as reported by Diaz-Balteiro and Rodriguez (2006). The asymptotic volume, in Mg/ha, was empirically taken as 10 times the mean productivity of each biomass species in each forest unit, in Mg/(ha.year). These

[10] Other biomass growth modeling are discussed in Scolforo et al. (2019).

productivity values were estimated accordingly to the reported values of eucalyptus yield in Binkley et al. (2017). Each forest unit was matched to a representative site in the work of Binkley et al., which was the reference for estimating each eucalyptus clone productivity in these forest units. The complete list of forest units, representative sites, and estimated productivities is displayed in Table 11.

Table 11 - Productivity data for each biomass species at each forest unit

Forest ID	Federative Unit	Representative Site	E. Urophylla [Mg/(ha.year)]	E. grandis x E. Camaldulensis [Mg/(ha.year)]
1	Bahia	Eunápolis	40	10
2	Espírito Santo	Aracruz	40	10
3	Goiás	Niquelândia	35	15
4	Maranhão	Urbano Santos	35	15
5	Mato Grosso	Rio Verde	50	40
6	Mato Grosso do Sul	Três Lagoas	40	10
7	Minas Gerais	Três Marias	30	10
8	Paraná	Telêmaco Borba	20	30
9	Rio Grande do Sul	Eldorado do Sul	40	30
10	Santa Catarina	Otacílio Costa	20	20
11	São Paulo	Botucatu	40	30
12	Tocantins	Brejinho de Nazaré	30	10
		Mean	**35,00**	**19,17**

Binkley et al. (2017) reported a variation of 2- to 6-fold on clone performance across sites. This indicates the relevance of accounting for uncertainties in the decision process. Thus, for each of the production sites, a variation of 50% from the nominal value reported in Table 11 is considered for the robust representation of biomass growth.

As considering the logistic curve directly into the model would result in a non-linear optimization model, the estimated logistic growth curves for each clone at each forest location were discretized into a 12-year time-horizon and inputted as the accumulated growth parameter (Figure 6).

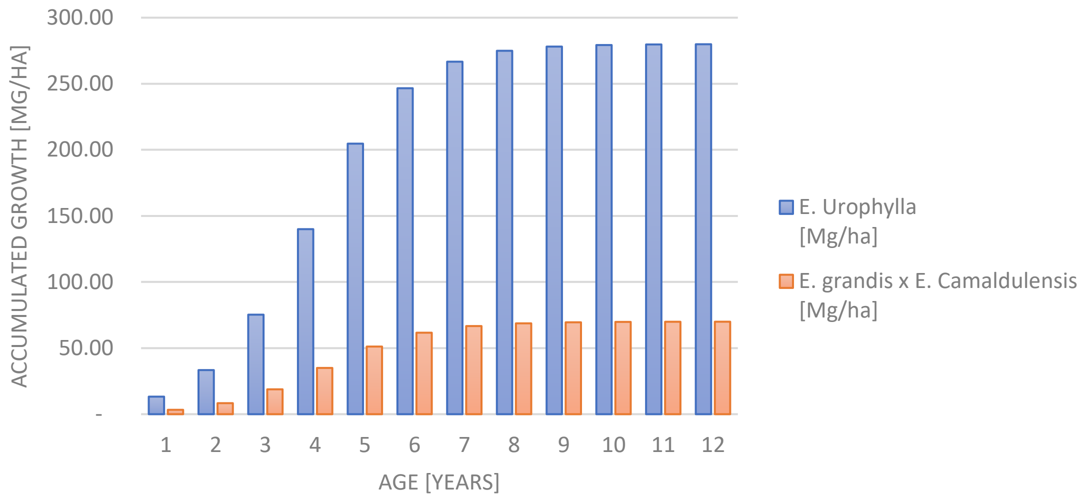

Figure 6 - Accumulated growth estimated for each year for E. urophylla and E. grandis x E. camaldulensis planted in Bahia UF.

Differences in biomass composition between the different biomass species and forest units will not be considered in the present work. All biomass species in all forest units will have their composition mapped a chemical pseudo-component named “Wood” in Set Q (Section 4.1.1.7), as stated by equation 146.

$$\begin{cases} x_{f,b,q} = 1 & if\ q = 'Wood' \\ x_{f,b,q} = 0 & otherwise \end{cases} \qquad \forall (f \in F, b \in B) \qquad \text{(eq. 146)}$$

4.1.2.4 Forest Operating Efficiency

The amount of biomass produced in the field must be harvested and brought to the production units. In the scope of the present work, only the losses from harvesting are considered in this process. Van der Merwe; Pulkki and Ackerman (2015) reported a 1.7% fiber loss in single-grip harvester operations on eucalyptus. Thus, forest operating efficiency is taken as 98.3% for all biomass species in this work.

4.1.2.5 Forest Operating Costs

Forest operating costs were taken from the FAMATO (FEDERAÇÃO DA AGRICULTURA E PECUÁRIA DO ESTADO DE MATO GROSSO, 2013) that maps all costs associated with eucalyptus plantation in Mato Grosso UF.

Soil handling, ant control, pre-plantation desiccation, soil chemical amendment, furrowing, fertilization, and other operations needed for starting a eucalyptus plantation are estimated at R$ 3.578,26 each hectare, interests and administrative costs included. These operating costs are incorporated into the planted land maintenance cost parameter for biomass with age 0 in the model. For the following year, FAMATO also suggests some rigorous maintenance, such as herbicides application and plagues control, with an estimated cost of R$ 446,39 for each hectare. From the year-2 and beyond, only plague control operations are recommended by FAMATO, with a value of R$ 91,00 for each hectare. This cost will also be taken as a reference for free land maintenance costs.

The reported costs are referenced in 2013 and were updated in this work to 2021-values according to the Brazilian price-index to the consumer (IPCA) historical data provided by the Central Bank of Brazil (BANCO CENTRAL DO BRASIL, 2021a). These updated costs are displayed in Table 12 and they are considered for all biomass species in all forest units in the model.

Table 12 **-** Forest Operating costs corrected by inflation.

Cost Description	Cost in 2013 [BRL/ha]	Cost in 2021 [BRL/ha]
Land maintenance for biomass age 0 (plantation costs)	3,578.26	5,215,26.
Land maintenance for biomass age 1 (following year pos-plantation)	446.39	650.67
Land maintenance for biomass age 2 and beyond	91.00	132.64
Free land maintenance	91.00	132.64

Source: Adapted from FAMARO (FEDERAÇÃO DA AGRICULTURA E PECUÁRIA DO ESTADO DE MATO GROSSO, 2013) using inflation data from Central Bank of Brazil (BANCO CENTRAL DO BRASIL, 2021a).

4.1.2.6 Forest Investments - Land Acquisition

Investments for non-planted lands in Brazil were taken from agricultural lands price study by Caetano Bacha, Stege, and Harbs (2016) and updated to 2021-values using Brazil Central Brank inflation historical data as displayed in Table 13. As prices were mapped for each Brazilian region, Table 14 relates which region each forest unit belongs to.

Table 13 - Land acquisition price in all five Brazilian regions.

Region	Price in 2016 [BRL/ha]	Price in 2021 [BRL/ha]
South	21.555,47	31,419.70
Southeast	12.224,19	17,818.23
Mid-West	12.764,40	18,605.66
Northeast	5.222,04	7,611.75
North	3.373,18	4,916.82

Source: Prices in 2016 by Caetano Bacha, Stege, and Harbs (2016) updated by inflation data in this work from the Central Bank of Brazil (BANCO CENTRAL DO BRASIL, 2021a).

Land acquisition for lands already planted with biomass will be given as a function of the wood already grown in it, i.e., given by a multiple of the accumulated growth parameter. This multiple is defined as BRL 603.67 per ton of dried wood, estimated from the wood price of USD 66.00 per wet ton of wood reported by Pereira et al. (2018) and converted to reais using the currency ratio of 5.00 BRL/USD (section 4.1.5.1). Then, these values were updated to 2021-values by the historical inflation data by Central Bank of Brazil (BANCO CENTRAL DO BRASIL, 2021a) and correct to dry weight considering 59.6% of solid content in wood as reported by Vinha Zanuncio et al. (2017) for *E. urophylla* logs left for drying in the field for 90 days.

Table 14 - Brazilian UFs considered in the model and its region.

UF	Region
Minas Gerais	Southeast
Bahia	Northeast
Goiás	Mid-West
São Paulo	Southeast
Tocantins	North
Maranhão	Northeast
Mato Grosso	Mid-west
Mato Grosso do Sul	Mid-west
Paraná	South
Piauí	Northeast
Rio Grande do Sul	South
Espírito Santo	Southeast
Santa Catarina	South

4.1.3 Production And Technological Parameters

As mentioned in section 4.1.1.6, the production technologies considered in the present work will be represented as wood handling, bleaching, chemical recovery, biomass boiler, steam turbine, and acid precipitation. These technologies are discussed in sections 4.1.3.1 to 4.1.3.5. Operating costs for these technologies are discussed in section 4.1.3.6 and investments in section 4.1.3.7.

4.1.3.1 Wood Handling

Wood handling is the first processing step in a pulp factory and is responsible for wood debarking and chipping. The wood chips are then classified and stored (BAJPAI, 2018). This set of operations aims at the reduction of chip dimension, as chip thickness is intimately related to the cooking chemicals diffusion and might result in a poor fiber separation or high rejects yield (DANG; NGUYEN, 2008).

The term “wood handling” comprises the cutting, debarking, chipping, storage, and screening operations with a global yield of 95% (RESSEL, 2008) from the pseudo-component “wood” to the pseudo-component “wood chips”. The remainder 5% are converted into the pseudo-component “wood fines” that may be burned in the biomass boiler for steam generation.

4.1.3.2 Kraft Cooking

Kraft cooking consists in treating the wood at high temperatures in the presence of alkali and sulfide ions for the removal of lignin (GIUDICI; PARK, 1996). The result of this cooking is a fibrous dark mass that still contains some residual lignin - the “Brown Pulp” - and a liquor containing most of the used cooking chemicals and the solids dissolved from the wood – the “Black Liquor.”

Accordingly to the ABTCP report (BACHMANN E ASSOCIADOS; ABTCP, 2011) on Pulp and Paper factories benchmark, the mean specific consumption is 3.7 m^3 of wood, for each air-dried metric ton (admt) of pulp for factories working with shortfiber wood as eucalyptus. Considering that air-dried ton is a unit that considers pulp humidity of 90% and adopting a wood density of 500 kg/m³ for eucalyptus wood (PAULO EICHLER et al., 2017), the dried-mass basis yield of brown pulp from fed wood chips is 48.6%.

The same report shows a total dried solids (organic and inorganic) generation of 1.45-ton per each admt of brown pulp leaving the digester. Considering the digester yield of 48.6% of brown pulp from fed wood chips and the conversion of admt to regular tons, the yield of total dried solids on digester is 78.4% for each ton of fed wood chips.

Summing brown pulp and dried solids yields results in total production of 1.27-ton of products for each ton of fed wood chips. The 0.27-ton excess is due to the cooking chemicals that are added to the process. The main chemicals used in Kraft cooking are Sodium Hydroxide (NaOH) and Sodium Sulfide (Na_2S). The latter display a very important role in accelerating delignification reactions improving cooking selectivity when compared to cooking made exclusively from sodium hydroxide (SIXTA; POTTHAST; KROTSCHEK, 2006). The mixture of the two components is called White Liquor and is considered as one of the pseudo-components in the utilities set U, with consumption of 0.27 metric tons for each metric ton of processed wood chips in the digester.

4.1.3.3 Bleaching

The fibrous mass that leaves the cooking digester may still present 1.5 to 4% of lignin that displays a dark color after cooking (SIXTA et al., 2006). Also, some other chromophores compounds must be removed for allowing pulp used as a raw material for tissue and P&W papers. The operations performed to remove the residual lignin and the other chromophores compounds are called pulp bleaching.

In the present work, all bleaching operations are grouped into a single representative operation called “Bleaching” that yields 90% of BEKP from brown pulp accordingly to the values reported by Mao (2007). The remaining 10% are considered as the pseudo-component “effluent”. It is worth mentioning that pulp drying and other product finishing operations such as packaging are also considered in the “Bleaching” representative process in the present work. Thus, the pulp leaving this stage is market ready.

Bleaching operations may be performed through several bleaching stages with the help of some bleaching chemicals such as Cl_2, ClO_2, NaOCl, O_3, O_2, H_2O_2, and others (SIXTA et al., 2006). In the present work, these chemicals are represented by the pseudo-component “Chlorine” used at a rate of 42.7 kg per each admt produced of BEKP as presented in the ABTCP report (BACHMANN E ASSOCIADOS; ABTCP, 2011). Considering the 90% yield of BEKP from brown pulp and the conversion from admt to metric tons, the consumption of “Chlorine” is 52.72kg for each ton of processed brown pulp.

4.1.3.4 Chemical Recovery, Biomass Boiler, And Utilities

One of the main aspects regarding the economic feasibility of the Kraft Process is the possibility of recovering the chemicals used in the cooking stage. The black liquor leaving the pre-bleaching stage is concentrated through a series of evaporators and is then burned in a Recovery Boiler. The burn of the organic chemicals, besides rendering possible the recovery of the inorganic components present in the black liquor, also allows steam generation that might be further consumed by other operations and/or to be converted into electric energy through steam turbines. The inorganic ashes remaining after the liquor is burnt may be recovered in Caustification and Lime Kiln sections as white liquor that are re-used In the cooking stage (KROTSCHECK; SIXTA, 2009).

Evaporation, Recovery Boiler, Caustification, and Lime Kiln are all grouped into the representative process “Chemical Recovery” that produces the utility “white liquor” from black liquor burning. Tran and Vakkilainen (2016) reported a typical recovery efficiency of 97%. Thus, it is assumed that 97% of the 270 kg of pseudo-component “white liquor” added to the cooking stage per each ton of wood chips processed is recovered. As “black liquor solids” yield from brown pulp is 78.4%, the yield of “white liquor” in “Chemical Recovery” is 334 kg per ton of burn black liquor solids.

Chemical recovery not only allows the recovery of cooking chemicals but is also essential to the energy balance of pulp mills. Francis, Towers, and Browne (2002) conducted an energy benchmark with pulp mills reporting the energy consumption of its main processing units. These reported values are grouped and converted to our reference units and considered as the energy consumption parameters for the model in the present work (table 15).

Table 15 **-** Energy consumptions grouped into the representative processes.

Representative Process	Steam [GJ/admt]	Electric Energy [MWh/admt]	Natural Gas. [GJ/admt]	Steam [GJ/ton RM]	Electric Energy [MWh/ton RM]	Natural Gas [Nm³/ton RM]
Wood handling	-	0.02	-	-	0.01	-
Kraft Cooking	2.20	0.15	-	0.99	0.07	-
Bleaching	4.60	0.24	-	4.37	0.23	-
Chemical Recovery	3.10	0.08	1.20	1.73	0.04	19.15

Source: Adapted from Francis, Towers, and Browne (2002). The originally reported values are displayed in reference to BEKP production (admt). These values are converted to a basis-unit of processed raw material (ton RM) using the yield parameters reported in the previous sections.

Francis, Towers, and Browne also reported the mean steam generation from benchmarked recovery boilers as 15.8 GJ of generating steam for each ton of black liquor solids burnt. The same report shows the mean conversion of steam into electricity as 100 kWh for each GJ of processed steam.

Steam may also be generated by burning the wood fines produced during wood chopping. This generation is estimated from the adoption of a 75% efficiency on the conversion of the calorific heat of biomass in energy in the form of steam as reported by Lian, Chua, and Chou (2010). The calorific heat of eucalyptus is taken from Eichler et al. (2017) that reported a 19.1 MJ for each dried kg of *E. Urophylla*. Thus, the final yield of steam considered in the present work is 14.33 GJ for each wood fine ton burnt.

4.1.3.5 Lignin Precipitation

Lignin precipitation data are taken from Kannangara (2015) that studied the acid precipitation of lignin from black liquor of softwood kraft cooking. Although the chemical composition of softwoods and hardwoods (the case of eucalyptus) might be different, the reported parameters are considered in the present work as a first estimate.

Kannangara (2015) reported an extraction yield of 67% of all dissolved lignin in black liquor that initially contained 34% of lignin. Thus, a 19.1% of lignin yield is considered for each ton of black liquor solids processed. The filtrate resulting from this operation is considered effluent, which should be treated as discussed in section 4.1.3.6.

The extraction process is conducted by acidification using CO_2. The solids are then washed with an H_2SO_4 solution. Kannangara (2015) reported consumption of 0.25 tons of CO_2 for each ton of solid lignin, i.e., 0.085 ton of CO_2 for each ton of processed black liquor solids, and 0.35 tons of H_2SO_4 for each ton of solid lignin, i.e., 0.12 tons of H_2SO_4 for each ton of processed black liquor solids. Both extraction and washing stages are grouped in the representative process “Acid precipitation” with these yield and consumptions factors.

All yield values for all technologies in Set Z are summarized in Tables 16 to 18 and utility consumption in Table 19.

Table 16 - Technology yield’s data as input to the model for chemical-to-chemical conversion.

Technology	Fed Chemical	Produced Chemical	Conversion Factor
Wood Preparation	Raw Wood	Wood Chips	0.950 [ton/ton]
		Wood Fines	0.050 [ton/ton]
Kraft Cooking	Wood Chips	Brown Pulp	0.486 [ton/ton]
		Black Liquor (as solid)	0.784 [ton/ton]
Bleaching	Brown Pulp	Bleached Pulp	0.900 [ton/ton]
Acid Precipitation	Black Liquor (as solids)	Lignin	0.228 [ton/ton]

Table 17 - Technology yield’s data as input to the model for chemical-to-utilities conversion.

Technology	Fed Chemical	Produced Utility	Conversion Factor
Chemical Recovery	Black Liquor (as solids)	Cooking Inorganics	0.334 [ton/ton]
		Steam	15.80 [GJ/ton]
Biomass Boiler	Wood Fines	Steam	14.33 [GJ/ton]

Table 18 - Technology yield's data as input to the model for utilities-to-utilities conversion.

Technology	Fed Utility	Produced Utility	Conversion Factor
Steam Turbine	Steam	Electricity	0.10 [MWh/GJ]

Table 19 - Technology consumption data as input to the model.

Technology	Reference Chemical	Demanded Utility	Consumption Factor
Wood Preparation	Raw Wood	Electricity	0.009 [MWh/ton]
Kraft Cooking	Wood Chips	Cooking Inorganics	0.270 [ton/ton]
Bleaching	Brown Pulp	Active Chlorine	0.098 [ton/ton]
		Electricity	0.231 [MWh/ton]
		Steam	4.370 [GJ/ton]
Chemical Recovery	Black Liquor (as solids)	Electricity	0.045 [MWh/ton]
		Steam	1.732 [GJ/ton]
		Natural Gas	19.153 [Nm^3/ton]
Acid Precipitation	Black Liquor (as solids)	CO_2	0.085 [ton/ton]
		Sulfuric Acid	0.119 [ton/ton]

4.1.3.6 Production Costs

Production variable costs associated with utility acquisition are given by the market prices discussed in section 4.1.5. Production fixed costs are considered null in the present work. Selling, General and Administrative (SG&A), and other typical fixed expenses are integrated into a variable production cost. These variable costs, excluding utility acquisition, are taken from the Suzano SA's earnings release regarding the 4th quarter from 2020 (SUZANO SA, 2021a). The mean cash cost reported for BEKP, excluding wood and utilities, was BRL 155.50 per each admt, i.e., BRL 172.78 per each completely dried metric tons. These variable costs are split evenly into Wood Handling, Cooking, Bleaching, and Chemical Recovery sections. The conversion factor for expressing them as a function of their main raw material is displayed in Table 20. These conversion factors were obtained composing all yield factors from the considered operation until the BEKP finished product. Variable costs for lignin acid precipitation are not included in Table 20 and will be considered the same as those regarding the Chemical Recovery section.

Table 20 - Conversion of pulp fixed costs of an illustrative pulp and paper manufacturer into variable production costs. The lignin acid precipitation section is not included in the calculations. Its cost will be taken as the same as the chemical recovery section.

Technology	Reference Raw Material	Cost [BRL/BEKP admt]	Conversion Factor [BEKP admt/reference raw material unit]	Cost [BRL/reference raw material unit]
Kraft Cooking	Wood Chips	43.06	0.44	18.85
Wood Handling	Wood	43.06	0.42	17.91
Bleaching	Brown Pulp	43.06	0.90	38.75
Chemical Recovery	Black Liquor solids	43.06	0.34	14.78

Source: Adapted from SUZANO SA (2021).

All effluents produced should be treated. Effluent treatment units are not modelled explicitly in the model, but implicitly by an effluent treatment cost taken as USD 43.00 for each 1000 m³ of treated effluent, according to Turton et al. (2012) considering both primary (filtration) and secondary (activated sludge) treatments. Considering a density of 1 ton/m³, the currency conversion of 5.00 BRL/USD (section 4.1.5.1) and updating prices from 2012 to 2021 accordingly to inflation reported by the Central Bank of Brazil (BANCO CENTRAL DO BRASIL, 2021a), yields a cost of BRL 0.33 for each ton of processed effluent.

4.1.3.7 Production Investment

The announcement from Suzano SA of a USD 2.8 billion investment in the construction of a 2.3 million capacity BEKP mill (SUZANO SA, 2021c) is taken as the reference for the Kraft technologies investment estimate. This investment is split evenly between Wood Handling, Kraft Cooking, Chemical Recovery, and Bleaching analogously to the procedure done for variables costs in section 4.1.3.6.

Steam turbine investment is taken from Jönsson et al. (2013) as EUR 151.4 million for a 1,000 MW turbine. This value is converted to BRL using the mean exchange rate from Jan-21 to Aug-21 as reported by the European Central Bank (2021) of 6.09 BRL per EUR and updated from 2013 to 2021 values using inflation data from the Central Bank of Brazil (BANCO CENTRAL DO BRASIL, 2021a). This reference capacity for this investment is stated in power units and is then translated into the amount of processed steam by considering that each GJ of steam is responsible for 0.1 MWh of produced electricity and that the turbine operates full-time and all its power is converted into electric energy. Thus, the reference capacity of a 1,000 MW steam turbine is considered as 10,000 GJ per hour of processed steam or 87,6000,000 GJ per year.

Biomass boiler investment is estimated from Lian, Chua, and Chou (2010) reporting an investment of USD 1.8 million for a processing capacity of 1.21 kg/s of biomass. This value is updated from 2010 to 2021 values using inflation data from the Central Bank of Brazil (BANCO CENTRAL DO BRASIL, 2021a) and the reference capacity is converted into yearly flowrate considering the full 24-hour operation for 365 days a year.

Lignin acid precipitation investment is estimated from Kannangara (2015) that reported a value of USD 12.1 million for an installed capacity of 70 tons per day of precipitated lignin. This reference capacity is converted from precipitated lignin production to processed black liquor solids using the yield reported in section 4.1.3.5. The investment value is converted to BRL using the exchange rate from section 4.1.5.1 and updated from 2015 to 2021 values using inflation data from the Central Bank of Brazil (BANCO CENTRAL DO BRASIL, 2021a).

Scale exponents for all technologies are considered as 0.6, as normally adopted in the chemical industry (MCKETTA JR, 1993).

4.1.4 Logistics Parameters

Logistics parameters are discussed in terms of storage (section 4.1.4.1), road transportation (section 4.1.4.2), and overseas operations (section 4.1.4.3).

4.1.4.1 Storage

In the present work, the building of owned storage facilities is not considered. Storage modeling will be taken as a purely variable cost operation as a function of the volume stored and the length of the storage. Kussano and Batalha (2012) reported storage costs for the main UFs of agribusiness in Brazil as displayed in Table 21.

These values are updated from 2012 to 2021 values using inflation data from the Central Bank of Brazil (BANCO CENTRAL DO BRASIL, 2021a) and are displayed in Table 21. The updated costs are then multiplied by 12 (considering products are kept stored for 12-month) and are considered as the storage costs for BEKP and all other chemicals pseudo-components. The cost for the UFs not listed in Table 21 will be taken as the mean value presented in the table.

Table 21 - Storage costs as reported by references and the values after correction by inflation for the main agribusiness UFs in Brazil.

Federative Unit	Cost as reported [BRL/(ton.month)]	Cost corrected by inflation [BRL/(ton.month)]
Goiás	20,90	32.26
Mato Grosso do Sul	21,91	33.82
Mato Grosso	17,77	27.43
Paraná	20,67	31.91
Rio Grande do Sul	21,71	33.52
Santa Catarina	26,90	41.53
Minas Gerais	20,51	31.66
São Paulo	22,49	34.72
Mean	**21,61**	**33.36**

Source: Costs from Kussano and Batalha (2012). Inflation data from the Central Bank of Brazil (BANCO CENTRAL DO BRASIL, 2021a).

No minimum storage policy is considered. Initial storage quantities for all pseudo-components in all locations are null.

4.1.4.2 Road Transportation

Freight costs for road transportation are estimated accordingly to the minimum fare policy for Road Freight defined by resolution 5946/2021 from the ANTT (National Agency on Terrestrial Transportation) (AGÊNCIA NACIONAL DE TRANSPORTES TERRESTRES, 2021). The road transportation is supposed to be done in a 3-axle trailer with 25 metric tons of capacity which results in a freight rate of BRL 0.11 per km per ton. As freight rate is defined considering the total weight of products - including its content water - and the flow rates are calculated in the model as dried tons, the cost parameter is converted to dry weight using the pseudo-component total solids content (Table 22).

Table 22 - Solid content for each pseudo-component considered in the model.

Pseudo-component	Solid Content
Wood Chips	59.60%
Brown Pulp	50.00%
Black Liquor Solids	15.00%
Lignin	80.00%
BEKP	100.00%
Wood Fines	59.60%

For the case of pseudo-component “wood” as well as biomass transportation from the forest units to production facilities, a freight rate of BRL 0.27 per ton per km is considered when correcting the reported value by Lopes, Vieira, and Rodrigues (2016) to inflation and biomass solid content. Biomass for all forest units is considered to present 59.6% solid content as reported by Vinha Zanuncio et al. (2017) for *E. urophylla* logs left for drying in the field for 90 days.

The distance between locations is defined accordingly to the reported distance in *Google Maps* (www.google.com.br/maps) between the representative cities of each location. For non-port locations, the UF’s capital is taken as the representative city, and for port location, the port’s city itself. The distance between a location to itself will be taken as a quarter of the squared root of the total UF area as reported by IBGE (2018).

4.1.4.3 Port Operating Costs And Maritime Freight

The export operations must be done through a port location. Thus, the material should be transferred from a production facility (Production layer P) or storage facility (Storage layer E) to a port location (Storage Layer E), from which it is transferred to a final overseas destination (Market Layer M). Two major costs components are observed at these locations: the port operating expenses and the sea freight.

The sea freight is estimated considering Antwerp, Baltimore, and Qingdao as the representative ports of European, North American, and Chinese markets, respectively. The Shanghai to Rotterdam Index from Drewry Shipping Consultants (2021) reports a rate of USD 14.254,00 for a 40-ft container departing from Shanghai to Rotterdam. Assuming that a 40-ft container is loaded upon 30.5 tons (SHAPOSHNYK et al., 2021) and that the distance from Shanghai to Rotterdam is 10.525 nautical miles (SEA-DISTANCES.ORG, 2021), this yields a base rate of USD 0,0445 per ton per nautical mile or BRL 0,222 per ton per nautical mile considering the exchange rate reported in section 4.1.5.1. This base rate is used to determine the freight rate for each overseas route accordingly to its nautical distance as displayed in Table 23.

Table 23 - Sea freight estimated for port locations and overseas markets considered in the model.

Domestic Port	Oversea Market	Representative Exterior Port	Distance [nautical miles]	Sea Freight [BRL/ton]
Santos	Europe	Antwerp	5.435	718,55
Santos	China	Qingdao	11.285	948,13
Santos	North America	Baltimore	5.000	718,55
Vila do Conde	Europa	Antwerp	4.185	985,58
Vila do Conde	China	Qingdao	10.931	1.006,16
Vila do Conde	North America	Baltimore	2.965	985,58
Paranaguá	Europa	Antwerp	5.557	735,68
Paranaguá	China	Qingdao	11.340	971,36
Paranaguá	North America	Baltimore	5.122	896,74
Suape	Europa	Antwerp	4.179	735,68
Suape	China	Qingdao	11.213	1.014,30
Suape	North America	Baltimore	3.710	896,74

Source: Distances from sea-distances.org (2021) and base-rate estimated from composing the freight index from Drewry Shipping Consultants (2021), container load from Shaposhnyk et al. (2021), the exchange rate from Central Bank of Brazil (2021), and distance from sea-distances.org (2021).

Port operating expenses are taken from the report by ANTAQ (AGÊNCIA NACIONAL DE TRANSPORTE AQUAVIÁRIO, 2021) and are displayed in Table 24.

Table 24 - Port operating costs.

Port	Operating Cost [BRL/Container]
Vila do Conde	68.92
Paranaguá	43.91
Santos	49.74
Suape	5.81

Source: ANTAQ (AGÊNCIA NACIONAL DE TRANSPORTE AQUAVIÁRIO, 2021)

The total transfer cost for overseas operations is given by the sum of sea freight and port operating expenses divided by the container capacity of 25 tons adopted in this work. As previously mentioned, the solid contents reported in Table 22 should also be used for correcting the capacity for each pseudo-component.

4.1.5 Market And Financial Parameters

Economics parameters used as input to the model and also to estimate other parameters for the case study are discussed in section 4.1.5.1. The different taxes configurations considered in the model are discussed in section 4.1.5.2. Demand and prices for BEKP, Lignin, and Electricity are discussed in sections 4.1.5.3, 4.1.5.4, and 4.1.5.5, respectively. Market aspects for other utilities, such as natural gas and white liquor, are discussed in section 4.1.5.6.

4.1.5.1 Inflation, Currency Exchange, And Interest Rates

The nominal prices are considered constant throughout the entire time horizon. Although they are still uncertain, their expected nominal price and range of possible variation is supposed to be constant. However, inflationary effects are very relevant to the Brazilian Economy (AFONSO; ARAÚJO; FAJARDO, 2016). These effects are incorporated into the model through the adoption of a real interest rate instead of a nominal one to discount cash flows to present value. According to Focus Market Readout from the Central Bank of Brazil (BANCO CENTRAL DO BRASIL, 2021b), the market median projection of nominal interest rates for Brazil for 2024 is at 6.5% (yearly) while inflation is at 3.0% which renders a real interest rate of 3.4%, used in the present work. From the same report, the expected exchange rate between BRL to USD for 2024 is 5,00. The 2024 year is adopted in the present work because it is the furthest projected year in the report and represents a more long-termed perspective for the Brazilian economy than closer projections.

4.1.5.2 Taxes

Taxes considered in the model are the ICMS (Tax on Goods and Services Circulation), PIS (Social Integration Program), and COFINS (Contribution to the financing of Social Security), applicable over sales, and the CSLL (Social Contribution on Net Profit) and IRPJ (Income Tax for Legal Person), applicable over the accounting profit for each period.

ICMS is dependent upon the origin and destination of the sold product as can be seen by Table 25 and 26 for interstates and intrastate operations, respectively (the term state is used interchangeably with UF in this work). These taxes are considered valid only for sales operations while the simple transfer of products from one facility to another (without any sale transaction) is assumed to be tax-free accordingly to *Súmula* 166 from the Brazilian Justice Superior Court (SUPERIOR TRIBUNAL DE JUSTIÇA, 1996) that states that the simple transference of a product to another location from the same tax-payer does not constitute a generator of ICMS. ICMS is also not applied to electricity sales (TORRES et al., 2003).

Table 25 - ICMS rate for operations from agents on different UFs.

Origin UF	Destination UF	Rate
South or Southeast UFs, excluding Espírito Santo	South or Southeast, excluding Espírito Santo UF	12%
South or Southeast UFs, excluding Espírito Santo	North, Northeast, Mid-West, or Espírito Santo UF	7%
North, Northeast, or Mid-West UFs, or Espírito Santo	South or Southeast, excluding Espírito Santo UF	12%
North, Northeast, or Mid-West UFs, or Espírito Santo	North, Northeast, Mid-West, or Espírito Santo UF	12%

Source: Torres et al. (2003)

PIS and COFINS present a fixed rate for each product independent from where (or to) the product is sold. Several tribute regimes are available, and the non-cumulative regime is the one considered in the present work. This regime is associated with rates of 1.65% and 7.6% for PIS and COFINS, respectively (FABRETTI, 2015).

Exports are free from PIS, COFINs, and ICMS (PÊGAS, 2008; TORRES et al., 2003). Thus, no domestic tax fee is considered on exports. The destination (clearance) taxes are also not considered, because prices adopted in the present work are taken under a CIF (Cost Insurance and Freight) incoterm[11], i.e., clearance costs are paid by the client when receiving the material at their port location.

[11] A discussion on the meaning of each incoterm is available in Malfliet (2011)

Table 26 - ICMS rate for operations between buyer and seller in the same UF.

UF	Rate
Acre	17%
Alagoas	17%
Amazonas	17%
Amapá	17%
Bahia	17%
Ceará	17%
Distrito Federal	17%
Espírito Santo	17%
Goiás	17%
Maranhão	17%
Mato Grosso	17%
Mato Grosso do Sul	17%
Minas Gerais	18%
Pará	17%
Paraíba	17%
Paraná	18%
Pernambuco	17%
Piauí	17%
Rio Grande do Norte	17%
Rio Grande do Sul	17%
Rio de Janeiro	19%
Rondônia	17%
Roraima	17%
Santa Catarina	17%
São Paulo	18%
Sergipe	17%
Tocantins	17%

Source: Contabilizei website (2021)

CSLL and IRPJ are applied over the accounting profit of each period only if it is positive. CSLL rate for non-financial institutions is of 9% (MINISTÉRIO DA ECONOMIA, 2020a). IRPJ rate is 15% on profits with an additional rate of 10% for the profit exceeding BRL 20.000 a month (MINISTÉRIO DA ECONOMIA, 2020b). In the present work, this progressive rate will be neglected and only the higher rate of 25% will be considered for any magnitude of positive profit. The two taxes are grouped into a single fee of 31.75%. The time for depreciation of productive investments is taken as 10 years.

4.1.5.3 BEKP Demand And Prices

Accordingly to the ABTCP (Brazilian Pulp and Paper Producers Association) sector report (FARINHA E SILVA; BUENO; NEVES, 2017) Brazilian pulp exports summed 5.603 tons in which Europe, China, and North America correspond to 89% (table 27). These three locations are then considered as the overseas market locations in layer M.

Table 27 - Brazilian pulp export data.

Market	Quantity [ton]	Share [%]
Europe	2.129	38%
China	1.849	33%
North America	1.009	18%
Other Asia and Oceania	504	9%
Latin America	112	2%
Total	**5.603**	**100%**

Source: ABTCP sector report (FARINHA E SILVA; BUENO; NEVES, 2017).

The domestic consumption of pulp is also relevant. According to a former ABTCP sector report (BACHMANN E ASSOCIADOS; ABTCP, 2011), the most representative paper segments in Brazil are corrugated packaging (53%), printing & writing (P&W, 24%), and tissue (11%). As corrugated packaging is mostly made from Softwood or Non-Bleached Hardwood Pulp (TWEDE et al., 2015) only P&W and tissue markets will be considered as domestic demand for BEKP. For assessing this demand, a list of the most important P&W and tissue paper producers was taken from the ABTCP report. The location and capacity for each of these producers were inferred from the producer's official website. These mapped capacities were then consolidated by the federal unit level considering that P&W paper is made of 70% cellulose (DE CARVALHO; DE ALMEIDA, 1997) and that tissue paper is composed integrally of cellulose. Each Federal Unit (UF) with a non-null mapped capacity of paper production was taken as a potential market location in Set M. The complete collected data is displayed in Appendix D.

Pulp prices are estimated from the 4Q-2020 earnings release from Suzano (SUZANO SA, 2021a) that reported a net price of BRL 2.479,00 per admt for exports and BRL 2.246,00 per admt for the domestic market. As exports are free from domestic taxes (section 4.1.5.2) the final billed price for pulp is taken as the net price reported by Suzano corrected to completely dried metric tons. The final billed price for domestic markets, however, should include ICMS, PIS, and COFINS taxes. As the final tax rate is origin-destination dependent (section 4.1.5.2), a representative 21% tax rate is adopted for all markets and added to the net price for Suzano as an estimate of the final billed price for all markets. The final converted values as input to the model are displayed in Table 28.

Table 28 - Pulp prices considered in the model.

Market	Net Price [USD/admt]	Billed Price [BRL/metric ton]
Europe	2,479.00	2,754.44
China	2,479.00	2,754.44
North America	2,479.00	2,754.44
Domestic Market	2,246.00	2,495.56

The pulp prices are also considered as an uncertain parameter. Suzano reported that BEKP prices on exports raised 27% in 4Q20 when compared with 4Q19 (SUZANO SA, 2021a). Thus, for the uncertain price representation in the robust model ($p = \bar{p} + \varepsilon\tilde{p}$) the nominal price ($\bar{p}$) is taken as those displayed in Table 28 with a variation ($\tilde{p}$) of 27% the value of $\bar{p}$. This variation is represented by a random variable ε contained in a unitary box ($|\varepsilon| \leq 1$).

4.1.5.4 Lignin Demand And Prices

Lignin will be considered as used only as a cement additive. Its demand will be estimated similarly to the procedure used for pulp. Cement producers' capacity data are taken from the Brazilian Chamber for the Construction Industry (CÂMARA BRASILEIRA DA INDÚSTRIA DE CONSTRUÇÃO, 2021). It is considered a 0.2% addition of lignin on cement as reported by Huang et al. (2018). The collected data for demand estimation is displayed in Table 29.

Prices for lignin were reported by L'Udmila et al. (2015) as ranging from 260 to 500 USD per metric ton. This range of variation is significant and, thus, lignin prices will be treated as an uncertain parameter. The nominal price ($\bar{p}$) from the uncertain price representation in the robust model ($p = \bar{p} + \varepsilon\tilde{p}$) is taken as the mean price of 380 USD in the range reported by L'Udmila et al. converted to BRL using the exchange rate from section 4.1.5.1, updated from 2015 to 2021 values using inflation data from Central Bank of Brazil (2021), added a 21% of taxes, yielding a value of BRL 2.845,58 per ton. The possible variation ($\tilde{p}$) is taken as BRL 898,60 per ton matching the reported variation by L'Udmila et al. (2015).

Table 29 - Production capacity data for cement in Brazil in 2017.

UF	Production [ton/year]	Potential Lignin Demand [ton/year]	Share [%]
Minas Gerais	11.577.225	23.154,45	24,46%
Paraná	5.836.992	11.673,98	12,33%
São Paulo	5.196.555	10.393,11	10,98%
Distrito Federal	2.620.265	5.240,53	5,54%
Ceará	2.461.470	4.922,94	5,20%
Paraíba	2.310.304	4.620,61	4,88%
Rio de Janeiro	1.926.186	3.852,37	4,07%
Sergipe	1.925.785	3.851,57	4,07%
Espírito Santo	1.493.544	2.987,09	3,16%
Goiás	1.485.986	2.971,97	3,14%
Santa Catarina	1.419.303	2.838,61	3,00%
Rio Grande do Sul	1.401.625	2.803,25	2,96%
Pará	1.333.064	2.666,13	2,82%
Bahia	1.086.172	2.172,34	2,29%
Mato Grosso	1.034.038	2.068,08	2,18%
Rio Grande do Norte	1.022.713	2.045,43	2,16%
Mato Grosso do Sul	637.028	1.274,06	1,35%
Amazonas	559.228	1.118,46	1,18%
Tocantins	538.969	1.077,94	1,14%
Maranhão	467.799	935,60	0,99%
Pernambuco	382.833	765,67	0,81%
Piauí	279.270	558,54	0,59%
Rondônia	206.445	412,89	0,44%
Alagoas	131.394	262,79	0,28%
Acre	-	-	0,00%
Roraima	-	-	0,00%
Amapá	-	-	0,00%
Total	**47.334.193**	**94.668,39**	**100,00%**

Source: Câmara Brasileira da Indústria de Construção (2021).

4.1.5.5 Electricity Demand And Prices

The electricity consumption of each UF in Brazil is displayed in Table 30. This consumption data is considered as the electricity demand for the model.

Table 30 - Electricity consumption per UF in 2016.

UF	Consumption 2016 [GWh]	Share [%]	Subsystem
São Paulo	127.171	*28,3%*	Southeast/Mid-West
Minas Gerais	53.076	*11,8%*	Southeast/Mid-West
Rio de Janeiro	29.886	*6,6%*	Southeast/Mid-West
Rio Grande do Sul	29.428	*6,5%*	South
Paraná	29.328	*6,5%*	South
Bahia	24.952	*5,5%*	Northeast
Santa Catarina	23.307	*5,2%*	South
Pará	19.916	*4,4%*	North
Goiás	14.790	*3,3%*	Southeast/Mid-West
Pernambuco	13.635	*3,0%*	Northeast
Ceará	11.914	*2,6%*	Northeast
Espírito Santo	9.836	*2,2%*	Southeast/Mid-West
Mato Grosso	8.032	*1,8%*	Southeast/Mid-West
Maranhão	6.824	*1,5%*	Northeast
Distrito Federal	6.511	*1,4%*	Southeast/Mid-West
Amazonas	5.991	*1,3%*	North
Rio Grande do Norte	5.589	*1,2%*	Northeast
Mato Grosso do Sul	5.246	*1,2%*	Southeast/Mid-West
Paraíba	5.189	*1,2%*	Northeast
Alagoas	4.881	*1,1%*	Northeast
Sergipe	3.784	*0,8%*	Northeast
Piauí	3.381	*0,8%*	Northeast
Rondônia	2.935	*0,7%*	North
Tocantins	2.178	*0,5%*	Northeast
Acre	1.017	*0,2%*	North
Roraima	915	*0,2%*	North
Amapá	119	*0,0%*	North
Total	**449.831**		

Source: Energy Research Company (EMPRESA DE PESQUISA ENERGÉTICA, 2017)

The consumptions reported in Table 30 are associated with a specific subsystem (region). Each of these subsystems has a specific energy fare regulated by the Electricity Commercial Chamber. Historical prices from 2012 to 2016 for each of these subsystems are displayed in Table 31 , which shows that energy prices present an intense variation. Thus, they are taken as uncertain parameters in the model. The nominal energy price ($\bar{p}$) at each UF is taken as the mean energy price of its subsystem on Table 31. The possible variation ($\tilde{p}$) is taken as the difference between the mean and lowest prices for each UF. No inflation correction is proposed for energy prices as it is mostly influenced by environmental factors and water scarcity.

Table 31 **-** Historical data for energy liquidation price for each subsystem from 2012 to 2016.

Subsystem	Fare 2012 [R$/kWH]	Fare 2013 [R$/kWH]	Fare 2014 [R$/kWH]	Fare 2015 [R$/kWH]	Fare 2016 [R$/kWH]	**Mean [R$/kWH]**	**Lowest [R$/kWH]**
North	253,24	290,72	601,21	166,89	122,19	**286,85**	**122,19**
Northeast	253,24	291,86	601,21	303,22	122,19	**314,34**	**122,19**
Southeast and Mid-West	259,57	290,72	601,21	116,08	122,19	**277,95**	**116,08**
South	259,57	290,72	601,21	110,55	122,19	**276,85**	**110,55**

Source: Energy Research Company (EMPRESA DE PESQUISA ENERGÉTICA, 2017).

4.1.5.6 Other Utilities

Natural Gas is regulated by the ANP (National Agency of Petroleum, Natural Gas and Biofuels) and its price is retrieved from the official supplier website for each UF. The collected data for each UF is displayed in Table 32.

All other utility prices are estimated by import data available on the Brazilian Tax Agency website (MINISTÉRIO DA ECONOMIA, 2021) using 2020 as a reference year. The collected prices for each utility were filtered considering only purchases over 1.000 kg of product and done by road transportation. These filters are applied for avoiding inclusion of spot and samples purchases that might present unusual prices. Both the reported FOB (Free on Board) price and freight were considered for composing the unitary product price in USD/ton. The composed price is converted to BRL using the exchange rate reported in section 4.1.5.1. The collected data and NCM (Mercosur Common Nomenclature) used in the database consult are displayed in Table 33.

As the tribute regime adopted in the present work is non-cumulative (section 4.1.5.2), PIS, COFINS, and ICMS are not included in the acquisition price for utilities.

Table 32 - Natural gas prices for each UF considered in the model.

UF	Price [BRL/Nm³]	Official Supplier	Source
Alagoas	2.3054	Algás	Algás (2021)
Bahia	2.0225	Bahiagás	Agerba (2021)
Ceará	2.3140	Cegás	Cegás (2021)
Distrito Federal	2.1816	Cebgás	Cebgás does not present its fares' information on their website. Representative fares for this UF are taken as the ones from Minas Gerais UF.
Espírito Santo	2.2114	Esgás	Agência de Regulação de Serviços Públicos Do Espírito Santo (2021)
Goiás	2.1816	Goiasgás	Goiasgás does not present its fares' information on their website. Representative fares for this UF are taken as the ones from Minas Gerais UF
Maranhão	2.3140	Gasmar	Gasmar does not present fares' information on its website. Representative fares for this UF are taken as the ones from Ceará.
Mato Grosso	2.3192	MTgas	MTgas do not present fares' information on their website. Representative fares for this UF are taken as the ones from Mato Grosso do Sul UF.
Mato Grosso do Sul	2.3192	Msgas	Msgás (2021)
Minas Gerais	2.1816	Gasmig	Gasmig (2021)
Pará	2.3192	Cia de Gás do Pará	Cia de Gás do Pará do not present fare information in their website. Representative fares for this UF are taken as the ones from Mato Grosso do Sul.
Paraíba	1.9777	Pbgás	Pbgás (2021)
Paraná	2.7312	Compagás	Compagás (2021)
Pernambuco	2.3054	Copergás	Copergás does not present its fares' information on their website. Representative fares for this UF are taken as the ones from Alagoas UF
Rio de Janeiro	2.6941	Naturgy	Naturgy (2021)
Rio Grande do Sul	2.2062	Sulgás	Sulgás (2021)
Santa Catarina	2.2766	Scgás	Scgás (2021)
São Paulo	2.2497	Comgás	Comgás (2021)
Sergipe	2.1516	Sergas	Sergas (2021)
Tocantins	2.0225	-	There is no piped natural gas distribution in Tocantins Representative fares for this UF are taken as the ones from Bahia.

Prices exclude ICMS, PIS, and COFINs as the tribute regime considered in the model is non-cumulative.

Table 33 - Estimated prices for utilities and NCM used for consultation.

Utility	Price [USD/ton]	Price [BRL/ton]	NCM considered
White Liquor	881.68	4,408.40	28151100 - Sodium hydroxide (caustic soda) solid
Chlorine	187.40	937.00	28011000 - Chlorine
CO_2	233.61	1,168.05	28112100 – Carbon dioxide
H_2SO_4	140.00	700.00	28070010 - Sulfuric acid

Source: Ministério da Economia (2021) and ITC (2021)

4.2 COMPUTATIONAL IMPLEMENTATION

The optimization model was computationally implemented in Python v.3.9.1 using the Pyomo v.5.8.6 library (HART et al., 2017). The pyomo model was used to build an abstract model, i.e., a model whose numerical values are not instantiated and thus represented by placeholder symbols, comprising the collections of all Sets, Parameters, Variables and Constraints developed in section 3.

A Microsoft Excel® spreadsheet was used as the user interface for collecting the parameters values to instantiate the optimization model. The Pandas v.1.2.4 library (REBACK et al., 2021) for Python was used for the ingestion of the data from the excel spreadsheet and to format it accordingly to the requirements for instantiating the Pyomo concrete model (i.e., a model with the numerical values instantiated) from the abstract model.

The solution was obtained through the Pyomo interface with the CPLEX v.12.09 solver (IBM, 2018) on a 32-GB RAM machine with Intel Core i7-9750H 2.6GHz CPU. The MILP gap defined for optimality was 0.01%.

Solutions obtained from all scenarios' runs were consumed by a web application built in Flask v.1.1.2 library (GRINBERG, 2018) for Python and data was visualized on dashboards built on the Plotly v.1.20.0 library (PLOTLY INC., 2019).

4.3 OPTIMIZATION SCENARIOS

Several optimization scenarios were considered varying the degree of conservatism on the polyhedral uncertainty set formulation (equations 24, 114, and 132). The solution of the first scenario was obtained with no MILP solution initialization. The other scenarios used the first scenario solution as a starter - when feasible. The list of the main optimization scenarios and their respective uncertainty parameters and solver runtime for reaching the optimality gap is displayed in Table 34.

Scenarios from Table 34 consider all parameters exactly as defined in section 4.1 differing only on the polyhedral uncertainty set definition. These scenarios are identified with the letter M on theirs ID. However, for further investigation some extra scenarios were run with some parameters shifted from their nominal values. Table 35 shows the scenarios in which lignin prices were raised from their nominal value to investigate the operation attractiveness (Scenarios' IDs for this investigation start with the letter L.). Tables 36 and 37 show the scenarios with reductions in transportation cost and productive investments, respectively, used for investigating decentralization/centralization trade-offs and strategies for increasing the operation´s attractiveness. The scenarios' IDs for transportation cost investigations start with the letter T and scenarios IDs for production investments investigations start with the letter I.

Table 34 – List of the main optimization runs (scenarios) and their respective values for uncertainty parameters and solver runtime.

Scenario ID	Uncertainty Parameters				Solver Runtime [s][12]	NPV [B BRL]
	Pulp Prices $\Gamma_{m,q=pulp}$	Lignin Prices $\Gamma_{m,q=lignin}$	Energy Prices $\Gamma_{p,u=electricity}$	Biomass Prod. $\Gamma_{f,b}$		
M.1	0	0	0	0	388.61	136.02
M.2	20	20	20	12	159.02	0
M.3	0	0	0	12	568.63	109.10
M.4	20	20	20	0	140.41	0
M.5	20	0	0	0	136.81	0
M.6	0	20	0	0	440.77	136.02
M.7	0	0	20	0	437.50	134.07
M.8	0	0	0	9	594.86	109.10
M.9	0	0	0	6	574.14	109.23
M.10	0	0	0	3	565.72	117.72
M.11	15	0	0	0	1202.81	0
M.12	10	0	0	0	2610.97	19.99
M.13	5	0	0	0	1139.78	53.36
M.14	14	0	0	0	5003.64	0.15
M.15	13	0	0	0	5438.36	2.10
M.16	12	0	0	0	2608.20	6.58
M.17	11	0	0	0	3659.13	11.74
M.18	9	0	0	0	2311.23	23.57

All scenarios from this list present the nominal value as those collected in section 4.1differing only regarding the choices of polyhedral uncertainty sets parameters.

[12] Solver runs were done in parallel to other computers' task and their runtimes should not be compared. They are displayed here only as a reference and no conclusions are to be drawn from this information.

Table 35 – List of the extra optimization scenarios for lignin price investigation and their respective values for uncertainty parameters and solver runtime.

Scenario ID	Uncertainty parameters taken from	Lignin price increase from nominal value	Solver Runtime [s][13]	NPV [B BRL]
L.1	Scenario M.1	+150%	562.94	136.02
L.2	Scenario M.1	+175%	559.75	136.02
L.3	Scenario M.1	+200%	616.70	136.02
L.4	Scenario M.1	+225%	555.00	136.02
L.5	Scenario M.1	+250%	1055.27	136.34
L.6	Scenario M.7	+150%	625.86	134.07
L.7	Scenario M.7	+175%	674.58	134.07
L.8	Scenario M.7	+200%	554.55	134.07
L.9	Scenario M.7	+225%	1152.88	134.34
L.10	Scenario M.7	+250%	1508.83	135.22

Table 36 – List of the extra optimization scenarios for transportation cost investigation and their respective values for uncertainty parameters and solver runtime

Scenario ID	Uncertainty parameters taken from	Transportation cost reduction from the nominal value	Solver Runtime [s][13]	NPV [B BRL]
T.1	Scenario M.1	-25%	596.98	140.38
T.2	Scenario M.1	-50%	554.36	144.75
T.3	Scenario M.1	-75%	801.92	149.28
T.4	Scenario M.5	-25%	336.56	0
T.5	Scenario M.5	-50%	1157.13	0
T.6	Scenario M.5	-75%	3506.05	79.05

Table 37 – List of the extra optimization scenarios for production investment investigation and their respective values for uncertainty parameters and solver runtime.

Scenario ID	Uncertainty parameters taken from	Production Investment reduction from the nominal value	Solver Runtime [s][13]	NPV [B BRL]
I.1	Scenario M.1	-25%	445.59	141.75
I.2	Scenario M.1	-50%	484.63	147.48
I.3	Scenario M.1	-75%	760.84	153.25
I.4	Scenario M.5	-25%	284.19	0
I.5	Scenario M.5	-50%	2348.09	0.74
I.6	Scenario M.5	-75%	2704.64	4.28

[13] Solver runs were done in parallel to other computers' task and their runtimes should not be compared. They are displayed here only as a reference and no conclusions are to be drawn from this information.

4.4 RESULTS AND DISCUSSIONS

Scenario M.1 resulted in an operating NPV of 136 billion BRL. This scenario represents a situation in which the polyhedral uncertainty-set constant is set to zero for all uncertain parameters, i.e., all parameters assume their nominal values. The NPV breakdown for this scenario is displayed in Figure 7. The operation is associated with a positive net present value in which chemical sales are the main positive contributors and logistic costs are the main negative ones.

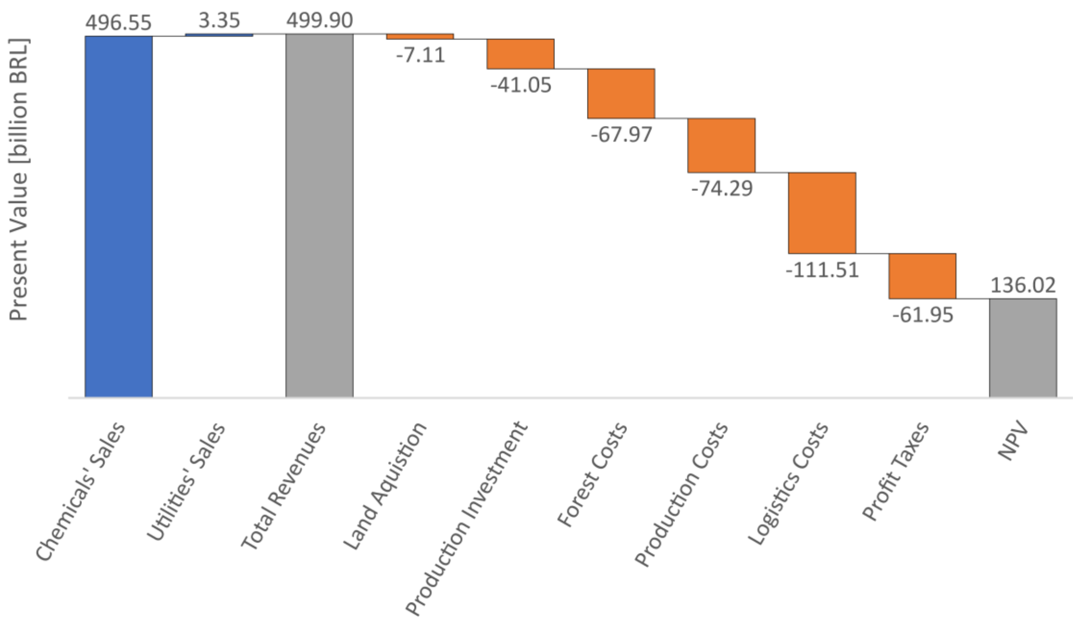

Figure 7 - The optimal NPV breakdown for scenario M.1.

Chemical sales represent the main source of revenues from the operation and come exclusively from BEKP sales. The lignin operation was not financially attractive under the nominal scenario. When all uncertainties polyhedral constants are set to zero, the lignin operation becomes financially attractive on scenario L.5, with lignin price of 9,959.54 BRL per ton, i.e., an increase of 250% from its nominal value. For this scenario, the overall biorefinery configuration remains virtually the same as in scenario M.1, with São Paulo chosen as the unique production facility fulfilling all BEKP and lignin demands. In scenario L.5, however, the operation has a reduced kraft recovery and steam turbine processing capacities, due to shifting part of the produced black liquor to the lignin acid-precipitation stage (Figure 8). All production capacity is installed in São Paulo. Wood handling, Biomass Boiler, Kraft Cooking, and Pulp Bleaching capacities are the same for both scenarios. Uncertainties were not considered in any of the two scenarios (M1 and L5).

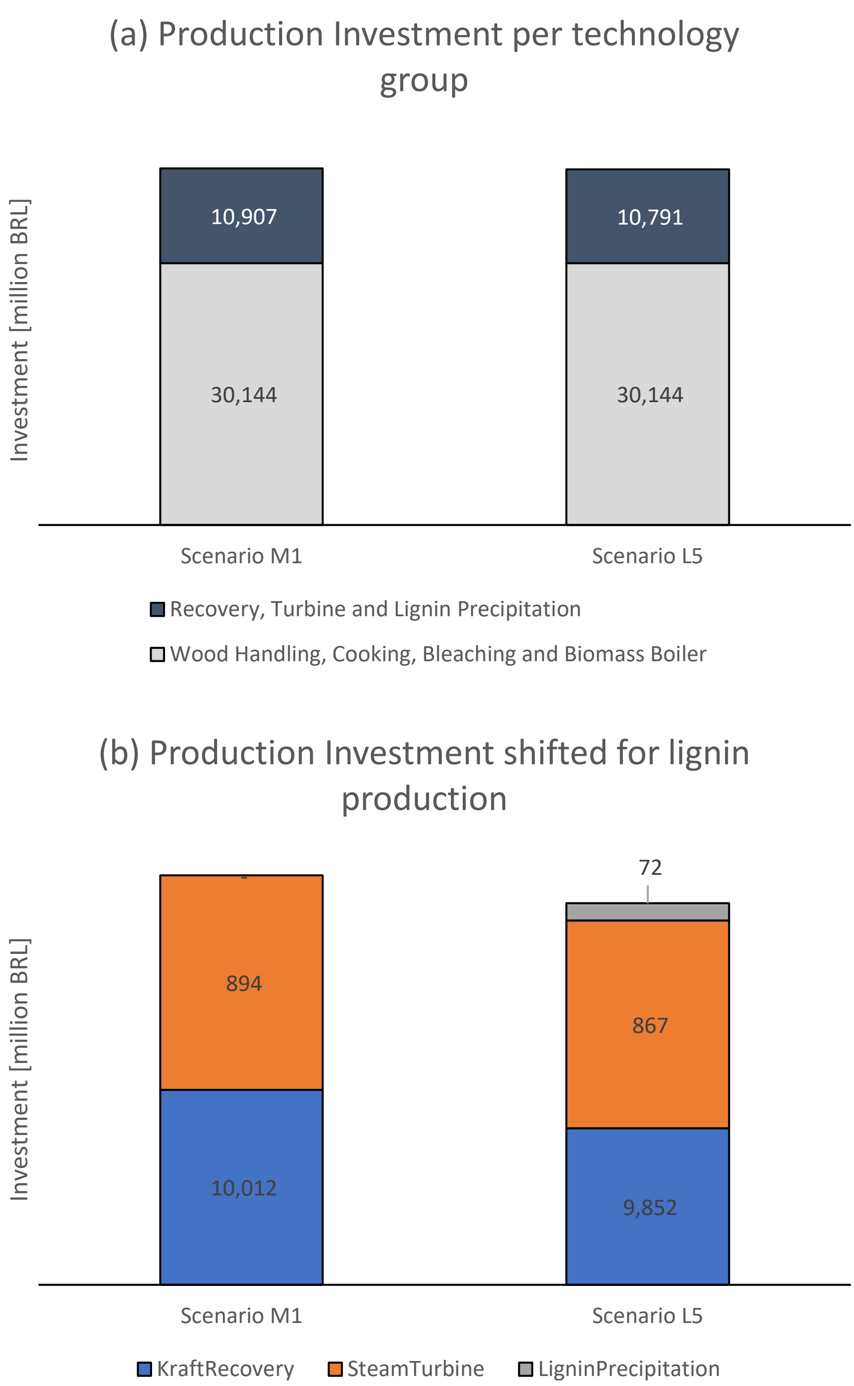

Figure 8 – Production Investment in each technology for different lignin price scenarios. Scenario M.1 is the one in which lignin operation is not financially attractive and scenario L5 (lignin prices increased by 250%) in which it is attractive. (a). The shift of black liquor processing to the lignin acid precipitation stage in scenario L.5 reduces kraft recovery boiler and steam turbine processing capacities (b). Production Investment shifted for lignin production.

The reduced steam turbine production in scenario L5 implies a lower revenue from electricity sales. Thus, the more profitable the electricity sales operation the more profitable the lignin operation must be to compensate for the lower energy generation. The inverse applies, if the energy operation is expected to be less profitable, the lignin operation has a lower opportunity cost and can become financially attractive under lower selling prices. However, even for scenario M.7 – which considers the worst-case electricity prices - lignin was not financially attractive. Under the worst-case electricity prices, lignin operation requires a smaller price increase for becoming financially attractive and the lignin operation is feasible with prices beyond 9,248.14 BRL per ton (scenarios L.9 and L.10), i.e., an increase of 225% and beyond from the nominal values.

These results suggest that developing higher-value applications for lignin may be important for the successful consolidation of the operation. However, it is worth noticing that the wash filtrate after lignin precipitation still presents some potential for integration to the mill (KANNANGARA, 2015) that was not considered in the model. This integration could lower the opportunity costs associated with lignin extraction and increase its attractiveness.

Although electricity profitability is important for defining lignin attractiveness, the utility sales presented a diminished relevance on the biorefinery profitability, representing only 6.7% of the present value for all operating revenues. As electricity is only a co-product from the main BEKP operation it is natural to expect diminished participation in the overall results. However, it is worth noticing that the electricity production flowsheet considered in the model has some simplifications that might lead to an underestimation of the electricity production potential. For instance, only a single type of steam was considered in the model. The differentiation of steam into high and medium/low-pressure types could enable extra energy generation through turbines that reduce the high-pressure steam produced in the recovery boiler to a medium/low-pressure steam used in the pulp processes. This conversion could provide extra electricity production potential for the same black liquor burnt, making the overall biorefinery configuration more attractive.

This potential, however, might be hindered by price uncertainties. Section 4.1.5.5 shows that electricity prices are subject to intense variation and should be considered carefully. Given that energy revenues present diminished participation on the operating revenue, the impacts of its price uncertainties were also diminished. For instance, the worst-case electricity prices scenario has an optimal NPV of 134 billion BRL, a decrease of 2 billion BRL or 1.5% from the nominal case. Even under this worst-case scenario, all operating decisions remained the same.

The only parameter whose uncertainty was able to severely impact operating decisions was BEKP prices. Every scenario with a polyhedral constant ($\Gamma_{m,q=pulp}$) greater than 15 presented a null optimal solution, i.e., the optimal configuration is to not build any biorefining operation. Figure 9 shows that the expected NPV for the operation is heavily influenced by the degree of conservatism constant on BEKP price uncertainties.

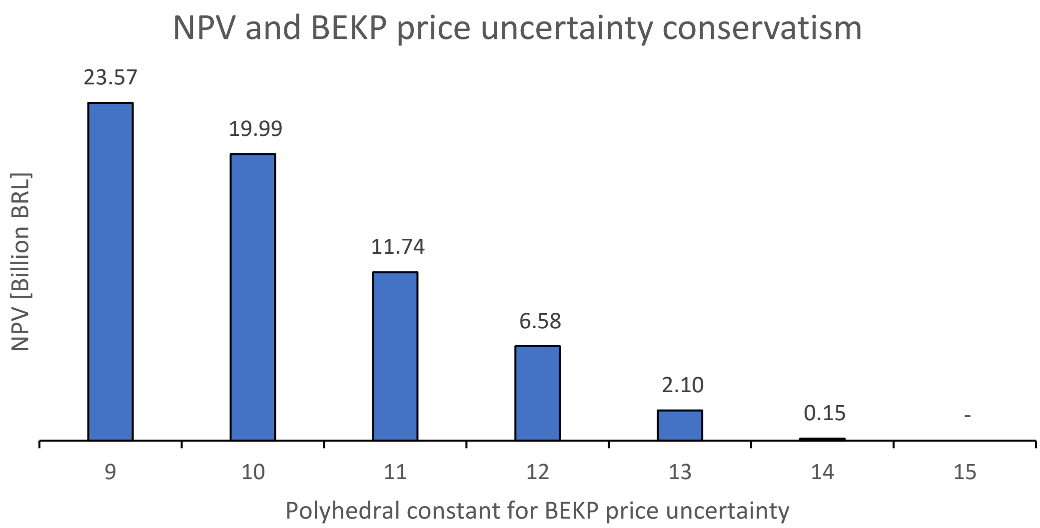

Figure 9 – Optimal NPV and pulp price uncertainty conservatism degree constant.

In scenario M.14 ($\Gamma_{m,q=pulp}$ = 14), the most conservative BEKP price with a non-null optimal solution, the optimal NPV is 150 MM BRL and the operation is designed to fulfill only part of the domestic BEKP demand (Figure 10). It is shown on Figure 10 that the domestic market is preferred in more stressful scenarios. Ceará and Pará states are the only BEKP markets that have none of theirs demand fulfilled. They are the furthest consumer markets from the single production capacity installed in Espírito Santo, distant 2,162 and 3,023 kilometers, respectively. In scenario M.15 ($\Gamma_{m,q=pulp}$ = 13), Espírito Santo is still the only installed production facility and the Ceará market becomes financially attractive to operate.

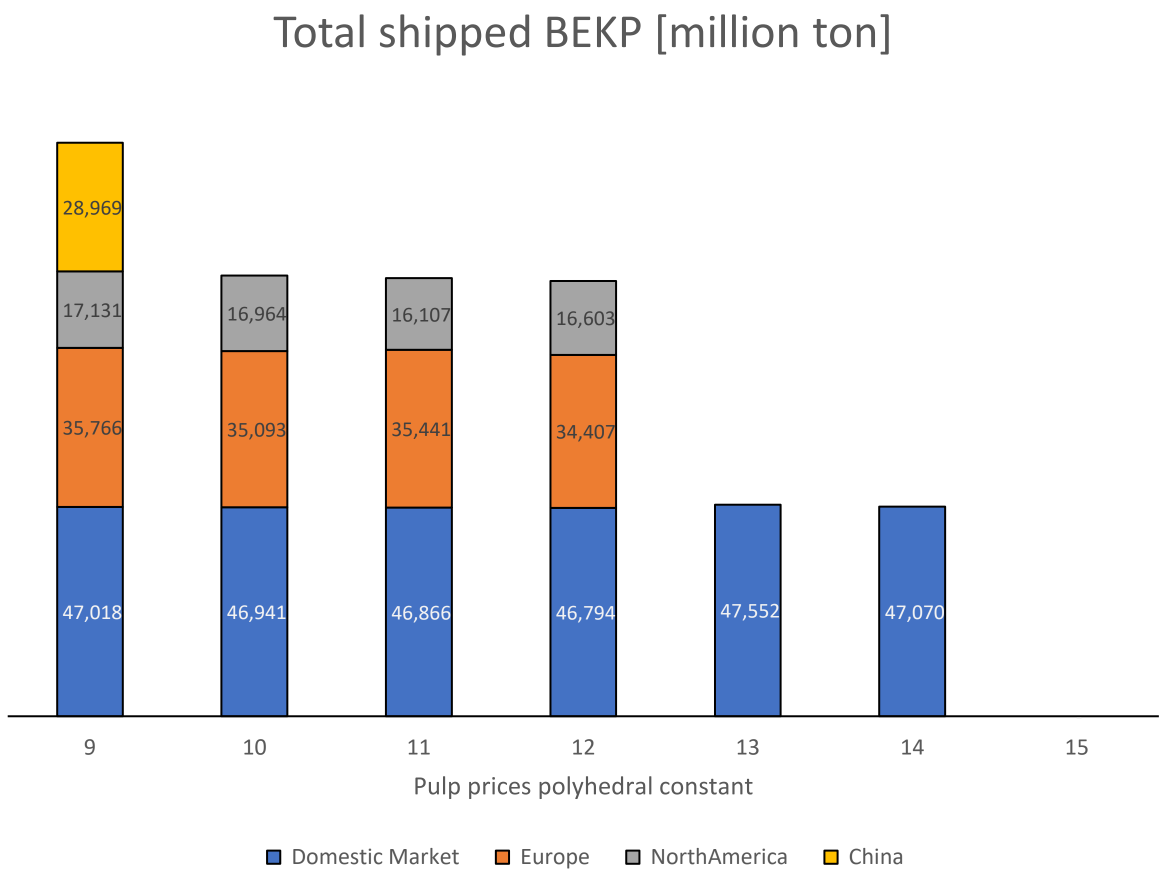

Figure 10 – Total BEKP shipped for each consumer market accordingly to the degree of conservatism on pulp price uncertainties.

Espírito Santo is among UFs with higher biomass productivity (40 $m^3 year^{-1} ha^{-1}$) and presents a strategic location for attending most of the pulp domestic market (Figure 11). It also presents the lowest interstate distance (53.7 km) among these biomass' most productive states (Figure 12). Lower interstate distances mean that forests are closer to the production facilities reducing biomass transportation costs. These factors make Espírito Santo an attractive spot for production, close to very productive forests and in a central location to most of the BEKP domestic market.

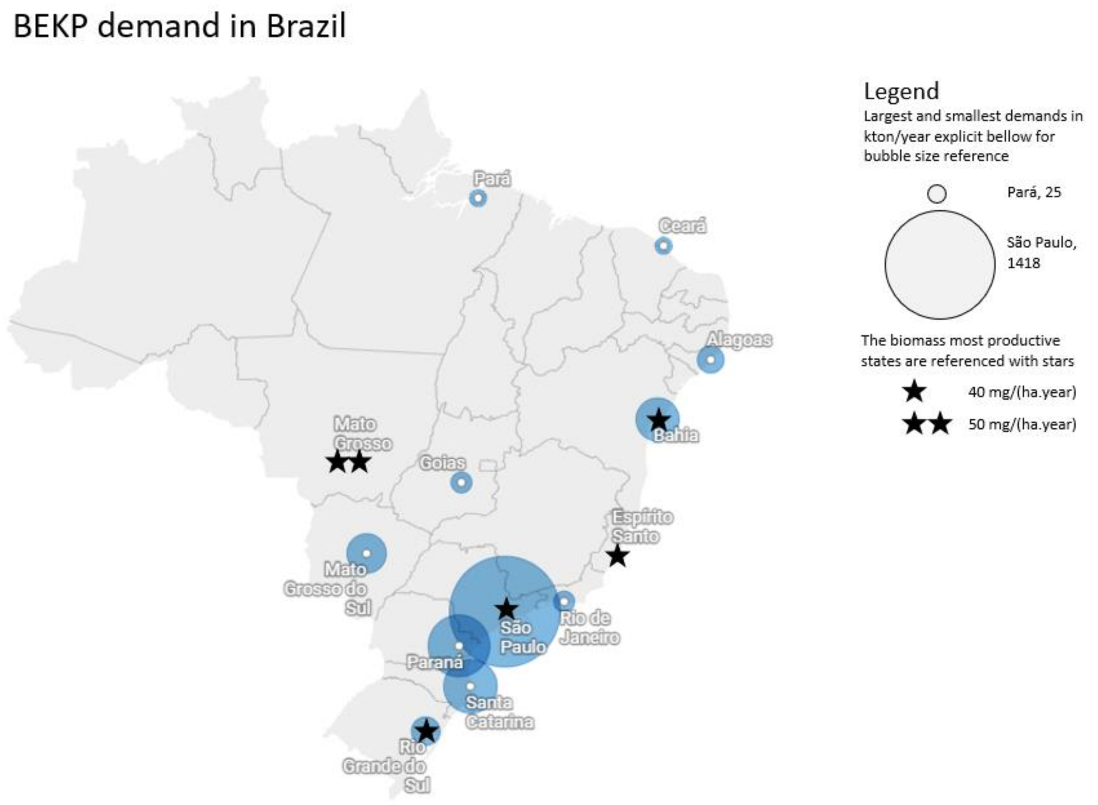

Figure 11 – Location of domestic BEKP market compared to the most productive forest locations.

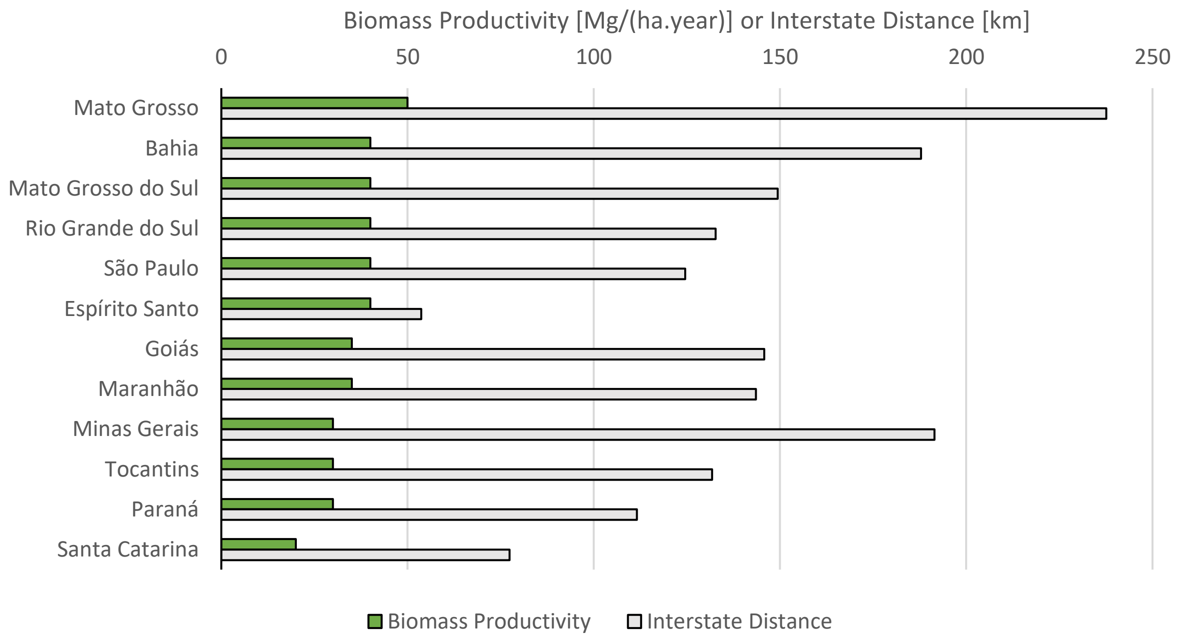

Figure 12 – Biomass productivity and interstate distance for all considered forest locations. Mato Grosso presents the highest biomass productivity and the highest interstate distance. Bahia, Espírito Santo, Mato Grosso do Sul, Rio Grande do Sul and São Paulo are the second most productive locations. Among these, Espírito Santo is the one with the lowest interstate distance.

Under less conservative uncertainties scenarios ($\Gamma_{m,q=pulp}$ ≤ 12) the overseas market becomes financially attractive (Figure 10). Even though Espírito Santo is competitive for BEKP domestic demand fulfillment, its closest port considered in the case study is Santos - distant 1,012 km - which is not competitive for reaching overseas markets. For scenarios in which the overseas BEKP market is considered financially attractive, the optimal BEKP production capacity is installed entirely in São Paulo. São Paulo has the same biomass productivity as Espírito Santo, presents the second-lowest interstate distance (124.6 km), and is very strategically located for reaching both the domestic BEKP market (Figure 11) and overseas markets, as Santos' port is distant only 82km from it. The first overseas markets to be fulfilled are Europe and North America, but from scenarios where the polyhedral constant ($\Gamma_{m,q=pulp}$) is lower or equal to 9, the China market – the furthest overseas market from Santos' port – becomes financially attractive as well.

One of the reasons why under price pressure the domestic market is preferred is the higher logistic costs associated with exports. For instance, Figure 7 shows that logistic costs are the major detractor of NPV for the nominal scenario. Figure 13 shows that exports contribute to 71% of the total net present revenues but are responsible for 92% of the logistic costs, i.e., the significance of exports on the logistic costs is not matched by their contribution to revenue generation. This cost-share considers only the sea freight component of cost and would be even higher if transportation from factories to port locations was included in the calculation.

This cost relevance is increased as BEKP was considered to be transported in containers in the model. Operation by containers is significantly more expensive than breakbulk, commonly deployed for commercial BEKP operations (HAMERI; BORG; ELORANTA, 2013). Also, container freight references were taken from October 2021 when fares were peaking high (Figure 14). These considerations lead to a conservative estimation of overseas transportation costs for BEKP that might hinder the operation's attractiveness.

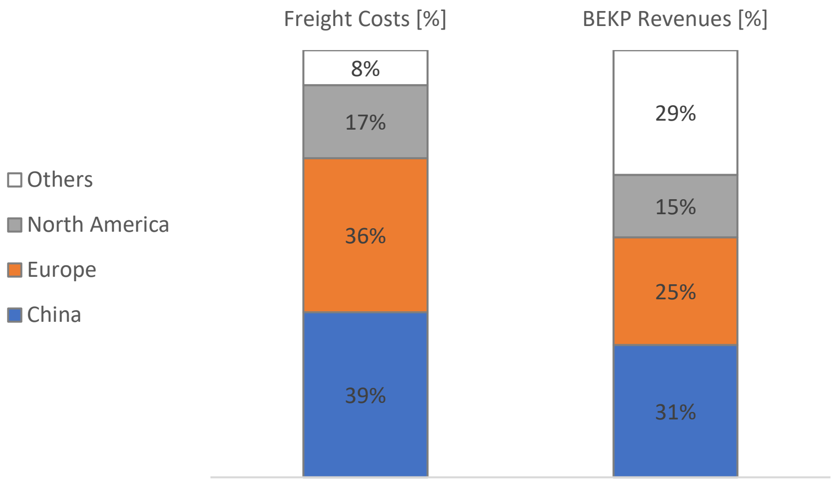

Figure 13 – Comparison of logistic costs and revenue share for domestic and external markets for scenario M.1.
External market freight costs consider only the sea freight component. Transportation from factories to port locations is considered as domestic transference and grouped in "others."

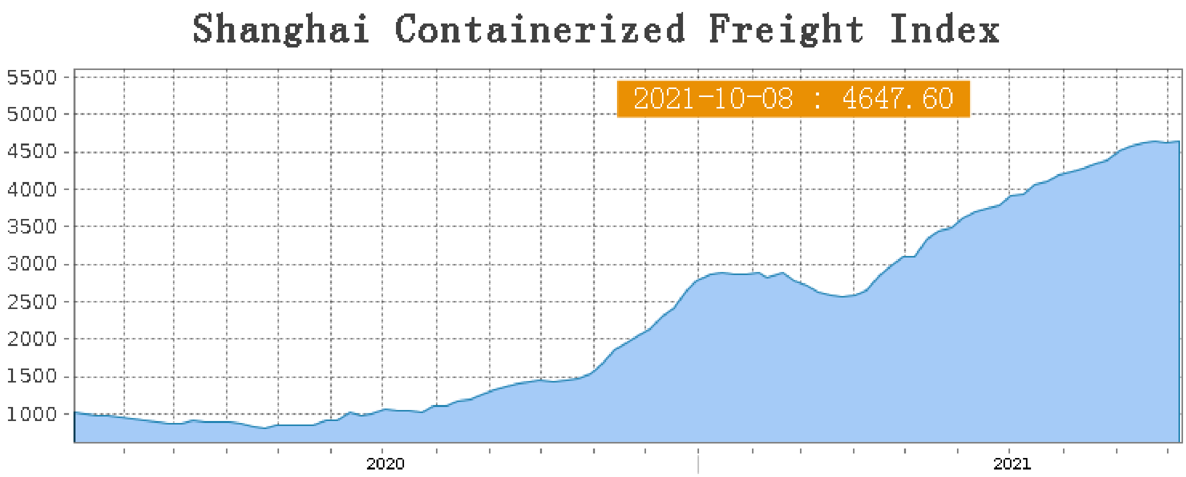

Figure 14 – Evolution of Shanghai Containerized Freight Index (SCFI) international indicator for measuring containerized maritime freight prices.
Source: Shanghai Shipping Exchange (2021).

The optimal logistic network for scenario M.18 ($\Gamma_{m,q=pulp}$ = 9) is shown in Figure 15. The exports are entirely done by the Santos port. The domestic market is mostly fulfilled from the production facility in São Paulo with no logistic intermediate. The exceptions are the Ceará market that has Minas Gerais as an intermediate and São Paulo, which produces the BEKP, sends it to Rio de Janeiro, and receives it back in São Paulo. The first hub is motivated by the methodology of distance estimation used in section 4.1.4.2 that yielded a longer distance to São Paulo – Ceará route (3,140 km) than the São Paulo – Minas Gerais – Ceará route (3,007 km). The second hub is motivated by the difference in the ICMS tax rate from different origins. For instance, a good sold to São Paulo from a seller also in São Paulo pays 18% of ICMS against 12% for the same good sold from a seller in Rio de Janeiro. Financially, this tax difference more than compensates for the extra transportation distance. However, the extra distance might be associated with a greater environmental impact, which reinforces the importance of public policies on the configuration of sustainable biorefinery operations.

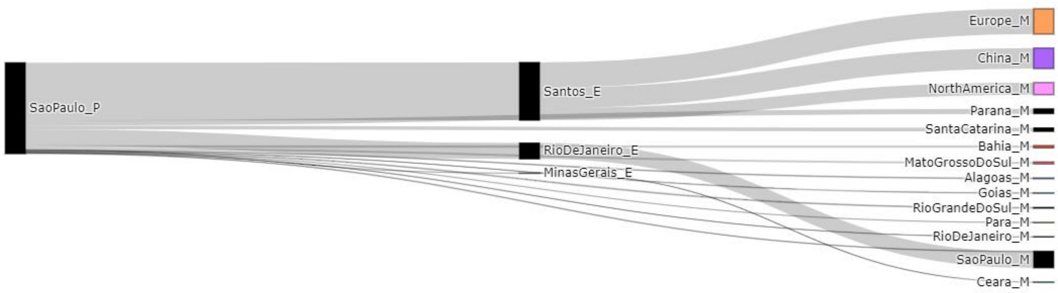

Figure 15 – Optimal logistic network for scenario M.18 which represents the first scenario in which all consumer markets become financially attractive.

The domestic transportation costs were taken considering road transportation done by 3-axle trucks. Infrastructure investments on better road routes and railways could lower domestic transportation costs. The reduction in transportation costs not only can increase the operations attractiveness but can also provide new optimal production arrangements. For instance, the 75% reduction of transportation costs in scenario T.6 could make the BEKP operation financially attractive even under the worst price consideration ($\Gamma_{m,q=pulp}$ = 20). For this scenario, the production capacity is installed in Mato Grosso, which presents the most productive forest (50 Mg $year^{-1}$ ha^{-1}) but is not attractive in main scenarios as it is far from any port location (≥ 1619 km) and the main BEKP consumer markets (≥ 711 km). This suggests that infrastructure investments connecting further UFs with abundant high-productive lands could be an important impulse for biorefineries consolidation.

The logistic cost reduction was able to shift capacity locations but the preference for a single centralized production location was still observed. This preference is associated with the gain of scale in which the total investment of a single production facility is lower than the same capacity distributed into smaller facilities. The gain of scale, on the other hand, is associated with larger logistic costs as the decentralized facilities may be installed closer to several consumer markets. Decentralization of production facilities was only observed in this work when investments' costs were reduced by 75% (scenarios I.3 and I.6), in which the benefits of gains of scale are diminished as the reference investment is lower.

For scenario I.3 that considered the reduction in production investments under no BEKP price uncertainty, São Paulo was still the preferred production facility fulfilling most of the domestic BEKP demand and the entire overseas demand (Figure 16). A small production unit in Bahia was also implemented for fulfilling Alagoas BEKP demand that is distant 583 km from Bahia and 2,426 km from São Paulo. A small production capacity was also installed in Maranhão for fulfilling Ceará and Pará's demands. The first is distant 887km from Maranhão and 3,140km from São Paulo. The second is distant 583 km from Maranhão and 2,884 km from São Paulo. This shows that the model was able to capture Brazil high territorial dimension influence on optimal facilities locations and transport configurations.

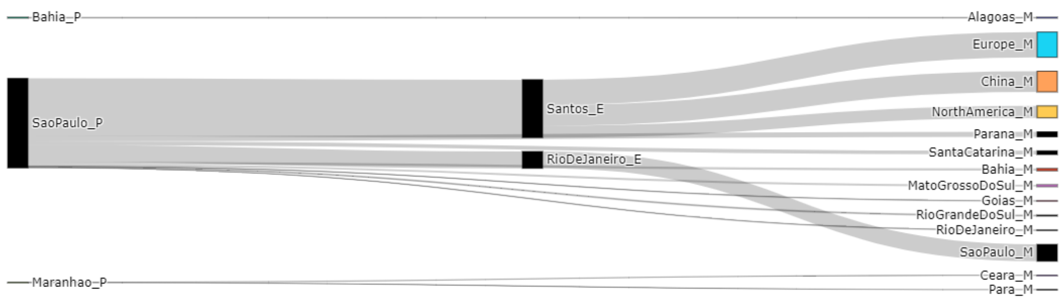

Figure 16 – Optimal logistic network for scenario I.3 that considered a 75% reduction in production investments but no BEKP price uncertainties.

For scenario I.6, which considered the production investment reduction under the worst-case BEKP price uncertainty, the overseas markets were not financially attractive, and Espírito Santo was the preferred production capacity location (Figure 17). A small production facility was implemented in Maranhão for fulfilling the BEKP demand from Pará, distant 583 km from Maranhão and 3,023 from Espírito Santo. And a facility in Rio Grande do Sul was installed for fulfilling its own BEKP demand, distant 2078 km from Espírito Santo. The capacity in Rio Grande do Sul in the first years of operation is also responsible for the partial fulfillment of Santa Catarina demand, as the first periods of operation still do not present enough mature forest for a full biomass supply in Espírito Santo. This result reinforces the importance of the multiperiod planning fitting biomass growth dynamics and that the model was able to take that into account in the optimal solutions.

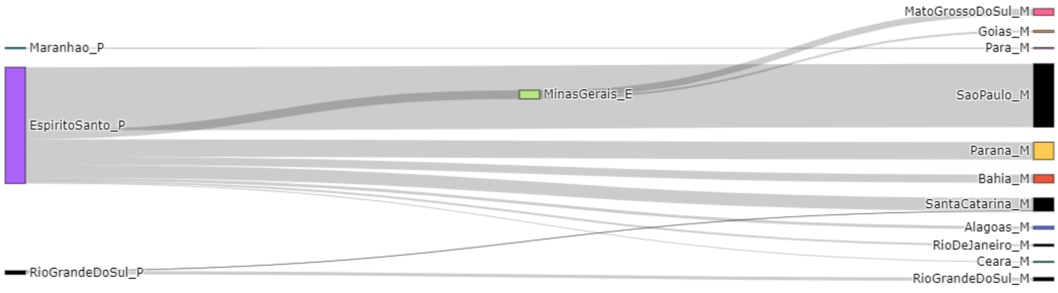

Figure 17 – Optimal logistic network for scenario I.6 that considered a 75% reduction in production investments under worst-case BEKP price uncertainties materialization.

The shifts of capacity locations produced by logistic costs reductions are also accompanied by shifts in the forest locations. In every scenario (M, L, T, and P), the production facility is fed exclusively with biomass from forests within the same state. This highlights the importance of an adequate description of forest dynamics as biomass availability may shift entire production facilities' installation decisions.

Biomass availability not only affects the sizing of the production facilities but also the level of occupation of this capacity. For instance, Figure 10 shows that the total shipped BEKP for each market increases as the degree of conservatism decreases. The difference in volume occurs especially within the first periods of operation (Figure 18). This may be explained by the biomass age distribution available for harvesting. On further periods, the planting and harvesting operation stabilizes and allows the biomass supply to become more stable. During the first years of operation, the biomass availability is not within its ideal distribution, making it necessary to harvest forests that are not yet mature (Figure 19). This operation is more expensive and demands lower price uncertainty for becoming financially attractive.

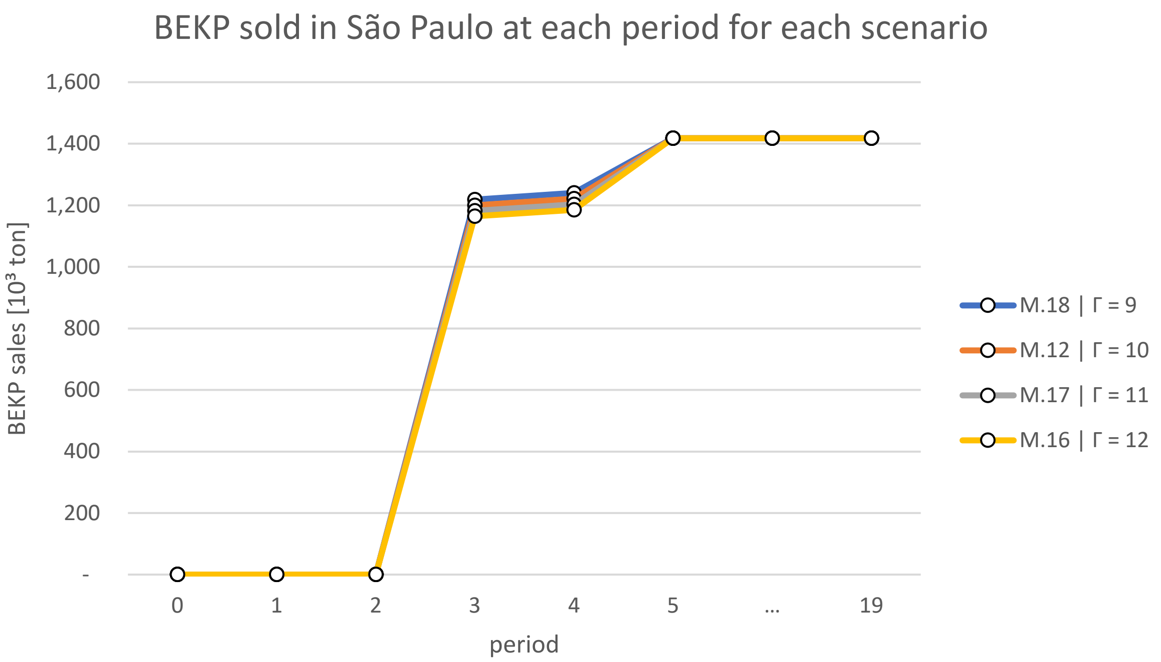

Figure 18 – Difference in total BEKP shipped volume within each period for consumer market São Paulo.

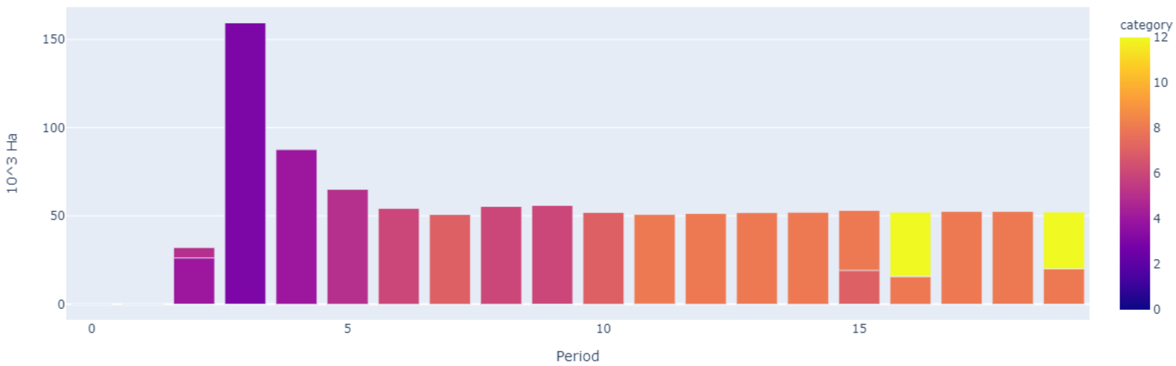

Figure 19 – Harvesting age profile.
The first periods are characterized by more intense harvesting as younger forests are being harvested and thus more land is needed for keeping the same level of biomass supply.

Even though biomass availability displays a significant role in shaping operating decisions, the degree of conservatism on forest uncertain is less influential on the overall profitability of the operation. Figure 20 shows that optimal NPV presents a steep decrease on scenarios with lower uncertainty conservatism (scenarios M.8 and M.1) and then stabilizes to virtually the same NPV for scenarios with polyhedral uncertainty constant ($\Gamma_{f,b}$) ranging from 6 and above (scenarios M.3, M.10, and M.09).

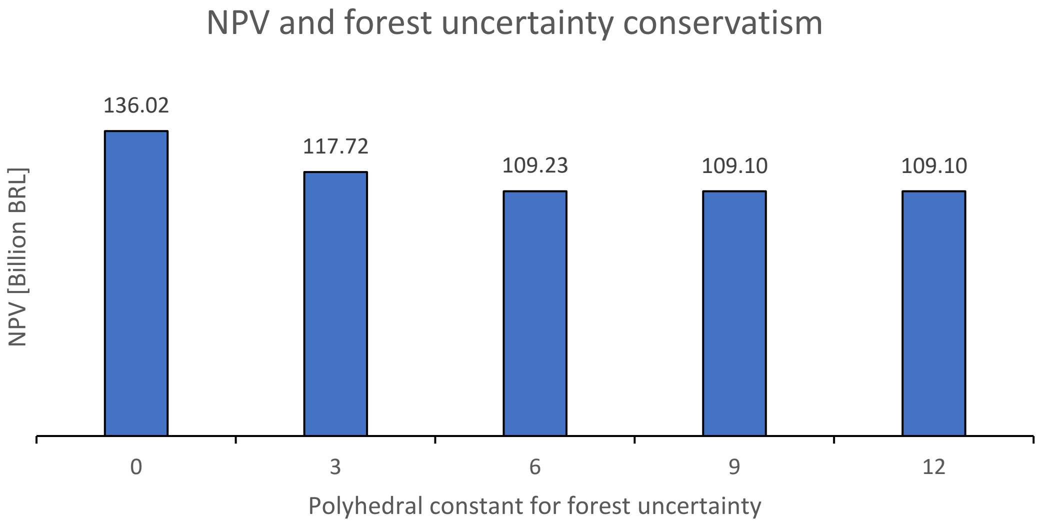

Figure 20 – Optimal NPV decreases as the degree of conservatism is increased for forest uncertainty.

Figure 21 shows that, under any biomass productivity uncertainty condition, the majority of harvested biomass is within 6 to 8 years old. This shows that the model was also able to identify the optimal harvesting ages commonly deployed for eucalyptus in Brazil (DIAZ-BALTEIRO; RODRIGUEZ, 2006). However, it should be noted that for the most conservative formulation ($\Gamma_{f,b}$ = 12), no harvested biomass is older than 6-years old. Thus, any formulation whose polyhedral constant is greater or equal to six has an optimal solution virtually equivalent to the worst-case scenario, which explains the NPV stabilization shown in Figure 20.

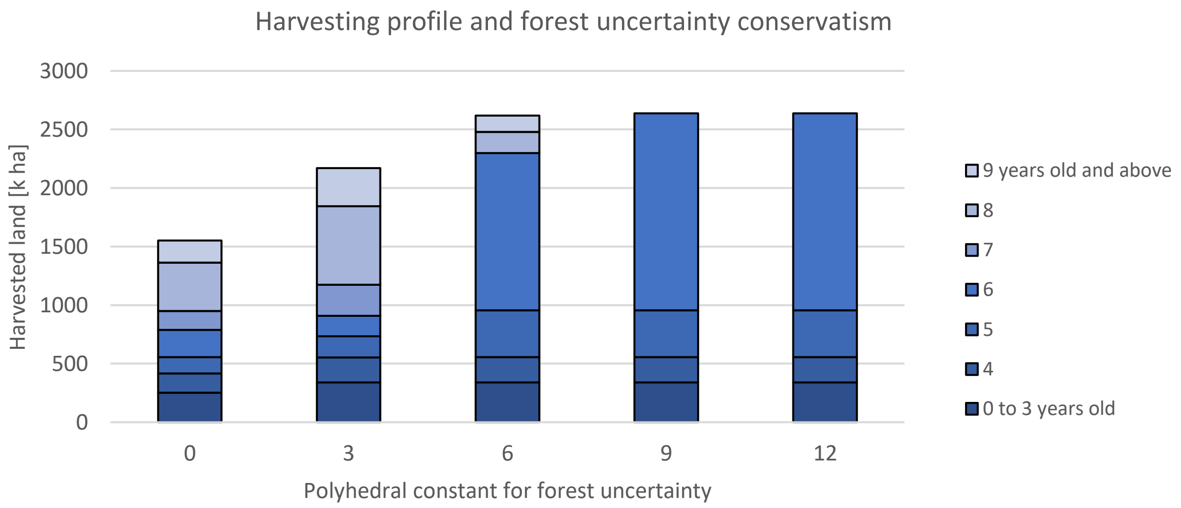

Figure 21 – Harvesting age profile forest uncertainty scenario.

The biomass growth is represented by a logistic curve with higher growth rates during the first years of the biomass plantation (Figure 6). Thus, a possible interpretation for the impact of the polyhedral formulation on forest uncertainty for the most conservative formulations is that the biomass in its first $\Gamma_{f,b}$ years presents the worst-case productivity and the nominal productivity for the following years. This effect is illustrated in Figure 22 in which can be seen that after having worst-case productivity on the most productive ages of the curve the aging of biomass is not effective in reverting the final expected accumulated biomass growth under the modeling assumptions of section 4.1.2.3. This explains the preference for harvesting younger trees in most conservative scenarios.

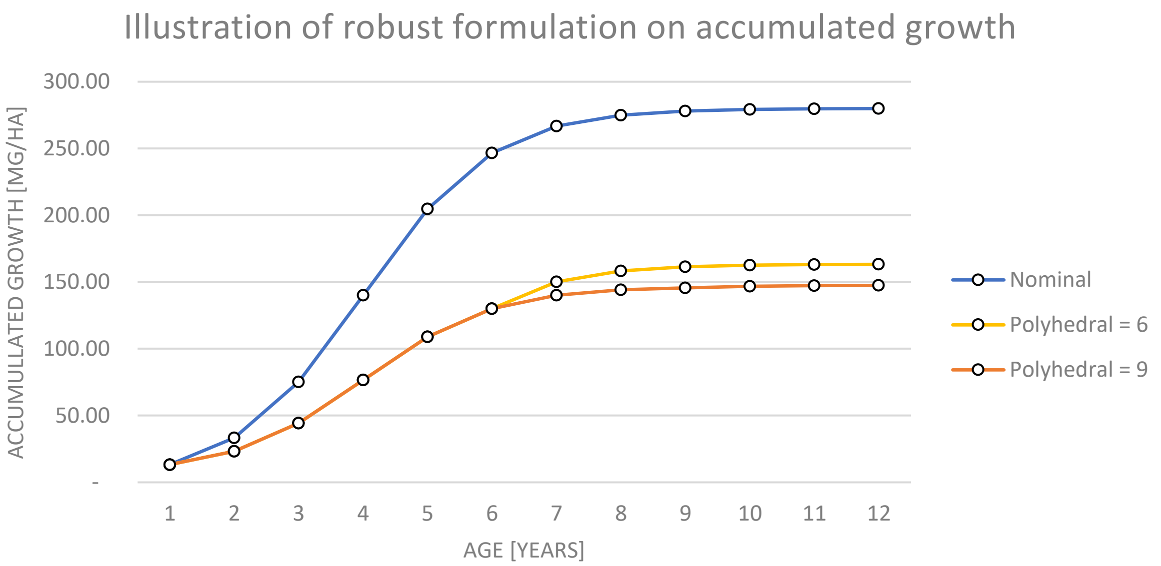

Figure 22 – Interpretation of the polyhedral robust formulation for biomass productivity for E. urophylla planted in Bahia.

When biomass productivity is uncertain, larger areas need to be cultivated to ensure wood supply levels even when facing the lower levels of productivity. For instance, scenario M.3, the most conservative regarding forest uncertainty, uses 70% more land than the nominal one. One of the major drawbacks of biorefineries operation is the competition for land usage with food crops and over-conservative solutions, such as M.3, may increase this land competition threatening the sustainable implantation of the operation. This stress out the relevance of the polyhedral formulation for controlling the degree of conservatism regarding uncertainties. For instance, scenario M.10, with the polyhedral constant of 3, uses 40% more land than the nominal formulation and still hedges for 3-years of severe productivity conditions within the biomass lifecycle, which is a reasonable hedge considering the majority of biomass is harvested within 6-years (Figure 21) and that severe droughts in Brazil usually do not last for several years[14].

For all scenarios, E. urophylla was the only planted biomass species in all forest units. This homogeneity is not interesting for a robust forest operation as plagues, diseases, and other environmental conditions might have different effects on different eucalyptus clone. Thus, planting several different clones might increase the operation robustness towards biomass productivity uncertainties and preserving the biodiversity of biomass planted areas. The current model formulation, however, does not capture clonal heterogeneity in the biomass growth uncertain, which explain the preference for a single biomass species in the optimal decision.

4.5 CONCLUSIONS FOR THE CASE STUDY

The case study shows that the optimal NPV for the nominal scenario is 136 billion BRL. The operation is associated with a positive net present value in which chemical sales are the main positive contributors and logistic costs are the main negative ones.

The lignin operation is not financially attractive under the nominal scenario and requires an increase of 225 or 250% from its nominal value depending on the uncertainty associated to the energy prices to become financially attractive. These results suggest that developing higher-value applications for lignin may be important for the successful consolidation of the operation.

Although electricity profitability is important for defining lignin attractiveness, the utility sales presented a diminished relevance on the overall biorefinery profitability, representing only 6.7% of the present value for all operating revenues.

[14] For a map of historical droughts in Brazil, see Bevacqua *et al.* (2021).

The only parameter whose uncertainty was able to severely impact operating decisions was BEKP prices. Every scenario with a polyhedral constant ($\Gamma_{m,q=pulp}$) greater than 15 presented a null optimal solution, i.e., the optimal solution is to not build any biorefining operation.

In scenario M.14 ($\Gamma_{m,q=pulp}$ = 14), the most conservative BEKP price yielding a non-null optimal solution, the optimal NPV is 150 million BRL and the operation is designed to fulfill only part of the domestic BEKP demand. Under less conservative uncertainties scenarios ($\Gamma_{m,q=pulp} \leq 12$) the overseas market becomes financially attractive. One of the reasons why under price pressure the domestic market is preferred is the higher logistic costs associated with exports.

The domestic market is mostly fulfilled from the production facility in São Paulo with no logistic intermediate. Some exceptions arise, motivated by the origin-destination dependent tax rate.

The reduction in transportation costs not only can increase the operations attractiveness but can also provide new optimal production arrangements. For instance, the 75% reduction of transportation costs could make the BEKP operation financially attractive even under the worst price consideration. For this scenario, the production capacity is installed in Mato Grosso, the location with higher biomass productivity, but unattractive on nominal scenarios due to its distance from ports and consumer markets.

Decentralization of production facilities was only observed in this work when investments' costs were reduced by 75%, in which the benefits of gains of scale are diminished as the reference investment is lower.

The shifts of capacity locations produced by logistic costs reductions are also accompanied by shifts in the forest locations. In every scenario (M, L, T, and P), the production facility is fed exclusively with biomass from forests within the same state. This highlights the importance of an adequate description of forest dynamics as biomass availability may shift entire production facilities' installation decisions.

Biomass availability not only affects the sizing of the production facilities but also the level of occupation of this capacity, especially on early periods of operation when initial plantations are not mature yet.

Under any scenario for biomass productivity, the majority of biomass is harvested within 6 to 8 years old, matching the optimal harvesting ages commonly deployed for eucalyptus in Brazil.

The uncertainty in biomass productivity was especially relevant to define the amount of occupied land. The most conservative solution for biomass productivity, uses 70% more land than the nominal one. This contrasts to an intermediate scenario, that still hedges for 3-years of severe productivity conditions and uses 40% more land than the nominal formulation. This reinforces the importance of the degree of conservatism to be controlled.

5 GENERAL CONCLUSIONS

A mathematical programming generic model was presented for the optimal design of biorefineries considering four interconnected decision layers: Biomass, Technology, Logistics, and Market. The model can capture forest systems dynamics and handle uncertainties on product selling prices and biomass productivity. The model capabilities were illustrated through a case study on a eucalyptus biorefinery that may produce BEKP, Lignin, and Electricity.

The case study showed that the layers interconnection is notably important for the optimal solution configuration. For instance, forest dynamics may render production spots unattractive, transportation costs may prohibit entire markets servicing, and tax policies may favor longer logistic networks. These integrated dynamics might be especially relevant for multi-product biorefineries in which several products compete for the same resources, requiring an integrated evaluation of trade-offs and opportunity costs.

The biomass dynamics displayed a vital role on the core strategic decisions, with biomass availability and forest distances driving decisions on all other layers. This reinforces the importance on the adequate modeling of the biomass growth dynamics for ensuring assertiveness of the optimal solutions. The adequate consideration of the supply networks is also relevant. For instance, the operation of some highly productive forest lands becomes financially attractive once logistic costs are reduced. The evaluation of these different logistic costs' scenarios may be useful for evaluating infrastructure investments decision.

The technological representation of the framework allows for the incorporation of complex process topologies with simple tabular data. This flexibility and ease-of-use are important for biorefineries design as several processing routes can branch from the same product along with several new integration points that results in a complex superstructure to be mathematically represented.

The proposed model was also proved useful to estimate minimum selling prices for products that might not be considered financially attractive under the nominal scenario. The case study also highlights the importance of ensuring high-value applications (with higher selling prices) for the new biorefinery products operation to be economic attractive.

The relevance of the high-volatile product selling prices in shaping the optimal solution exposes the vulnerabilities of the solution to the uncertainty in parameters estimation. A robust formulation integrating a box and polyhedral uncertainty set was implemented for both products selling prices and biomass productivity. The proposed formulation allowed for hedging against uncertainties at the same time as controlling for the degree of conservatism of the solution.

The choice of conservatism level was demonstrated as an important feature of the framework. Under a full conservative approach in the case study, the entire biorefinery operation is considered financially unattractive, contrasting with an opportunity of over 136 billion BRL in net present value for the operation in the nominal scenario. In between, some still conservative designs were proposed that could provide robustness for the operation and still benefit from the biorefining opportunities. For the forest layer decisions, the over-conservatism has been shown harmful as it proposes an excessive usage of land to ensure a stable wood supply. This excessive land usage might compete with lands for food crops which is not desirable for sustainability principles.

6 SUGGESTED FURTHER WORKS

To improve the proposed model and to further deal with the scientific challenges on biorefinery decision-making processes, the following points are suggested for further works:

I. **The integration of recourse actions as an adjustable robust optimization formulation** allowing for recourse actions to be made upon the realization of uncertainties. This is especially relevant for uncertainties on biomass productivity, as recourse actions would allow decision-makers to reduce the conservative excess in land usage in early periods and adjust forest plantation planning upon the uncertainties' materialization.

II. **The construction of a robust formulation that captures the influence of Eucalyptus clonal heterogeneity in the uncertainty behavior for biomass productivity**. This would allow decision-maker to evaluate clonal diversity as a strategy for increasing the robustness of the operation.

III. **The incorporation of sustainability assessment or other environmental performance evaluation** (such as GHG emissions and land usage) within the decision framework.

Beyond the generic model, other improvements are suggested in the case study as well:

I. **The adoption of a climate/geological-based segmentation of the Forest Layer instead of political one**. This segmentation would better describe the influence of climate, soil, and other environmental variables on biomass growth rates.

II. **The inclusion of other high-value products and conversion routes in the model superstructure**, such as the thermochemical valorization of black liquor and the biological valorization of hemicelluloses.

III. **The consideration of a more diverse biomass set**, such as other eucalyptus clones, other forest species and non-forest biomass. This would allow the evaluation of the competitiveness of each biomass type to each biorefining product at each region. It would also allow the evaluation of synergies in integrating process operations (utilities, raw materials and others) among different sourced Biorefineries.

IV. **The more detailed description of the P&P processes dynamics**. For instance, CO_2 produced in the lime kiln combustion might be used as a raw material for the acid precipitation of lignin. Also, the washed filtrated, that still contains part of lignin, might be used as a weak liquor for burning in the recovery boiler. These might be processing alternatives for a more economically attractive lignin extraction process and their adequate description and incorporation into the model would allow for a more assertive evaluation of the lignin business model.

V. **The better description of effluents and residues on the subset Set R of the model**.

REFERENCES[15]

ABDELAZIZ, O. Y. *et al.* Conceptual Design of a Kraft Lignin Biorefinery for the Production of Valuable Chemicals via Oxidative Depolymerization. **ACS Sustainable Chemistry and Engineering**, v. 8, n. 23, p. 8823–8829, 2020.

AFONSO, J. R.; ARAÚJO, E. C.; FAJARDO, B. G. The role of fiscal and monetary policies in the Brazilian economy: Understanding recent institutional reforms and economic changes. **Quarterly Review of Economics and Finance**, v. 62, p. 41–55, 2016.

AGÊNCIA DE REGULAÇÃO DE SERVIÇOS PÚBLICOS DO ESPÍRITO SANTO. **Resolução ARSP 049/2021.** ESPÍRITO SANTO (Federative Unit), 2021. Available at: <https://arsp.es.gov.br/Media/arsi/Legislação/Resoluções Gás Natural/ARSP/2021/ResolucaoARSPn049_2021.pdf>. Accessed in: 7 Sep. 2021

AGÊNCIA NACIONAL DE TRANSPORTE AQUAVIÁRIO. **Anuário Estatístico**. Available at: <http://web.antaq.gov.br/Anuario/>. Accessed in: 31 Aug. 2021.

AGÊNCIA NACIONAL DE TRANSPORTES TERRESTRES. **Resolução 5949/2021.** BRAZIL, 2021. Available at: <https://anttlegis.antt.gov.br/action/ActionDatalegis.php?acao=detalharAto&tipo=RES&numeroAto=00005949&seqAto=000&valorAno=2021&orgao=DG/ANTT/MI&codTipo=&desItem=&desItemFim=&cod_menu=5408&cod_modulo=161&pesquisa=true>. Accessed in: 6 Sep. 2021

AGERBA. **Resolução AGERBA 36/2021.**BAHIA (Federative Unit), 28 Jul. 2021. Available at: <http://www.agerba.ba.gov.br/node/2313>. Accessed in: 7 Sep. 2021

AHMED, S.; SHAPIRO, A. The sample average approximation method for stochastic programs with integer recourse. **SIAM J Optim**, v. 24, 2002.

AJAO, O. *et al.* Hemicellulose based integrated forest biorefineries: Implementation strategies. **Industrial Crops and Products**, v. 126, p. 250–260, 2018.

ALEX MARVIN, W. *et al.* Economic Optimization of a Lignocellulosic Biomass-to-Ethanol Supply Chain. **Chemical Engineering Science**, v. 67, n. 1, p. 68–79, 2012.

---

[15] In accordance with the Brazilian National Standards Organization (ABNT NBR 6023)

ALGÁS. **Gás Industrial - Algás - Gás de Alagoas S.A.** Available at: <https://algas.com.br/gas-natural/gas-industrial/>. Accessed in: 7 Sep. 2021.

AN, H.; WILHELM, W. E.; SEARCY, S. W. A mathematical model to design a lignocellulosic biofuel supply chain system with a case study based on a region in Central Texas. **Bioresource Technology**, v. 102, n. 17, p. 7860–7870, 2011.

AWUDU, I.; ZHANG, J. Uncertainties and sustainability concepts in biofuel supply chain management: A review. **Renewable and Sustainable Energy Reviews**, v. 16, n. 2, p. 1359–1368, 2012.

AZADEH, A.; VAFA ARANI, H.; DASHTI, H. A stochastic programming approach towards optimization of biofuel supply chain. **Energy**, v. 76, p. 513–525, 2014.

BACHMANN E ASSOCIADOS; ABTCP. **Análise Comparativa do Desempenho de Fábricas de Celulose e Papel 2010.** Curitiba, 2011.

BAIRAMZADEH, S.; PISHVAEE, M. S.; SAIDI-MEHRABAD, M. Multiobjective Robust Possibilistic Programming Approach to Sustainable Bioethanol Supply Chain Design under Multiple Uncertainties. **Industrial and Engineering Chemistry Research**, v. 55, n. 1, p. 237–256, 2016.

BAIRAMZADEH, S.; SAIDI-MEHRABAD, M.; PISHVAEE, M. S. Modeling different types of uncertainty in biofuel supply network design and planning: A robust optimization approach. **Renewable Energy**, v. 116, p. 500–517, 2018.

BAJPAI, P. Raw Material Preparation. In: BAJPAI, P. (Ed.). . **Biermann’s Handbook of Pulp and Paper**. 3rd. ed. Kanpur: Elsevier Inc., 2018. p. 279–294.

BANCO CENTRAL DO BRASIL. **Inflation targeting track record**. Available at: <https://www.bcb.gov.br/en/monetarypolicy/historicalpath>. Accessed in: 15 Aug. 2021a.

BANCO CENTRAL DO BRASIL. **Focus - Market Readout (27-ago-2021)**. Available at: <https://www.bcb.gov.br/en/publications/focusmarketreadout/27082021>. Accessed in: 4 Sep. 2021b.

BAO, B. *et al.* A shortcut method for the preliminary synthesis of process-technology pathways: An optimization approach and application for the conceptual design of integrated biorefineries. **Computers and Chemical Engineering**, v. 35, n. 8, p. 1374–1383, 2011.

BECKHAM, G. T. *et al.* Opportunities and challenges in biological lignin valorization. **Current Opinion in Biotechnology**, v. 42, p. 40–53, 2016.

BEN-TAL, A. *et al.* Adjustable robust solutions of uncertain linear programs. **Mathematical Programming**, v. 99, n. 2, p. 351–376, 2004.

BEN-TAL, A.; EL GAHOUI, L.; NEMIROSVSKI, A. **Robust Optimization**. New Jersey, USA: Princeton University Press, 2009, 576p.

BERGAMINI, M. L. *et al.* An improved piecewise outer-approximation algorithm for the global optimization of MINLP models involving concave and bilinear terms. **Computers and Chemical Engineering**, v. 32, n. 3, p. 477–493, 2008.

BERTSIMAS, D.; BROWN, D. B.; CARAMANIS, C. Theory and applications of robust optimization. **SIAM Review**, v. 53, n. 3, p. 464–501, 2011.

BERTSIMAS, D.; SIM, M. The price of robustness. **Operations Research**, v. 52, n. 1, p. 35–53, 2004.

BEVACQUA, A. G. *et al.* Spatial and temporal patterns of propagation from meteorological to hydrological droughts in Brazil. **Journal of Hydrology**, v. 603, p. 126902, 2021.

BHARDWAJ, N.; VERMA, P. Microbial Xylanases: A Helping Module for the Enzyme Biorefinery Platform. **Bioenergy Research**, p. 129–152, 2021.

BHATIA, S. K. *et al.* Recent developments in pretreatment technologies on lignocellulosic biomass: Effect of key parameters, technological improvements, and challenges. **Bioresource Technology**, v. 300, p. 122724, 2020.

BINKLEY, D. *et al.* The interactions of climate, spacing and genetics on clonal Eucalyptus plantations across Brazil and Uruguay. **Forest Ecology and Management**, v. 405, p. 271–283, 2017.

BIRGE, J. R.; LOUVEAUX, F. **Introduction to Stochastic Programming**. New York, NY: Springer New York, 2011. 485p.

BO PAPER. **BO Paper - About**. Available at: <http://bopapergroup.com/en/institucional/about/>. Accessed in: 6 Sep. 2021.

BOJARSKI, A. D. *et al.* Incorporating environmental impacts and regulations in a holistic supply chains modeling: An LCA approach. **Computers and Chemical Engineering**, v. 33, n. 10, p. 1747–1759, 2009.

BORDONAL, R. DE O. *et al.* Sustainability of sugarcane production in Brazil. A review. **Agronomy for Sustainable Development 2018 38:2**, v. 38, n. 2, p. 1–23, 2018.

BOWLING, I. M.; PONCE-ORTEGA, J. M.; EL-HALWAGI, M. M. Facility location and supply chain optimization for a biorefinery. **Industrial and Engineering Chemistry Research**, v. 50, n. 10, p. 6276–6286, 2011.

BRAZILIAN TREE INDUSTRY. **IBÁ Annual Report**, 2021.

BRIDGWATER, A. V. Renewable fuels and chemicals by thermal processing of biomass. **Chemical Engineering Journal**, v. 91, n. 2–3, p. 87–102, 2003.

CAETANO BACHA, C.; STEGE, A.; HARBS, R. Ciclos de preços de terras agrícolas no Brasil. **Revista de Política Agrícola**, v. 25, n. 4, p. 18–37, 2016.

CÂMARA BRASILEIRA DA INDÚSTRIA DE CONSTRUÇÃO. **Banco de Dados - CBIC**. Available at: <http://www.cbicdados.com.br/menu/materiais-de-construcao/cimento>. Accessed in: 4 Sep. 2021.

CARRILLO, I. *et al.* Comparative study of cellulosic components isolated from different Eucalyptus species. **Cellulose**, v. 25, n. 2, p. 1011–1029, 2018.

CARTA GOIÁS. **Demonstrações Financeira 2016 e 2015**. Available at: <http://www.cartafabril.com.br/wp-content/uploads/2017/10/dfs-carta-goias-2015-2016.pdf>. Accessed in: 6 Sep. 2021.

CEGÁS. **Tabela de tarifas atual – Cegás**. Available at: <https://www.cegas.com.br/tabela-de-tarifas-atual/>. Accessed in: 7 Sep. 2021.

CHANDRA, R. *et al.* Algal biorefinery: A sustainable approach to valorize algal-based biomass towards multiple product recovery. **Bioresource Technology**, v. 278, p. 346–359, 2019.

CHEALI, P. *et al.* Upgrading of lignocellulosic biorefinery to value-added chemicals: Sustainability and economics of bioethanol-derivatives. **Biomass and Bioenergy**, v. 75, p. 282–300, 2015.

CHEN, Q.; GROSSMANN, I. E. Recent Developments and Challenges in Optimization-Based Process Synthesis. **Annual Review of Chemical and Biomolecular Engineering**, v. 8, p. 249–283, 2017.

CHRISTOPHER, L. P. Integrated Forest Biorefineries: Current State and Development Potential. In: CHRISTOPHER, L. P. (Ed.). . **Integrated Forest Biorefineries: Challenges and Opportunities**. Cambridge, UK: Roya Society of Chemistryl, p. 1-66, 2013.

CIA CANOINHAS DE PAPEL. **Cia Canoinhas | Arquivo Informações da Empresa - Cia Canoinhas**. Available at: <http://www.canoinhas.com.br/empresa/>. Accessed in: 6 Sep. 2021.

COLLETTE, Y.; SIARRY, P. **Multiobjective Optimization**. Berlin, Heidelberg: Springer Berlin Heidelberg, 2004. 293p.

COMGAS. **Tarifas Industrial – Comgas**. Available at: <https://www.comgas.com.br/tarifas/industrial/>. Accessed in: 7 Sep. 2021.

COMPAGAS. **Tabela de preços INDUSTRIAL**. Available at: <http://agv.compagas.com.br/index.php?action=uiprecos.index&segmento=1>. Accessed in: 7 Sep. 2021.

CONTABILIZEI. **ICMS: o que é,como calcular e a Tabela ICMS completa**. Available at: <https://www.contabilizei.com.br/contabilidade-online/tabela-icms/>. Accessed in: 4 Sep. 2021.

ČUČEK, L. *et al.* Multi-period synthesis of optimally integrated biomass and bioenergy supply network. **Computers and Chemical Engineering**, v. 66, p. 57–70, 2014.

CVG. **CVG – Cahdam**. Available at: <https://www.cvg.ind.br/>. Accessed in: 6 Sep. 2021.

DAL-MAS, M. *et al.* Strategic design and investment capacity planning of the ethanol supply chain under price uncertainty. **Biomass and Bioenergy**, v. 35, n. 5, p. 2059–2071, 2011.

DANG, V. Q.; NGUYEN, K. L. A universal kinetic model for characterisation of the effect of chip thickness on kraft pulping. **Bioresource Technology**, v. 99, p. 1486–1490, 2008.

DE BHOWMICK, G.; SARMAH, A. K.; SEN, R. Lignocellulosic biorefinery as a model for sustainable development of biofuels and value added products. **Bioresource Technology**, v. 247, p. 1144–1154, 2018.

DE CARVALHO, E. A.; DE ALMEIDA, S. L. M. **Caulim e Carbonato de Cálcilo: Competição na Indústria de Papel**. Rio de Janeiro: CETEM - Centro de Tecnologia Mineral, 1997.

DIAZ-BALTEIRO, L.; RODRIGUEZ, L. C. E. Optimal rotations on Eucalyptus plantations including carbon sequestration-A comparison of results in Brazil and Spain. **Forest Ecology and Management**, v. 229, n. 1–3, p. 247–258, 2006.

DREWRY SHIPPING CONSULTANTS. **World Container Index - 09 Sep**. Available at: <https://www.drewry.co.uk/supply-chain-advisors/supply-chain-expertise/world-container-index-assessed-by-drewry>. Accessed in: 11 Sep. 2021.

DUNNETT, A.; ADJIMAN, C.; SHAH, N. Biomass to heat supply chains applications of process optimization. **Process Safety and Environmental Protection**, v. 85, n. 5 B, p. 419–429, 2007.

DUNNETT, A. J.; ADJIMAN, C. S.; SHAH, N. A spatially explicit whole-system model of the lignocellulosic bioethanol supply chain: An assessment of decentralised processing potential. **Biotechnology for Biofuels**, v. 1, p. 1–17, 2008.

EASON, J. P.; CREMASCHI, S. A multi-objective superstructure optimization approach to biofeedstocks-to-biofuels systems design. **Biomass and Bioenergy**, v. 63, p. 64–75, 2014.

EICHLER, P. *et al.* Potential assessment of eucalyptus grown for biorefinery processes. **Agronomy Science and Biotechnology**, v. 3, n. 1, p. 01–11, 2017.

EKŞIOĞLU, S. D. *et al.* Analyzing the design and management of biomass-to-biorefinery supply chain. **Computers and Industrial Engineering**, v. 57, n. 4, p. 1342–1352, 2009.

EL-HALWAGI, A. *et al.* Optimizing safety-constrained solvent selection for process systems with economic uncertainties. **Journal of Loss Prevention in the Process Industries**, v. 26, n. 3, p. 495–498, 2013.

ELIA, J. A. *et al.* Optimal energy supply network determination and life cycle analysis for hybrid coal, biomass, and natural gas to liquid (CBGTL) plants using carbon-based hydrogen production. **Computers and Chemical Engineering**, v. 35, n. 8, p. 1399–1430, 2011.

EMPRESA DE PESQUISA ENERGÉTICA. **2017 Statistical Yearbook of electricity.**Brasília, Brazil., 2017. 230p.

EUROPEAN CENTRAL BANK. **Brazilian real (BRL)**. Available at: <https://www.ecb.europa.eu/stats/policy_and_exchange_rates/euro_reference_exchange_rates/html/eurofxref-graph-brl.en.html>. Accessed in: 7 Sep. 2021.

FABRETTI, L. C. **Contabilidade Tributária**. 15th. ed. São Paulo, Brazil: Editora Atlas, 2015. 424p.

FARINHA E SILVA, C. A.; BUENO, J. M.; NEVES, M. R. A INDÚSTRIA DE CELULOSE E PAPEL NO BRASIL. **Guia ABTCP - Fornecedores e Fabricantes**, p. 16–28, 2017.

FEDERAÇÃO DA AGRICULTURA E PECUÁRIA DO ESTADO DE MATO GROSSO. **Diagnóstico de florestas plantadas do Estado de Mato Grosso**. Cuiabá, Brazil, 2013. 106p.

FRANCIS, D. W.; TOWERS, M. T.; BROWNE, T. C. **Energy Cost reduction in the Pulp and Paper Industry - An Energy Benchmarking Perspective**. Montreal, Canada: Pulp and Paper research Institute of Canada, 2002. 28p.

GAO, J.; YOU, F. Modeling framework and computational algorithm for hedging against uncertainty in sustainable supply chain design using functional-unit-based life cycle optimization. **Computers and Chemical Engineering**, v. 107, p. 221–236, 2017.

GASMIG. **Industrial Tarifas**. Available at: <http://www.gasmig.com.br/NossosServicos/Industrial/Paginas/Tarifas.aspx>. Accessed in: 7 Sep. 2021.

GEBRESLASSIE, B. H.; WAYMIRE, R.; YOU, F. Sustainable design and synthesis of algae-based biorefinery for simultaneous hydrocarbon biofuel production and carbon sequestration. **AIChE Journal**, v. 59, n. 5, p. 1599–1621, 2013.

GEBRESLASSIE, B. H.; YAO, Y.; YOU, F. Design under uncertainty of hydrocarbon biorefinery supply chains: Multiobjective stochastic programming models, decomposition algorithm, and a Comparison between CVaR and downside risk. **AIChE Journal**, v. 58, n. 7, p. 2155–2179, 2012.

GIAROLA, S.; BEZZO, F.; SHAH, N. A risk management approach to the economic and environmental strategic design of ethanol supply chains. **Biomass and Bioenergy**, v. 58, p. 31–51, 2013.

GIUDICI, R.; PARK, S. W. Kinetic Model for Kraft Pulping of Hardwood. **Industrial and Engineering Chemistry Research**, v. 35, n. 3, p. 856–863, 1996.

GIULIANO, A.; POLETTO, M.; BARLETTA, D. Process optimization of a multi-product biorefinery: The effect of biomass seasonality. **Chemical Engineering Research and Design**, v. 107, p. 236–252, 2016.

GONELA, V. *et al.* Stochastic optimization of sustainable hybrid generation bioethanol supply chains. **Transportation Research Part E: Logistics and Transportation Review**, v. 77, p. 1–28, 2015.

GONELA, V.; ZHANG, J.; OSMANI, A. Stochastic optimization of sustainable industrial symbiosis based hybrid generation bioethanol supply chains. **Computers and Industrial Engineering**, v. 87, p. 40–65, 2015.

GONZÁLEZ-DELGADO, Á. D.; KAFAROV, V.; EL-HALWAGI, M. Development of a topology of microalgae-based biorefinery: Process synthesis and optimization using a combined forward-backward screening and superstructure approach. **Clean Technologies and Environmental Policy**, v. 17, n. 8, p. 2213–2228, 2015.

GRINBERG, M. Flask Web Development. **O'Reilly**, p. 1–314, 2018.

GROSSMANN, I. E. *et al.* Recent advances in mathematical programming techniques for the optimization of process systems under uncertainty. **Computers and Chemical Engineering**, v. 91, p. 3–14, 2016.

GROSSMANN, I. E. **Advanced Optimization for Process Systems Engineering**. Cambridge, USA: Cambridge University Press, 2021. 102p.

GROSSMANN, I. E.; GUILLÉN-GOSÁLBEZ, G. Scope for the application of mathematical programming techniques in the synthesis and planning of sustainable processes. **Computers and Chemical Engineering**, v. 34, n. 9, p. 1365–1376, 2010.

HAMERI, A.-P.; BORG, A.; ELORANTA, E. Vendor-managed inventory in a global maritime supply chain – The case of a Brazilian pulp producer. **Maritime Economics & Logistics 2013 16:2**, v. 16, n. 2, p. 207–227, 2013.

HART, W. E. *et al.* **Pyomo — Optimization Modeling in Python**. 2. ed. Cham, Switzerland: Springer International Publishing, 2017. 231p.

HOLLADAY, J. E. *et al.* **Top Value-Added Chemicals from Biomass Volume II — Results of Screening for Potential Candidates from Biorefinery Lignin. Prepared for the U.S. Department of Energy under Contract DE-AC05-76RL01830**. Springfield, USA: National Technical Information Service, U.S. Department of Commerce, 2007. 79p.

HUANG, C. *et al.* Preparation of lignosulfonates from biorefinery lignins by sulfomethylation and their application as a water reducer for concrete. **Polymers**, v. 10, n. 8, 2018.

HUANG, Y.; CHEN, C. W.; FAN, Y. Multistage optimization of the supply chains of biofuels. **Transportation Research Part E: Logistics and Transportation Review**, v. 46, n. 6, p. 820–830, 2010.

IBGE. **Áreas Territoriais**. Available at: <https://www.ibge.gov.br/geociencias/organizacao-do-territorio/estrutura-territorial/15761-areas-dos-municipios.html?edicao=24050&t=acesso-ao-produto>. Accessed in: 31 Aug. 2021.

IBGE. **Tabela 5930: Área total existente em 31/12 dos efetivos da silvicultura, por espécie florestal**. Available at: <https://sidra.ibge.gov.br/tabela/5930#resultado>. Accessed in: 24 Jul. 2022.

IBM. **ILOG CPLEX Manuals**. Available at: <https://www.ibm.com/support/pages/ilog-cplex-manuals>. Accessed in: 17 Sep. 2021.

IEA. **World Energy Outlook**. Available at: <www.iea.org/weo>. Accessed in: 1 Jun. 2022.

INSTITUTO BRASILEIRO DE ÁRVORES. **Relatório Ibá 2015**. Available at: <www.iba.org>. Accessed in: 2 Sep. 2021.

INTERNATIONAL PAPER. **Paper Mills and Forestry Unit**. Available at: <https://www.internationalpaper.com/company/regions/south-america/paper-mills>. Accessed in: 6 Sep. 2021.

IPEL. **SOBRE NÓS | IPEL**. Available at: <https://www.ipelpapel.com.br/sobre-nos>. Accessed in: 6 Sep. 2021.

ITC. **Trade Map - Trade statistics for international business development**. Available at: <https://www.trademap.org/>. Accessed in: 7 Sep. 2021.

JĘDRZEJCZAK, P. *et al.* The role of lignin and lignin-based materials in sustainable construction – A comprehensive review. **International Journal of Biological Macromolecules**, v. 187, p. 624–650, 2021.

JOLLIET, O. *et al.* IMPACT 2002+: A New Life Cycle Impact Assessment Methodology. **International Journal of Life Cycle Assessment**, v. 8, n. 6, p. 324–330, 2003.

JÖNSSON, J. *et al.* Comparison of options for utilization of a potential steam surplus at kraft pulp mills — Economic performance and CO 2 emissions. **International Journal of Energy Research**, v. 37, n. 9, p. 1017–1035, 2013.

KANNANGARA, M. S. **Development and integration of acid predicpitation based lignin biorefineries in kraft pulping mills**. Montreál, Canada: Université de Montréal, 2015,184p.

KELLOWAY, A.; DAOUTIDIS, P. Process synthesis of biorefineries: Optimization of biomass conversion to fuels and chemicals. **Industrial and Engineering Chemistry Research**, v. 53, n. 13, p. 5261–5273, 2014.

KIM, J.; REALFF, M. J.; LEE, J. H. Optimal design and global sensitivity analysis of biomass supply chain networks for biofuels under uncertainty. **Computers and Chemical Engineering**, v. 35, n. 9, p. 1738–1751, 2011.

KIMBERLY-CLARK. **Global Sustainability Report Addendum 2020 Data and Disclosures**. Available at: <https://www.kimberly-clark.com/en-us/responsibility/annualreports>. Accessed in: 6 Sep. 2021.

KIRTANIA, K. Thermochemical Conversion Processes for Waste Biorefinery. **Waste Biorefinery: Potential and Perspectives**, p. 129–156, 2018.

KISS, A. A.; GRIEVINK, J. Process systems engineering developments in Europe from an industrial and academic perspective. **Computers & Chemical Engineering**, v. 138, p. 106823, 2020.

KOSTIN, A. *et al.* Optimization-based approach for maximizing profitability of bioethanol supply chain in Brazil. **Computers and Chemical Engineering**, v. 115, p. 121–132, 2018.

KOSTIN, A. M. *et al.* Design and planning of infrastructures for bioethanol and sugar production under demand uncertainty. **Chemical Engineering Research and Design**, v. 90, n. 3, p. 359–376, 2012.

KROTSCHECK, A. W.; SIXTA, H. Recovery. In: SIXTA, H. (Ed.). . **Handbook of Pulp**. Weinheim, Germany: Wiley-VCH Verlag GmbH, 2009. p. 967–996.

KUMAR, B.; VERMA, P. Biomass-based biorefineries: An important architype towards a circular economy. **Fuel**, v. 288, p. 119622, 2021.

KUSSANO, M. R.; BATALHA, M. O. Custos logísticos agroindustriais: Avaliação do escoamento da soja em grão do Mato Grosso para o mercado externo. **Gestao e Producao**, v. 19, n. 3, p. 619–632, 2012.

LEDUC, S. *et al.* Optimizing biodiesel production in India. **Applied Energy**, v. 86, n. SUPPL. 1, p. S125–S131, 2009.

LI, Q.; HU, G. Supply chain design under uncertainty for advanced biofuel production based on bio-oil gasification. **Energy**, v. 74, n. C, p. 576–584, 2014.

LI, Z.; FLOUDAS, C. A. **Robust Counterpart Optimization: Uncertainty Sets, Formulations and probabilistic Guarantees**. FOCAPO (Foundations of Computer-Aided Process Operations). **Anais**.2012.

LIAN, Z. T.; CHUA, K. J.; CHOU, S. K. A thermoeconomic analysis of biomass energy for trigeneration. **Applied Energy**, v. 87, n. 1, p. 84–95, 2010.

LIM, J. S. *et al.* A multi-period model for optimal planning of an integrated, resource-efficient rice mill. **Computers and Chemical Engineering**, v. 52, p. 77–89, 2013.

LOPES, E. DA S.; VIEIRA, T. P.; RODRIGUES, C. K. Avaliação técnica e de custos do transporte rodoviário com diferentes espécies e sortimentos de madeira. **Floresta**, v. 46, n. 3, p. 297–305, 2016.

LOSSAU, S. *et al.* Brazil's current and future land balances: Is there residual land for bioenergy production? **Biomass and Bioenergy**, v. 81, p. 452–461, 2015.

ĽUDMILA, H. *et al.* Lignin, potential products and their market value. **Wood research**, v. 60, n. 6, p. 973–986, 2015.

MAITY, S. K. Opportunities, recent trends and challenges of integrated biorefinery: Part I. **Renewable and Sustainable Energy Reviews**, v. 43, p. 1427–1445, 2015.

MALFLIET, J. Incoterms 2010 and the mode of transport: how to choose the right term. **Eur. JL Reform 13**, 2011.

MANKAR, A. R. *et al.* Pretreatment of lignocellulosic biomass: A review on recent advances. **Bioresource Technology**, v. 334, p. 125235, 2021.

MAO, H. **Technical evaluation of a hardwood biorefinery using the "near-neutral" hemicellulose extraction process**. Orono, USA: The University of Maine, 2007, 230p.

MARTINEZ-HERNANDEZ, E.; SADHUKHAN, J.; CAMPBELL, G. M. Integration of bioethanol as an in-process material in biorefineries using mass pinch analysis. **Applied Energy**, v. 104, p. 517–526, 2013.

MARTINEZ-HERNANDEZ, E.; TIBESSART, A.; CAMPBELL, G. M. Conceptual design of integrated production of arabinoxylan products using bioethanol pinch analysis. **Food and Bioproducts Processing**, v. 112, p. 1–8, 2018.

MARUFUZZAMAN, M.; EKSIOGLU, S. D.; HUANG, Y. Two-stage stochastic programming supply chain model for biodiesel production via wastewater treatment. **Computers and Operations Research**, v. 49, p. 1–17, 2014.

MAVROTAS, G. Effective implementation of the ε-constraint method in Multi-Objective Mathematical Programming problems. **Applied Mathematics and Computation**, v. 213, n. 2, p. 455–465, 2009.

MCKETTA JR, J. J. **Encyclopedia of Chemical Processing and Design: Volume 44**. Ney York: CRC Press, 1993, 277p.

MEDINA-GONZÁLEZ, S. *et al.* Systematic approach for the design of sustainable supply chains under quality uncertainty. **Energy Conversion and Management**, v. 149, p. 722–737, 2017.

MEDINA-GONZÁLEZ, S.; ESPUÑA, A.; PUIGJANER, L. An efficient uncertainty representation for the design of sustainable energy generation systems. **Chemical Engineering Research and Design**, v. 131, p. 144–159, 2018.

MENCARELLI, L. *et al.* A review on superstructure optimization approaches in process system engineering. **Computers & Chemical Engineering**, v. 136, p. 106808, 2020.

MENON, V.; RAO, M. Trends in bioconversion of lignocellulose: Biofuels, platform chemicals & biorefinery concept. **Progress in Energy and Combustion Science**, v. 38, n. 4, p. 522–550, 2012.

MILI SA. **Mili SA website**. Available at: <https://www.mili.com.br/amili/>. Accessed in: 6 Sep. 2021.

MINISTÉRIO DA ECONOMIA. **Contribuição Social sobre o Lucro Líquido CSLL** . Available at: <https://www.gov.br/receitafederal/pt-br/assuntos/orientacao-tributaria/tributos/CSLL>. Accessed in: 4 Sep. 2021a.

MINISTÉRIO DA ECONOMIA. **IRPJ (Imposto sobre a renda das pessoas jurídicas)** . Available at: <https://www.gov.br/receitafederal/pt-br/assuntos/orientacao-tributaria/tributos/IRPJ>. Accessed in: 4 Sep. 2021b.

MINISTÉRIO DA ECONOMIA. **Estatísticas de Comércio Exterior em Dados Abertos — Português (Brasil)**. Available at: <https://www.gov.br/produtividade-e-comercio-exterior/pt-br/assuntos/comercio-exterior/estatisticas/base-de-dados-bruta>. Accessed in: 4 Sep. 2021.

MOHSENI, S.; PISHVAEE, M. S.; SAHEBI, H. Robust design and planning of microalgae biomass-to-biodiesel supply chain: A case study in Iran. **Energy**, v. 111, p. 736–755, 2016.

MORYA, R. *et al.* Recent advances in black liquor valorization. **Bioresource Technology**, v. 350, p. 126916, 2022.

MSGÁS. **Industrial - Tarifas**. Available at: <https://www.msgas.com.br/segmentos/industrial/tarifas>. Accessed in: 7 Sep. 2021.

MULVEY, J. M.; VANDERBEI, R. J.; ZENIOS, S. A. Robust Optimization of Large-Scale Systems. **Operations Research**, v. 43, n. 2, p. 264–281,1995.

MUSCAT, A. *et al.* The battle for biomass: A systematic review of food-feed-fuel competition. **Global Food Security**, v. 25, p. 100330, 2020.

NATURGY. **CEG Estrutura Tarifária**. Available at: <https://www.naturgy.com.br/atendimento/tarifas/tarifa_rio_de_janeiro>. Accessed in: 7 Sep. 2021.

NG, D. K. S. *et al.* A Hierarchical Approach to the Synthesis and Analysis of Integrated Biorefineries. In: **Design for Energy and the Environment**. CRC Press, 2009. p. 451–458.

NG, D. K. S.; NG, K. S.; NG, R. T. L. Integrated Biorefineries. **Encyclopedia of Sustainable Technologies**, p. 299–314, 2017.

NG, R. T. L.; HASSIM, M. H.; NG, D. K. S. Process synthesis and optimization of a sustainable integrated biorefinery via fuzzy optimization. **AIChE Journal**, v. 59, n. 11, p. 4212–4227, 2013.

OHRA-AHO, T. *et al.* Carbohydrate composition in Eucalyptus wood and pulps – Comparison between Py-GC/MS and acid hydrolysis. **Journal of Analytical and Applied Pyrolysis**, v. 129, n. May 2017, p. 215–220, 2018.

OKOLIE, J. A. *et al.* Next-generation biofuels and platform biochemicals from lignocellulosic biomass. **International Journal of Energy Research**, v. 45, n. 10, p. 14145–14169, 2021.

OSMANI, A.; ZHANG, J. Stochastic optimization of a multi-feedstock lignocellulosic-based bioethanol supply chain under multiple uncertainties. **Energy**, v. 59, p. 157–172, 2013.

OSMANI, A.; ZHANG, J. Economic and environmental optimization of a large scale sustainable dual feedstock lignocellulosic-based bioethanol supply chain in a stochastic environment. **Applied Energy**, v. 114, n. 2014, p. 572–587, 2014.

PÄTÄRI, S. *et al.* Global sustainability megaforces in shaping the future of the European pulp and paper industry towards a bioeconomy. **Forest Policy and Economics**, v. 66, p. 38–46, 2016.

PAULO EICHLER *et al.* Potential assessment of eucalyptus grown for biorefinery processes. **Agronomy Science and Biotechnology**, v. 3, n. 1, p. 01–11, 2017.

PBGÁS. **Tarifas - PBGÁS – Companhia Paraibana de Gás**. Available at: <http://www.pbgas.com.br/?page_id=1477>. Accessed in: 7 Sep. 2021.

PÊGAS, P. H. **PIS e COFINS**. Rio de Janeiro, Brazil: Freitos Bastos Editora, 2008.

PENA-VERGARA, G. *et al.* Energy from planted forest and its residues characterization in Brazil. **Energy**, v. 239, p. 122243, 2022.

PEREIRA, G. C. Q. *et al.* Process design and economics of a flexible ethanol-butanol plant annexed to a eucalyptus kraft pulp mill. **Bioresource Technology**, v. 250, n. November 2017, p. 345–354, 2018.

PÉREZ-FORTES, M. *et al.* Design of regional and sustainable bio-based networks for electricity generation using a multi-objective MILP approach. **Energy**, v. 44, n. 1, p. 79–95, 2012.

PHAM, V.; EL-HALWAGI, M. Process synthesis and optimization of biorefinery configurations. **AIChE Journal**, v. 58, n. 4, p. 1212–1221, 2012.

PISHVAEE, M. S.; RAZMI, J.; TORABI, S. A. Robust possibilistic programming for socially responsible supply chain network design: A new approach. **Fuzzy Sets and Systems**, v. 206, p. 1–20, 2012.

PLOTLY INC. **plotly/plotly.py: The interactive graphing library for Python (includes Plotly Express)**. Available at: <https://github.com/plotly/plotly.py>. Accessed in: 7 Aug. 2022.

PRE-CONSULTANTS. **The Eco-indicator 99 - A damage oriented method for Life Cycle Impact Assessment - Manual for Designers** Amersfoort, Netherlands, 2000.

RAFIONE, T. *et al.* The Green Integrated Forest Biorefinery: An innovative concept for the pulp and paper mills. **Applied Thermal Engineering**, v. 73, n. 1, p. 74–81, 2014.

RAMAN, R.; GROSSMANN, I. E. Modeling and computational techniques for logic based integer programming. **Computers and Chemical Engineering**, v. 18, n. 7, p. 563–578, 1994.

REBACK, J. *et al.* **pandas-dev/pandas: Pandas 1.2.4**, 12 Apr. 2021. Available at: <https://zenodo.org/record/4681666>. Accessed in: 7 Aug. 2022

RESSEL, J. B. Wood Yard Operations. **Handbook of Pulp**, v. 1, p. 69–107, 2008.

RYAN, M. G. *et al.* An experimental test of the causes of forest growth decline with stand age. **Ecological Monographs**, v. 74, n. 3, p. 393–414, 2004.

SANTHER. **Home - Santher**. Available at: <https://www.santher.com.br/#quem-somos>. Accessed in: 6 Sep. 2021.

SANTIBAÑEZ-AGUILAR, J. E. *et al.* Optimal planning of a biomass conversion system considering economic and environmental aspects. **Industrial and Engineering Chemistry Research**, v. 50, n. 14, p. 8558–8570, 2011.

SANTIBAÑEZ-AGUILAR, J. E. *et al.* Stochastic design of biorefinery supply chains considering economic and environmental objectives. **Journal of Cleaner Production**, v. 136, n. April, p. 224–245, 2016.

SCGAS. **SCGAS - Companhia de Gás de Santa Catarina**. Available at: <https://www.scgas.com.br/scgas/site/tarifas-e-simuladores/entenda-a-tarifa-tg2>. Accessed in: 7 Sep. 2021.

SCHNEIDER, M. N.; IACONI, A.; LAROCCA, S. Oleochemical Biorefinery. **Chemicals and Fuels from Bio-Based Building Blocks**, p. 519–534, 2016.

SCHRÖDER, T.; LAUVEN, L. P.; GELDERMANN, J. Improving biorefinery planning: Integration of spatial data using exact optimization nested in an evolutionary strategy. **European Journal of Operational Research**, v. 264, n. 3, p. 1005–1019, 2018.

SCOLFORO, H. F. *et al.* Yield pattern of eucalypt clones across tropical Brazil: An approach to clonal grouping. **Forest Ecology and Management**, v. 432, n. August 2018, p. 30–39, 2019.

SEA-DISTANCES.ORG. **SEA-DISTANCES.ORG - Distances**. Available at: <https://sea-distances.org/>. Accessed in: 11 Sep. 2021.

SEN GUPTA, S.; SHASTRI, Y.; BHARTIYA, S. Model-based optimisation of biodiesel production from microalgae. **Computers and Chemical Engineering**, v. 89, p. 222–249, 2016.

SERGAS. **Tarifas Praticadas – SERGAS – Sergipe Gás S/A**. Available at: <https://www.sergipegas.com.br/wp/tarifas-praticadas/>. Accessed in: 7 Sep. 2021.

SHABANI, N. *et al.* Tactical supply chain planning for a forest biomass power plant under supply uncertainty. **Energy**, v. 78, p. 346–355, 2014.

SHABANI, N.; SOWLATI, T. A hybrid multi-stage stochastic programming-robust optimization model for maximizing the supply chain of a forest-based biomass power plant considering uncertainties. **Journal of Cleaner Production**, v. 112, p. 3285–3293, 2016.

SHANGHAI SHIPPING EXCHANGE. **Shanghai Containerized Freight Index**. Available at: <https://en.sse.net.cn/indices/scfinew.jsp>. Accessed in: 12 oct. 2021.

SHAPOSHNYK, V. *et al.* Determining the possibility of Using removable Equipment for Transporting 20- and 40-feet-long Containers on an Universal platform Wagon. **Eastern-European Journal of Enterprise Technologies**, v. 1, p. 14–21, 2021.

SHARMA, P.; SARKER, B. R.; ROMAGNOLI, J. A. A decision support tool for strategic planning of sustainable biorefineries. **Computers and Chemical Engineering**, v. 35, n. 9, p. 1767–1781, 2011.

SINGH, N. *et al.* Global status of lignocellulosic biorefinery: Challenges and perspectives. **Bioresource Technology**, v. 344, p. 126415, 2022.

SIXTA, H. Introduction. In: SIXTA, H. (Ed.). . **Handbook of Pulp**. Weinheim, Germany: Wiley-VCH Verlag GmbH, 2006. p. 2–19.

SIXTA, H. *et al.* Pulp Bleaching. In: SIXTA, H. (Ed.). . **Handbook of Pulp**. Weinheim, Germany: Wiley-VCH Verlag GmbH, 2006. p. 609–932.

SIXTA, H.; POTTHAST, A.; KROTSCHEK, A. W. Chemical Pulping Processes. In: SIXTA, H. (Ed.). . **Handbook of Pulp**. Weinheim, Germany: Wiley-VCH Verlag GmbH, 2006. p. 109–229.

SMITH, J. C.; TASKIN, Z. C. A Tutorial Guide to Mixed-Integer Programming Models and Solution Techniques. In: LIM, G. J.; LEE, E. K. (Eds.). . **Optimization in Medicine and Biology**. 1st. ed. Boca Raton, USA: Auerbach Publications, 2008.

SOFTYS/CMPC. **Relatório Sustentabilidade 2020**. Available at: <https://www.sepac.com.br/pdf/softys-relatorio-de-sustentabilidade-2020.pdf>. Accessed in: 6 Sep. 2021.

SULGÁS. **Sulgás - Companhia de Gás do Estado do Rio Grande do Sul - Tabela tarifária**. Available at: <https://www.sulgas.rs.gov.br/sulgas/industrial/tabela-de-precos>. Accessed in: 7 Sep. 2021.

SUPERIOR TRIBUNAL DE JUSTIÇA. **Súmula n. 166. Não constitui fato gerador do ICMS o simples deslocamento de mercadoria de um para outro estabelecimento do mesmo contribuinte.Diário da Justiça**BRAZIL., 1996. Available at: <https://www.stj.jus.br/docs_internet/revista/eletronica/stj-revista-sumulas-2010_12_capSumula166.pdf>. Accessed in: 6 Sep. 2021

SUSAETA, A.; ROSSATO, F. G. Efficiency of pulp and paper industry in the production of pulp and bioelectricity in Brazil. **Forest Policy and Economics**, v. 128, p. 102484, 2021.

SUZANO SA. **Earning Release for 4Q2020**. Available at: <https://ir.suzano.com.br/English/financial-information/results-center/default.aspx>. Accessed in: 6 Sep. 2021a.

SUZANO SA. **Suzano Production Capacity**. Available at: <https://ir.suzano.com.br/English/the-company/production-capacity/default.aspx>. Accessed in: 6 Sep. 2021b.

SUZANO SA. **Suzano to invest $2.8 billion in the first fossil-free pulp plant in Brazil**. Available at: <https://www.suzano.com.br/en/suzano-to-invest-2-8-billion-in-the-first-fossil-free-pulp-plant-in-brazil/>. Accessed in: 6 Sep. 2021c.

TAN, R. R. *et al.* A fuzzy multiple-objective approach to the optimization of bioenergy system footprints. **Chemical Engineering Research and Design**, v. 87, n. 9, p. 1162–1170, 2009.

TAY, D. H. S. *et al.* Fuzzy optimization approach for the synthesis of a sustainable integrated biorefinery. **Industrial and Engineering Chemistry Research**, v. 50, n. 3, p. 1652–1665, 2011.

TONG, K. *et al.* Optimal design of advanced drop-in hydrocarbon biofuel supply chain integrating with existing petroleum refineries under uncertainty. **Biomass and Bioenergy**, v. 60, p. 108–120, 2014a.

TONG, K. *et al.* Stochastic programming approach to optimal design and operations of integrated hydrocarbon biofuel and petroleum supply chains. **ACS Sustainable Chemistry and Engineering**, v. 2, n. 1, p. 49–61, 2014b.

TORRES, D. *et al.* **Revelando o sistema tributário brasileiro**. 2nd. ed. São Paulo: Editora Sinafresp, 2003.

TRAN, H.; VAKKILAINEN, E. K. The kraft chemical recovery process. **Tappi Journal**, 2016.

TURTON, R. *et al.* **Analysis, synthesis, and design of chemical processes**. 3rd. ed. Upper Saddle River, USA: Prentice Hall, 2009, 108p.

TWEDE, D. *et al.* **Cartons , Crates and Corrugated Board: Handbook of Paper and Wood Packaging Technology**. 2nd. ed. Lancaster, USA: DEStech Publications, Inc., 2015, 83p.

VAN DER MERWE, J. P.; PULKKI, R.; ACKERMAN, P. Fibre losses during debranching and debarking of Eucalyptus pulp logs using a single-grip harvester. **Southern Forests**, v. 77, n. 4, p. 309–313, 2015.

VAN DYKEN, S.; BAKKEN, B. H.; SKJELBRED, H. I. Linear mixed-integer models for biomass supply chains with transport, storage and processing. **Energy**, v. 35, n. 3, p. 1338–1350, 2010.

VINHA ZANUNCIO, A. J. *et al.* Importância da secagem da madeira para o transporte forestal e abastecimento de fábricas de polpa celulósica. **Cerne**, v. 23, n. 2, p. 147–152, 2017.

WALTHER, G.; SCHATKA, A.; SPENGLER, T. S. Design of regional production networks for second generation synthetic bio-fuel - A case study in Northern

Germany. **European Journal of Operational Research**, v. 218, n. 1, p. 280–292, 2012.

WECD. **Our Common Future (The Brundtland Report)**. Oxford, UK: Oxford University Press, 1987, 300p.

WHEELER, J. *et al.* Combining multi-attribute decision-making methods with multi-objective optimization in the design of biomass supply chains. **Computers and Chemical Engineering**, v. 113, p. 11–31, 2018.

WU, X. *et al.* Photocatalytic transformations of lignocellulosic biomass into chemicals. **Chemical Society Reviews**, v. 49, n. 17, p. 6198–6223, 2020.

YILMAZ BALAMAN, Ş.; SELIM, H. A fuzzy multiobjective linear programming model for design and management of anaerobic digestion based bioenergy supply chains. **Energy**, v. 74, n. C, p. 928–940, 2014.

YILMAZ BALAMAN, Ş.; SELIM, H. A decision model for cost effective design of biomass based green energy supply chains. **Bioresource Technology**, v. 191, p. 97–109, 2015.

YOU, F. *et al.* Optimal design of sustainable cellulosic biofuel supply chains: Multiobjective optimization coupled with life cycle assessment and input-output analysis. **AIChE Journal**, v. 58, n. 4, p. 1157–1180, 2012.

YOU, F.; WANG, B. Life cycle optimization of biomass-to-liquid supply chains with distributed-centralized processing networks. **Industrial and Engineering Chemistry Research**, v. 50, n. 17, p. 10102–10127, 2011.

ZAMBONI, A.; SHAH, N.; BEZZO, F. Spatially explicit static model for the strategic design of future bioethanol production systems. 1. cost minimization. **Energy and Fuels**, v. 23, n. 10, p. 5121–5133, 2009a.

ZAMBONI, A.; SHAH, N.; BEZZO, F. Spatially explicit static model for the strategic design of future bioethanol production systems. 2. multi-objective environmental optimization. **Energy and Fuels**, v. 23, n. 10, p. 5134–5143, 2009b.

ZHANG, Y. X.; WANG, X. J. Geographical spatial distribution and productivity dynamic change of eucalyptus plantations in China. **Scientific Reports 2021 11:1**, v. 11, n. 1, p. 1–15, 2021.

ZHAO, S.; YOU, F. Resilient supply chain design and operations with decision-dependent uncertainty using a data-driven robust optimization approach. **AIChE Journal**, v. 65, n. 3, p. 1006–1021, 2019.

ZIMMER, T. *et al.* Modeling the impact of competing utilization paths on biomass-to-liquid (BtL) supply chains. **Applied Energy**, v. 208, n. August, p. 954–971, 2017.

ZORE, Ž. *et al.* Maximizing the sustainability net present value of renewable energy supply networks. **Chemical Engineering Research and Design**, v. 131, p. 245–265, 2018.

ZORE, Ž.; ČUČEK, L.; KRAVANJA, Z. Syntheses of sustainable supply networks with a new composite criterion – Sustainability profit. **Computers and Chemical Engineering**, v. 102, p. 139–155, 2017.

APPENDIX A – LIST OF MODEL SETS

B Set of biomass species

E Set of storage facilities' location

E_{non_port} The subset of E comprising locations that have no connections to overseas markets (non-port locations)

F Set of forest units' locations

P Set of production facilities' location

M Set of consumer markets' location

$M_{overseas}$ The subset of M comprising the overseas markets' locations. These markets cannot be accessed by non-port locations.

I Set of ages considered for all biomass species

Q Set of chemical pseudo-components

R Set of residues and effluents

U Set of utilities

T Set of periods

$T^{perpetuity}$ Artificial set of extra-operating periods for perpetuity constraints

Z Set of conversion technologies

APPENDIX B – LIST OF MODEL VARIABLES

Symbol[16]	Description	Domain
$A_{f,t}^{free,bought}$	Amount of free land (with no planted biomass) bought from third parties at a forest unit *f* and period *t*.	Non-Negative Reals
$A_{f,t}^{free,owned}$	Area of owned free land (with no planted biomass) available at a forest unit *f* at the end of period *t*.	Non-Negative Reals
$A_{f,t}^{free,thirds}$	Area of free lands (with no planted biomass) owned by third parties and available at each forest unit *f* at the end of a period *t*. This area is available for buying in the next period.	Non-Negative Reals
$A_{f,b,i,t}^{harvested}$	Area of land harvested at a forest unit *f* planted with biomass *b* with age *I* on period *t*.	Non-Negative Reals
$A_{f,b,t}^{newly\_planted}$	Area of lands in the forest unit *f* that were planted in the period *t* with biomass species *b*.	Non-Negative Reals
$A_{f,b,i,t}^{owned}$	Area of owned planted lands available at each forest unit *f* planted with biomass *b* with age *I* at the end of period *t*.	Non-Negative Reals
$A_{f,b,i,t}^{planted,bought}$	Area of lands bought from third parties at a forest unit *f* planted with biomass *b* with age *I* at a given period *t*.	Non-Negative Reals
$A_{f,b,i,t}^{thirds}$	Area of lands owned by third parties available at each forest unit *f* planted with biomass *b* with age *I* at the end of a period *t*. This areas area is available for buying in the next period.	Non-Negative Reals

[16] Variables present the form $X_{subscript\ 1, subscript\ 2, \ldots, subscript\ n}^{superscript\ 1, superscript\ 2, \ldots, superscript\ n}$ and are order alphabetically in respect to the name **X**. For variables with the same name X, superscripts will be used for ordering.

$C_{f,b,t}^{harvest}$	Costs associated with the harvesting of lands planted with biomass *b* on a forest unit *f* at a period *t*.	Non-Negative Reals
$C_{t}^{harvest,total}$	Total harvesting costs at a period *t*.	Non-Negative Reals
$C_{f,b,t}^{maintenance,F}$	Costs for maintaining the lands planted with biomass *b* on a forest unit *f* at a period *t*.	Non-Negative Reals
$C_{f,t}^{maintenance,F,free}$	Cost for maintaining the free lands (with no planted biomass) on a forest unit *f* at a period *t*.	Non-Negative Reals
$C_{t}^{maintenance,F,total}$	Total forest maintenance cost for a period *t.*	Non-Negative Reals
$C_{p,t}^{production,P}$	Production costs on a production facility *p* at a period *t.*	Non-Negative Reals
$C_{t}^{production}$	Total production costs at a period *t* considering all production facilities.	Non-Negative Reals
$C_{e,t}^{storage,E}$	Storage costs on storage facility *e* at a period *t.*	Non-Negative Reals
$C_{t}^{storage,E,total}$	Total storage costs on layer E at a period *t.*	Non-Negative Reals
$C_{p,t}^{storage,P}$	Storage costs on a production facility *p* at a period *t.*	Non-Negative Reals
$C_{t}^{storage,P,total}$	Total storage costs on layer P at a period *t.*	Non-Negative Reals
C_{t}^{total}	Total operating costs at a period *t.*	Non-Negative Reals
$C_{f,p,t}^{transp,biomass,FP}$	Costs for biomass transportation from a forest unit *f* to a production unit *p* at a period *t*.	Non-Negative Reals
$C_{t}^{transp,biomass}$	Total costs with biomass transportation at a period *t.*	Non-Negative Reals

$C_{t}^{transp,E}$	Total transportation costs originating from layer E at a period *t.*	Non-Negative Reals
$C_{e,e',q,t}^{transp,EE}$	Transportation costs from a storage facility *e* to another *e'* for the chemical pseudo-component *q* at a period *t.*	Non-Negative Reals
$C_{e,m,,q,t}^{transp,EM}$	Transportation costs from a storage facility *e* to a consumer market *m* for the chemical pseudo-component *q* at a period *t.*	Non-Negative Reals
$C_{t}^{transp,P}$	Total transportation costs originating from layer P at a period *t.*	Non-Negative Reals
$C_{p,e,q,t}^{transp,PE}$	Transportation costs from a production facility *p* to a storage facility *e* for the chemical pseudo-component *q* at a period *t.*	Non-Negative Reals
$C_{p,m,q,t}^{transp,PM}$	Transportation costs from a production facility *p* to a consumer market *m* for the chemical pseudo-component *q* at a period *t.*	Non-Negative Reals
$C_{p,p',q,t}^{transp,PP}$	Transportation costs from a production facility *p* to another *p'* for the chemical pseudo-component *q* at a period *t.*	Non-Negative Reals
$FEM_{e,m,q,t}$	Amount of chemical pseudo-component *q* sold to a consumer market *m* from a storage facility *e* at a period *t*.	Non-Negative Reals
$FF_{f,p,b,t}^{demand}$	Amount of biomass *b* harvested at a forest unit *f* and sent to production facility *p* at a period *t.*	Non-Negative Reals
$FF_{f,b,t}^{harvested}$	Amount of harvested biomass from a forest unit *f* planted with biomass *b* at each period *t*.	Non-Negative Reals

$\boldsymbol{FFP_{p,q,t}}$	Amount of chemical pseudo-component *q* sent from all forest units to a given production facility *p* at a period *t*.	Non-Negative Reals
$\boldsymbol{FM_{m,q,t}}$	Amount of the chemical pseudo-component *q* sold to a consumer market *m* at a period *t.*	Non-Negative Reals
$\boldsymbol{FPE_{p,e,q,t}}$	Amount of chemical pseudo-component *q* sent from a production facility *p* to a storage unity *e* at a period *t*.	Non-Negative Reals
$\boldsymbol{FPM_{p,m,q,t}}$	Amount of chemical pseudo-component *q* sent from a production facility *p* to a consumer market *m* at a period *t*.	Non-Negative Reals
$\boldsymbol{FPZ_{p,z,q,t}}$	Amount of chemical pseudo-component *q* produced at a production facility *p* by a technology *z* at a period *t*.	Non-Negative Reals
$\boldsymbol{FRZ_{p,z,r,t}}$	Amount of residue *r* produced by a technology *z* within a production facility *p* at a period *t.*	Non-Negative Reals
$\boldsymbol{FTE_{e,e',q,t}}$	Amount of a chemical pseudo-component *q* transferred from a storage facility *e* to another *e'* at a period *t.*	Non-Negative Reals
$\boldsymbol{FTP_{p',p,q,t}}$	Amount of chemical pseudo-component *q* transferred from a production facility *p'* to another production facility *p* at a period *t*.	Non-Negative Reals
$\boldsymbol{FU_{p,u,t}^{bought}}$	Amount of a utility *u* bought by a production facility *p* at a period *t.*	Non-Negative Reals
$\boldsymbol{FU_{p,z,u,t}^{interconversion}}$	Amount of a utility *u* that is fed to a technology *z* to be converted into another utility within the production facility *p* at a period *t.*	Non-Negative Reals
$\boldsymbol{FU_{p,z,u}^{interconversion,max}}$	The maximum fed of a utility *u* to be converted into another utility by the	Non-Negative Reals

	technology *z* within a production facility *p* considering all operating periods.	
$FU_{p,z,u,t}^{needed}$	Amount of a utility *u* demanded by a technology *z* within a production facility *p* at a period *t*.	Non-Negative Reals
$FU_{p,z,u_{prod},t}^{produced}$	Amount of a utility *u* produced by a technology *z* within a production facility *p* at a period *t.*	Non-Negative Reals
$FU_{p,u,t}^{sold}$	Amount of a utility *u* sold by a production facility *p* at a period *t.*	Non-Negative Reals
$FZ_{p,z,q,t}$	Amount of the chemical pseudo-component *q* processed by a technology *z* within a production facility *p* at a period *t*.	Non-Negative Reals
$FZ_{p,z,q}^{max}$	The maximum fed of a pseudo-component *q* to be converted by the technology *z* within a production facility *p* considering all operating periods.	Non-Negative Reals
$I_{f,t}^{forest}$	Investment at a period *t* for the acquisition of lands on a forest unit *f.*	Non-Negative Reals
$I_{t}^{forest,total}$	Investment at a period *t* for the acquisition of lands on all forest units.	Non-Negative Reals
$\tilde{I}_{p,z,q}^{prod,q}$	Investment on a technology *z* for converting a chemical pseudo-component *q* within production facility *p* obtained by piecewise linear approximation.	Non-Negative Reals
$\tilde{I}_{p,z,u}^{prod,u}$	Investment on a technology *z* for converting a utility *u* within production facility *p* obtained by piecewise linear approximation.	Non-Negative Reals
$\tilde{I}_{p,z}^{production}$	Total investment on a technology *z* within a production facility *p*.	Non-Negative Reals

$\boldsymbol{I^{production,total}}$	Total production investment considering all production facilities and all technologies.	Non-Negative Reals
$\boldsymbol{I^{storage}}$	Total storage investment considering all production and storage facilities and all chemical pseudo-components.	Non-Negative Reals
$\boldsymbol{\tilde{I}_{e,q}^{storage.E}}$	Investment in storage capacity for a chemical pseudo-component *q* within a storage facility *e* obtained by piecewise linear approximation.	Non-Negative Reals
$\boldsymbol{\tilde{I}_{p,q}^{storage.P}}$	Investment on storage capacity for a chemical pseudo-component *q* within a production facility *p* obtained by piecewise linear approximation.	Non-Negative Reals
$\boldsymbol{L_t}$	Total profit at a period *t*.	Reals
$\boldsymbol{me_{e,q,t}}$	Amount of chemical pseudo-component *q* stored at a storage facility *e* at a period *t*.	Non-Negative Reals
$\boldsymbol{me_{e,q}^{max}}$	Maximum stored quantity of a chemical pseudo-component *q* within a storage location *e* considering all periods.	Non-Negative Reals
$\boldsymbol{mp_{p,q,t}}$	Amount of chemical pseudo-component *q* stored at a production facility *p* at a period *t.*	Non-Negative Reals
$\boldsymbol{mp_{e,q}^{max}}$	Maximum stored quantity of a chemical pseudo-component *q* within a production facility *p* considering all periods.	Non-Negative Reals
$\boldsymbol{NPV}$	Net Present Value for the operation's cash flows.	Reals
$\boldsymbol{R_{q,t}}$	Total revenue (net of sales taxes) for a chemical pseudo-component *q* at a period *t* considering all sources and destinations.	Non-Negative Reals

R_t^{total}	Total revenue (net of sales tax) at a period *t* considering all chemical pseudo-component and utilities.	Non-Negative Reals
$RE_{e,m,q,t}$	Revenue (net of sales taxes) from a chemical pseudo-component *q* sold from a storage facility *e* to a consumer market *m* at a period *t.*	Non-Negative Reals
$RP_{p,m,q,t}$	Revenue (net of sales taxes) from a chemical pseudo-component *q* sold from a production facility *p* to a consumer market *m* at a period *t.*	Non-Negative Reals
$RU_{p,u,t}$	Revenue (net of sales taxes) from a utility *u* sold within a production facility *p* at a period *t.*	Non-Negative Reals
Tax_t^{Profit}	Profit tax paid at a period *t.*	Non-Negative Reals
$w_{e,q,n}^{lin,arm,e}$	Binary linearization variable for the piecewise linear approximation of the investment function for the storage of a chemical pseudo-component *q* within a storage facility *e.*	Non-Negative Reals
$w_{p,q,n}^{lin,arm,p}$	Binary linearization variable for the piecewise linear approximation of the investment function for the storage of a chemical pseudo-component *q* within a production facility *p.*	Non-Negative Reals
$w_{p,z,q,n}^{lin,prod,q}$	Binary linearization variable for the piecewise linear approximation of the investment function for the technology *z* implemented within a production facility *p* processing a chemical pseudo-component *q*.	Binary

$\boldsymbol{w_{p,z,u,n}^{lin,prod,u}}$	Binary linearization variable for the piecewise linear approximation of the investment function for the technology *z* implemented within a production facility *p* processing a utility *u*.	Binary
$\boldsymbol{ye_e}$	Binary that takes the value of 1 if it is decided to build a storage facility at a location *e* and 0 otherwise	Binary
$\boldsymbol{yp_p}$	Binary that takes the value of 1 if it is decided to build a production facility at a location *p* and 0 otherwise.	Binary
$\boldsymbol{ypz_{p,z}}$	Binary that takes the value of 1 if it is decided to implement a technology *z* within production facility *p* and 0 otherwise.	Binary
$\boldsymbol{\delta_{e,q,n}^{lin,armE}}$	Continuous linearization variable for the piecewise linear approximation of the investment function for the storage of a chemical pseudo-component *q* within a storage facility *e.*	Non-Negative Reals
$\boldsymbol{\delta_{p,q,n}^{lin,armP}}$	Continuous linearization variable for the piecewise linear approximation of the investment function for the storage of a chemical pseudo-component *q* within a production facility *p.*	Non-Negative Reals
$\boldsymbol{\delta_{p,z,q,n}^{lin,prod,q}}$	Continuous linearization variable for the piecewise linear approximation of the investment function for the technology *z* implemented within a production facility *p* processing a chemical pseudo-component *q*.	Non-Negative Reals
$\boldsymbol{\delta_{p,z,u,n}^{lin,prod,u}}$	Continuous linearization variable for the piecewise linear approximation of the	Non-Negative Reals

	investment function for the technology *z* implemented within a production facility *p* processing a utility *u*.	
$\boldsymbol{U_{f,b,\mathrm{i},\mathrm{n},t}^{harvest}}$	Auxiliary variable for the robust counterpart formulation for the produced biomass equation.	Non-Negative Reals
$\boldsymbol{W_{f,b,i,n,t}^{harvest}}$	Auxiliary variable for the robust counterpart formulation for the produced biomass equation.	Non-Negative Reals
$\boldsymbol{W_{e,m,q,t}^{revenue,E}}$	Auxiliary variable for the robust counterpart formulation for the chemicals selling revenues from layer E equation.	Non-Negative Reals
$\boldsymbol{W_{p,m,q,t}^{revenue,P}}$	Auxiliary variable for the robust counterpart formulation for the chemicals selling revenues from layer E equation.	Non-Negative Reals
$\boldsymbol{Z_{f,b,i,t}^{harvest}}$	Auxiliary variable for the robust counterpart formulation for the produced biomass equation.	Non-Negative Reals
$\boldsymbol{Z_{m,q}^{revenue,E}}$	Auxiliary variable for the robust counterpart formulation for the chemicals selling revenues from layer E equation.	Non-Negative Reals
$\boldsymbol{Z_{m,q}^{revenue,P}}$	Auxiliary variable for the robust counterpart formulation for the chemicals selling revenues from layer E equation.	Non-Negative Reals
$\xi_{f,b,t}^{growth}$	The random variable representing the uncertainties in the growth increment parameter. It is displayed in regular formatting as it is managed implicitly in	Reals

	the Optimization model through a robust counterpart formulation.	
$\xi_{m,q,t}^{price,q}$	The random variable representing the uncertainties in chemicals selling prices. It is displayed in regular formatting as it is managed implicitly in the Optimization model through a robust counterpart formulation.	Reals
$\xi_{p,u,t}^{price,u}$	The random variable representing the uncertainties in utilities selling prices. It is displayed in regular formatting as it is managed implicitly in the Optimization model through a robust counterpart formulation.	Reals

APPENDIX C – LIST OF MODEL PARAMETERS

Symbol[17]	**Description**
$A_{f,initial}^{free,owned}$	Owned land area initially available at each forest unit *f* with no planted biomass.
$A_{f,initial}^{free,thirds}$	Third parties' owned land area initially available at each forest unit *f* with no planted biomass. This area is available for buying.
$A_{f,b,i,initial}^{owned}$	Owned land area initially available at each forest unit *f* planted with biomass species *b* with age *i*.
$A_{f,b,i,initial}^{thirds}$	Third parties' owned land area initially available at each forest unit *f* planted with biomass species *b* with age *i*. This area is available for buying.
$c_{f,b,i,t}^{harvest}$	Cost for harvesting a unit of land planted with biomass *b* with age *i* on a forest location *f* at a period *t*.
$c_{f,b,i,t}^{maintenance,F}$	Cost for maintaining a unit of planted land with biomass *b* with age *i* on a forest unit *f* at a period *t*.
$c_{f,t}^{maintenance,F,free}$	Cost for maintaining a unit of free land (with no planted biomass) on a forest unit *f* at a period *t*.
$c_{p,z,t}^{prod,fix}$	Fixed costs for operating a technology *z* within a production facility *p* at a period *t.*
$c_{p,z,q,t}^{prod,var,q}$	Cost for processing a unit of pseudo-component *q* by technology *z* within a production facility *p* at a period *t*. Utilities acquisition is excluded from this cost.
$c_{p,z,u,t}^{prod,var,u}$	Cost for processing a unit of utility *u* by technology *z* within a production facility *p* at a period *t*. Other utilities acquisition is excluded from this cost.
$c_{p,r,t}^{residue}$	Cost for treating a unit of residue or effluent *r* within a production facility *p* at a period *t*.
$c_{e,t}^{stor,E,fix}$	Fixed costs for operating a storage facility *e* at a period *t*.

[17] Parameters present the form $X_{subscript\ 1,subscript\ 2,\ldots,subscript\ n}^{superscript\ 1,superscript\ 2,\ldots,superscript\ n}$ and are ordered alphabetically in respect to the name X. For parameters with the same name X, superscripts will be used for ordering.

$c_{e,q,t}^{stor,E,var}$	Variable (unitary) cost for operating a storage facility *e* at a period *t* in function of the stored amount of the chemical pseudo-component *q* at that period.
$c_{p,q,t}^{stor,\mathrm{P},var}$	Variable (unitary) cost for storage within a production facility *p* at a period t in function of the stored amount of the chemical pseudo-component *q* at that period.
$c_{f,p,b,t}^{transp,biomass}$	Unitary transportation cost for the biomass *b* from a forest unit *f* to a production unit *p* at a period *t*.
$c_{e,e\prime,q,t}^{transp,EE}$	Unitary transportation cost of a chemical pseudo-component *q* from a storage facility *e* to another *e'* at a period *t*.
$c_{e,m,q,t}^{transp,EM}$	Unitary transportation cost of a chemical pseudo-component *q* from a storage facility *e* to a consumer market *m* at a period *t*.
$c_{p,\mathrm{e},q,t}^{transp,PE}$	Unitary transportation cost of a chemical pseudo-component *q* from a production facility *p* to a storage facility *e* at a period *t*.
$c_{p,m,q,t}^{transp,PM}$	Unitary transportation cost of a chemical pseudo-component *q* from a production facility *p* to a consumer market *m* at a period *t*.
$c_{p,p',q,t}^{transp,PP}$	Unitary transportation cost of a chemical pseudo-component *q* from a production facility *p* to another *p'* at a period *t*.
$c_{p,u,t}^{utility}$	Unitary cost for buying a utility *u* within a production facility *p* at a period *t*.
$conv\_intu_{z,u,u_{prod}}$	Yield for a technology *z* when converting a utility *u* into another utility *uprod*.
$conv\_q_{z,q,qprod}$	Yield for a technology *z* when converting a chemical pseudo-component *q* into *qprod*.
$conv\_r_{z,q,r}$	Ratio of a residue *r* generated to the amount of chemical pseudo-component *q* processed by a technology *z.*
$conv\_u_{z,q,uprod}$	Yield for a technology *z* when converting a chemical pseudo-component *q* into a utility *u.*

$Fdem_{m,q,t}$	Market demand for a chemical pseudo-component *q* for a consumer market *m* at a period *t*.
$FU_{z,u}^{ref}$	Reference capacity level for the conversion of a utility *u* by the technology z that corresponds to the reference technology investment ($i_{z,q}^{prod,q}$).
$FU_{z,u}^{ref,x}$	X[th] element of the reference vector used for piecewise linear approximation of the investment function for technology *z* in respect to the flow of the converted utility *u*. At each of these flow points, the approximated function will match exactly the original non-linear function. In between these points, the original function is linearly approximated.
$FZ_{z,q}^{ref}$	Reference capacity level for the conversion of a chemical pseudo-component *q* by the technology z that corresponds to the reference technology investment ($i_{z,q}^{prod,q}$)
$FZ_{z,q}^{ref,x}$	X[th] element of the reference vector used for piecewise linear approximation of the investment function for technology *z* in respect to the flow of the converted pseudo-component *q*. At each of these flow points, the approximated function will match exactly the original non-linear function. In between these points, the original function is linearly approximated.
$Growth_{f,b,i}^{accumulated}$	The amount of available biomass for harvesting for a given biomass *b* planted at a forest unit *f* when reaching age *i.* This parameter is uncertain.
$Growth_{f,b,i,t}^{incremented}$	The increment in the amount of available biomass *b* when aged from the previous period *t – 1* to the next period *t* when it reaches age *i*.
$\overline{Growth_{f,b,i}^{increment}}$	The expected or nominal value for the growth increment parameter of a biomass *b* at a forest location *f* when reaching age *i.*

$Growth^{\widetilde{increment}}_{f,b,\iota}$	The possible fluctuation in the value of the growth increment parameter of a biomass *b* at a forest location *f* when reaching age *i.*
$i^{free}_{f,t}$	Acquisition price for free lands (with no biomass planted) on a forest location *f* at a period *t*.
$i^{planted}_{f,b,i,t}$	Acquisition price for planted lands with biomass *b* with age *i* on a forest location *f* at a period *t*.
$i^{prod\_q}_{z,q}$	Reference investment for a technology *z* considering the reference processing capacity for the pseudo-component *q* ($FZ^{ref}_{z,q}$).
$i^{prod\_u}_{z,\mathrm{u}}$	Reference investment for a technology *z* considering the reference processing capacity for the utility *u* ($FU^{ref}_{z,\mathrm{u}}$).
$i^{storage.E}_{q}$	Reference investment for a storage facility on layer E considering the reference storage capacity for the pseudo-component *q* (me^{ref}_{q}).
$i^{storage.P}_{q}$	Reference investment for a storage facility on layer P considering the reference storage capacity for the pseudo-component *q* (mp^{ref}_{q}).
$imax$	Maximum age considered in Set I. All biomass with ages beyond this maximum is considered to not observe any changes in any of its properties and is then grouped as single age biomass.
int_{rate}	Interest rate considered for present value calculations.
$M^{arm,p,q}$	Big-M parameter used for imposing null storage at a production unit *p* for a given pseudo-component *q* if the production unit *p* is chosen not to be built.
$M^{conversion,z,q}$	Big-M parameter used for imposing no feed of a pseudo-component *q* to a technology *z* if it is not able to process it.
$M^{conversion,z,u}$	Big-M parameter used for imposing no feed of a utility *u* (for conversion to other utility) to a technology *z* if it is not able to process it.

$M^{demand,p,u}$	Maximum allowed amount of a utility *u* that can be sold by a production facility *p*.
$M^{supply,p,u}$	Maximum allowed amount of a utility *u* that can be bought by a production facility *p*.
$M^{tec,z,q}$	Big-M parameter used for imposing null feed to a technology z within a production facility *p* if this technology is chosen not to be implemented within the production facility.
$M^{transf,p,q}$	Big-M parameter used for imposing null transference of a pseudo-component *q* from a production unit *p* to a production unit *p'* if the second is chosen not to be built.
$M^{transf,\mathrm{e},q}$	Big-M parameter used for imposing null transference of a pseudo-component *q* from a storage facility *e* to another storage facility if the second is chosen not to be built.
$m_q^{mín}$	Fraction of the total sales of a given chemical pseudo-component *q* that must be kept under storage.
$me_{e,q,initial}$	Amount of chemical pseudo-component *q* initially stored at a storage facility *e*.
me_q^{ref}	Reference storage capacity for a chemical pseudo-component *q* associated with an investment of $i_q^{storage.E}$.
$me_q^{ref,\mathrm{x}}$	X^th^ element of the reference vector used for piecewise linear approximation of the investment function for storage facility *e* in respect to the volume stored of the pseudo-component *q*. At each of these points, the approximated function will match exactly the original non-linear function. In between these points, the original function is linearly approximated.
$mp_{p,q,initial}$	Amount of chemical pseudo-component *q* initially stored at a production facility *p*.
mp_q^{ref}	Reference storage capacity for a chemical pseudo-component *q* associated with an investment of $i_q^{storage.P}$.
$mp_q^{ref,\mathrm{x}}$	X^th^ element of the reference vector used for piecewise linear approximation of the investment function for storage

	capacity within a production facility *p* in respect to the volume stored of the pseudo-component *q*. At each of these points, the approximated function will match exactly the original non-linear function. In between these points, the original function is linearly approximated.
$n^{prod\_q,z,q}$	Scale exponent for the investment function of technology *z* in respect to the processing capacity of a chemical pseudo-component *q*.
$n^{prod\_u,z,u}$	Scale exponent for investment function of technology *z* in respect to the processing capacity of a utility *u*.
$n^{storage,q}$	Scale exponent for investment function for storage in respect to the storage capacity of a pseudo-component *q*.
$n\_lin\_arm\_e$	Number of linearization points for the storage investment approximation function in layer E.
$n\_lin\_arm\_p$	Number of linearization points for the storage investment approximation function in layer P.
n_lin_prod	Number of linearization points for the production investment approximation function.
$pq_{m,q,t}$	Uncertain unitary selling price of a chemical pseudo-component *q* on a consumer market *m* at a period *t*.
$\overline{pq}_{m,q,t}$	The expected or nominal value for the unitary selling price of a chemical pseudo-component *q* on a consumer market *m* at a period *t.*
$\widetilde{pq}_{m,q,t}$	The possible fluctuation in the unitary selling price of a chemical pseudo-component *q* on a consumer market *m* at a period *t.*
$pu_{p,u,t}$	Uncertain unitary selling price of a utility *u* within a production unit *p* at a period *t.*
$\overline{pu}_{p,\mathrm{u},t}$	The expected or nominal value for the unitary selling price of a utility *u* within a production unit *p* at a period *t.*
$\widetilde{pu}_{p,\mathrm{u},t}$	The possible fluctuation in the unitary selling price of a utility *u* within a production unit *p* at a period *t.*

$t_{construction}$	Duration of the construction period for storage and production facilities.
t_{last}	Last period of Set T.
tax_{rate}^{profit}	Tax rate incident on accounting profit.
$tax_{e,m,q}^{sales,E}$	Tax rate incident on the sale of a chemical pseudo-component *q* when originated on a storage facility *e* to a consumer market *m.*
$tax_{p,m,q}^{sales,P}$	Tax rate incident on the sale of a chemical pseudo-component *q* when originated on a production facility *p* to a consumer market *m.*
$tax_{p,u}^{sales,U}$	Tax rate incident on the sale of utility *u* within a production facility *p*.
$utl_{z,q,u}$	The consumption of utility *u* by a technology *z* for processing a unit of the chemical pseudo-component *q*.
$x_{f,b,q}$	Chemical composition of a biomass *b* given as the mass ratio of a chemical pseudo-component *q* present in biomass and the amount of biomass.
$\eta_{b}^{harvest}$	Yield of harvesting operations for a biomass *b*. Defined as the ratio between the amount of harvested biomass that can be sent to production facilities and the amount of the total biomass initially available on the harvested area.
$\Psi_{f,b,t}^{growth}$	Constant defining the size of the box set that limits the uncertainty representative variable for growth increment for a forest unit *f* planted with biomass *b* at a period *t.*
$\Psi_{m,q,t}^{price,q}$	Constant defining the size of the box set that limits the uncertainty representative variable for the unitary selling price of a chemical pseudo-component *q* on a consumer market *m* at a period *t.*
$\Psi_{p,u,t}^{price,u}$	Constant defining the size of the box set that limits the uncertainty representative variable for the unitary selling price of a utility *u* within a production unit *p* at a period *t*.

$\Gamma_{f,b}^{growth}$ Constant defining the size of the polyhedral set that limits the uncertainty representatives' variables for growth increment of the same forest unit *f* and planted biomass *b.*

$\Gamma_{m,q}^{price,q}$ Constant defining the size of the polyhedral set that limits the uncertainty representatives' variables for the unitary selling price of a chemical pseudo-component *q* on a consumer market *m* at a period *t.*

$\Gamma_{p,u}^{price,u}$ Constant defining the size of the polyhedral set that limits the uncertainty representatives' variables for the unitary selling price of a utility *u* within a production unit *p* at a period *t.*

APPENDIX D – BEKP DOMESTIC DEMAND ESTIMATED DATA

Company	Product	Location	Capacity [ton/year]	Pulp Demand [ton/year]	Source
Suzano (Suzano, Limeira and Rio Verde)	PW	São Paulo	800	560,000	Company website (SUZANO SA, 2021b)
IP (Mogi Guaçu and Luiz Antônio)	PW	São Paulo	795	556,500	Company website (INTERNATIONAL PAPER, 2021)
Suzano (Mucuri)	PW	Bahia	250	175,000	Company website (SUZANO SA, 2021b)
IP (Três Lagoas)	PW	Mato Grosso do Sul	234	163,800	Company website (INTERNATIONAL PAPER, 2021)
CPMC (Mogi das Cruzes and Caieras)	Tissue	São Paulo	140	140,000	Total volume for company taken from ABTCP Sector Guide (FARINHA E SILVA; BUENO; NEVES, 2017) and locations on the company website (SOFTYS/CMPC, 2021)
Sepac (Curitiba and Mallet)	Tissue	Paraná	130	130,000	Total volume for company taken from ABTCP Sector Guide (FARINHA E SILVA; BUENO; NEVES, 2017) and locations on the company website (SOFTYS/CMPC, 2021). Note: Sepac was acquired by CMPC, and their website is integrated into SOFTYS/CMPC.
Santher (Penha and Bragança Paulista)	Tissue	São Paulo	113	113,333	Total volume for the company taken from ABTCP Sector Guide (FARINHA E SILVA; BUENO; NEVES, 2017) and split evenly between the mill locations reported on the company website (SANTHER, 2021)

BO Paper (Arapoti and Jaguariaíva)	PW	Paraná	160	112,000	Company website (BO PAPER, 2021)
CVG (Volta Grande)	Tissue	Santa Catarina	100	100,000	Total volume for company taken from ABTCP Sector Guide (FARINHA E SILVA; BUENO; NEVES, 2017) and locations on the company website (CVG, 2021)
Milli (Maceió)	Tissue	Alagoas	70	70,000	Total volume for the company taken from ABTCP Sector Guide (FARINHA E SILVA; BUENO; NEVES, 2017) and split evenly between the mill locations reported on the company website (MILI SA, 2021)
Milli (Curitiba)	Tissue	Paraná	70	70,000	Total volume for the company taken from ABTCP Sector Guide (FARINHA E SILVA; BUENO; NEVES, 2017) and split evenly between the mill locations reported on the company website (MILI SA, 2021)
Mili (Três Barras)	Tissue	Santa Catarina	70	70,000	Total volume for the company taken from ABTCP Sector Guide (FARINHA E SILVA; BUENO; NEVES, 2017) and split evenly between the mill locations reported on the company website (MILI SA, 2021)
Indaial (Indaial)	Tissue	Santa Catarina	70	70,000	Total volume for company taken from ABTCP Sector Guide (FARINHA E SILVA; BUENO; NEVES, 2017) and locations from the company website (IPEL, 2021).
Santher (Guaíba)	Tissue	Rio Grande do Sul	57	56,667	Total volume for the company taken from ABTCP Sector

					Guide (FARINHA E SILVA; BUENO; NEVES, 2017) and split evenly between the mill locations reported on the company website (SANTHER, 2021)
Canoinhas (Canoinhas)	Tissue	Santa Catarina	50	50,000	Total volume for company taken from ABTCP Sector Guide (FARINHA E SILVA; BUENO; NEVES, 2017) and locations from the company website (CIA CANOINHAS DE PAPEL, 2021).
Kimberly-Clark (Suzano and Mogi das Cruzes)	Tissue	São Paulo	48	48,000	Total volume for company taken from ABTCP Sector Guide (FARINHA E SILVA; BUENO; NEVES, 2017) and split evenly between the mill locations reported in the company sustainability report (KIMBERLY-CLARK, 2021)
Carta Fabril (Anápolis)	Tissue	Goiás	40	40,000	Total volume for company taken from ABTCP Sector Guide (FARINHA E SILVA; BUENO; NEVES, 2017) and split evenly between the mill locations reported in the company finance report (CARTA GOIÁS, 2016)
Carta Fabril (São Gonçalo)	Tissue	Rio de Janeiro	40	40,000	Total volume for company taken from ABTCP Sector Guide (FARINHA E SILVA; BUENO; NEVES, 2017) and split evenly between the mill locations reported in the company finance report (CARTA GOIÁS, 2016)

Suzano (Facepa)	Tissue	Ceará	25	25,000	Company website (SUZANO SA, 2021b). Total reported volume from FACEPA was split evenly into Fortaleza, Ceará and Belem, Pará units.
Suzano (Facepa)	Tissue	Pará	25	25,000	Company website (SUZANO SA, 2021b). Total reported volume from FACEPA was split evenly into Fortaleza, Ceará and Belem, Pará units.
Kimberly-Clark (Camaçari)	Tissue	Bahia	24	24,000	Total volume for company taken from ABTCP Sector Guide (FARINHA E SILVA; BUENO; NEVES, 2017) and split evenly between the mill locations reported in the company sustainability report (KIMBERLY-CLARK, 2021)
Kimberly-Clark (Eldorado do Sul)	Tissue	Rio Grande do Sul	24	24,000	Total volume for company taken from ABTCP Sector Guide (FARINHA E SILVA; BUENO; NEVES, 2017) and split evenly between the mill locations reported in the company sustainability report (KIMBERLY-CLARK, 2021)
Kimberly-Clark (Correia Pinto)	Tissue	Santa Catarina	24	24,000	Total volume for company taken from ABTCP Sector Guide (FARINHA E SILVA; BUENO; NEVES, 2017) and split evenly between the mill locations reported in the company sustainability report (KIMBERLY-CLARK, 2021)